CELL MODELS FOR STUDYING THE INTERPLAY BETWEEN CONJUGATIVE METABOLISM AND EFFLUX TRANSPORTERS: ESTABLISHING UGT1A1, UGT2B7 AND MRP3 TRANSFECTED MDCK CELL LINES

Erkka Järvinen
University of Helsinki
Faculty of Pharmacy
Division of Pharmaceutical Chemistry and Technology

November 2015

HELSINGIN YLIOPISTO
HELSINGFORS UNIVERSITET
UNIVERSITY OF HELSINKI

Faculty	Department
Faculty of Pharmacy	Division of Pharmaceutical Chemistry and Technology

Author
Erkka Järvinen

Title
Cell models for studying the interplay between conjugative metabolism and efflux transporters: Establishing UGT1A1, UGT2B7 and MRP3 transfected MDCK cell lines

Subject
Pharmaceutical chemistry

Level	Month and year	Number of pages
Master's thesis	November 2015	112 (+ 3 Appendices)

Abstract
UDP-glucuronosyltransferases (UGTs) catalyse glucuronidation reactions between glucuronic acid and drug molecules, which contain nucleophilic groups, mostly hydroxyls, amines or carboxylic acids. Glucuronidation is the most important reaction in the conjugative drug metabolism. Because these conjugates are not usually able to cross cell membranes passively, they need active efflux transport. Efflux transporters mostly belong to superfamily of ATP-binding cassette transporters (ABC). Subfamily C of ABC transporters (ABCC) are known to be involved in efflux transport of glucuronides. Especially MRP2 (*ABCC2*) and MRP3 (*ABCC3*) play key roles in the elimination of glucuronide conjugates of drugs. MRP2 is localized in the apical membranes of hepatocytes and enterocytes, whereas MRP3 is localized in the basolateral membranes of the respective cells. On the other hand, UGT1A1 and UGT2B7 are highly expressed in liver and small intestine and are the most important UGTs in drug metabolism. It is known, that UGTs and efflux transporters work together forming interplay to eliminate drugs. Therefore, studying both of them in the same *in vitro* system is in important focus of drug metabolism studies.

The Madin Darby canine kidney cell line (MDCK) is one of the standard *in vitro* tools in drug metabolism studies. In this study, MDCK was chosen for a cell line to co-express UGTs (UGT1A1 or UGT2B7) and efflux transporters (MRP2 and MRP3 simultaneously. Therefore, cloning of the *UGT2B7* cDNA and the *ABCC3* cDNA encoding MRP3 was aimed in this study. On the other hand, the *UGT1A1* cDNA was already cloned in-house and MRP2 expressing MDCK cells were established earlier.

Cloning of the *UGT2B7* cDNA was not successful in this study despite of several different strategies such as PCR-amplification of the cDNA fragment using kidney or liver sscDNA as template. Cloning of the *ABCC3* cDNA encoding MRP3 was achieved and a mammalian expression vector containing this cDNA was constructed. In addition, the mammalian expression vector containing the *UGT1A1* cDNA was used to establish MDCK-UGT1A1 cells and this cell line was characterized regarding the expression of *UGT1A1* mRNA and UGT1A1 protein amount. Furthermore, establishment of MDCK-UGT1A1-MRP2 cell line was attempted in this study without success.

The mammalian expression vector containing the *ABCC3* cDNA encoding MRP3 could be used for future experiments to achieve novel cell lines such as MDCK-UGT1A1-MRP3 and MDCK-UGT1A1-MRP2-MRP3 for drug metabolism studies. In addition, the novel cell line MDCK-UGT1A1 could be used for drug metabolism studies in further experiments, but also as a cell line for further establishment of above cell lines. On the other hand, the cloning of the UGT2B7 cDNA needs optimization and several different strategies should be used to achieve the mammalian expression vector containing this cDNA.

Keywords
UGT1A1, UGT2B7, MRP2, MRP3, MDCK, interplay, glucuronidation, efflux transport

Where deposited
Division of Pharmaceutical Chemistry and Technology, Faculty of Pharmacy, University of Helsinki

Additional information
Supervisors: Professor Jörg König and Professor Martin F. Fromm

HELSINGIN YLIOPISTO
HELSINGFORS UNIVERSITET
UNIVERSITY OF HELSINKI

Tiedekunta	Osasto
Farmasian tiedekunta	Farmaseuttisen kemian ja teknologian osasto

Tekijä
Erkka Järvinen

Työn nimi
Solumallit konjugatiivisen lääkeainemetabolian ja efflux-kuljetuksen vuorovaikutuksen tutkimukseen: UGT1A1, UGT2B7 ja MRP3 -transfektoitujen MDCK-solulinjojen muodostus

Oppiaine
Farmaseuttinen kemia

Työn laji	Aika	Sivumäärä
Pro gradu	Marraskuu 2015	112 (+ 3 liitettä)

Tiivistelmä
UDP-glukuronosyylitransferaasit (UGT:t) katalysoivat glukuronidaatioreaktiota, jossa glukuronidihappo liittyy lääkeaineiden nukleofiilisiin ryhmiin kuten hydroksyyleihin, amiineihin tai karboksyylihappoihin. Glukuronidaatio on kaikkein tärkein metaboliareaktio konjugatiivisessa lääkeainemetaboliassa. Glukuronidikonjugaatit eivät pysty pääsääntöisesti läpäisemään solukalvoja passiivisesti, joten ne täytyy kuljettaa aktiivisesti ulos soluista. Efflux-transportterit vastaavat yhdisteiden aktiivisesta kuljetuksesta ulos soluista. Suurin osa efflux-transporttereista kuuluu adenosiinitrifosfaattia (ATP) sitovien efflux-transportterien perheeseen (ABC), joista etenkin C-alaperhe (ABCC) osallistuu glukuronidikonjugaattien kuljetukseen ulos soluista. MRP2 (*ABCC2*) ja MRP3 (*ABCC3*) ovat tärkeässä asemassa tässä kuljetuksessa. MRP2 on lokalisoitunut hepatosyyttien ja enterosyyttien apikaalimembraanille, kun taas MRP3 on lokalisoitunut vastaavien solujen basolateraalimembraanille. Lisäksi UGT1A1 ja UGT2B7 ekspressoituvat suuressa määrin maksassa ja ohutsuolessa, ja ovat täten kaikkein tärkeimpiä UGT-entsyymejä lääkeainemetaboliassa. Tiedetään, että UGT:t ja efflux-transportterit osallistuvat yhdessä lääkeaineiden eliminaatioon ja muodostavat täten yhteispelin. Tämän takia on tärkeää tutkia kumpaakin prosessia samassa *in vitro* mallissa.

Madin Darby koiran munuaissolulinja (MDCK) on yksi perustyökaluista lääkeainemetaboliatutkimuksissa. Tässä tutkimuksessa MDCK-solut valittiin solulinjaksi, jossa ekspressoidaan samanaikaisesti UGT:t (UGT1A1 tai UGT2B7) sekä MRP:t (MRP2 ja MRP3). Tätä varten tämän tutkimuksen tavoite oli kloonata *UGT2B7*:n ja *ABCC3*:n, joka koodaa MRP3:a, cDNA:t. Toisaalta, *UGT1A1*:n cDNA oli kloonattu ja MRP2:ta ekspressoivat MDCK-solut oli muodostettu jo aikaisemmin tässä laboratoriossa.

UGT2B7:n cDNA:n kloonaus ei onnistunut tässä tutkimuksessa, vaikka useita eri strategioita yritettiin, kuten cDNA fragmentin PCR-amplifikaatiota maksa- ja munuais-sscDNA:sta. Toisaalta, *ABCC3*:n cDNA, joka koodaa MRP3:a, saatiin kloonattua ja nisäkäsekspressiovektori, joka sisältää tämän cDNA:n, saatiin muodostettua. Lisäksi nisäkäsekspressiovektoria, joka sisältää *UGT1A1* cDNA:n, käytettiin muodostamaan MDCK-UGT1A1 solulinja, jonka UGT1A1 mRNA-ekspressio ja proteeniekspressio karakterisoitiin. Toisaalta, MDCK-UGT1A1-MRP2 solulinjaa ei saatu muodostettua yrityksistä huolimatta.

ABCC3:n cDNA:n, joka koodaa MRP3:a, sisältämää ekspressiovektoria voidaan käyttää tulevaisuudessa eri MDCK solulinjojen transfektointiin, jotta saataisiin muodostettua esimerkiksi MDCK-UGT1A1-MRP3 ja MDCK-UGT1A1-MRP2-MRP3 solulinjat lääkeainemetaboliatutkimusta varten. Lisäksi tässä tutkimuksessa muodostettua uutta MDCK-UGT1A1 solulinjaa voidaan käyttää tulevaisuudessa lääkeainemetaboliatutkimuksessa, mutta myös yllämainittujen solulinjojen muodostamiseen. Toisaalta, *UGT2B7*:n cDNA:n kloonaus vaatii lisää optimisaatiota.

Avainsanat
UGT1A1, UGT2B7, MRP2, MRP3, MDCK, glukuronidisaatio, yhteispeli, efflux-kuljetus

Säilytyspaikka
Farmaseuttisen kemian ja teknologian osasto, Farmasian tiedekunta, Helsingin yliopisto

Muita tietoja
Ohjaajat Professori Jörg König ja Professori Martin F. Fromm

TABLE OF CONTENTS

ABBREVIATIONS

ABC	Adenosine triphosphate binding cassette transporter superfamily
ADP	Adenosine diphosphate
APS	Ammonium peroxydisulphate
ATP	Adenosine triphosphate
BCRP	Breast cancer resistance protein
bp	Base pair
BSA	Bovine serum albumin
cDNA	Complementary deoxyribonucleic acid
CYP	Cytochrome P450
dATP	Deoxyadenosine triphosphate
dCTP	Deoxycytidine triphosphate
dGTP	Deoxyguanosine triphosphate
DMSO	Dimethyl sulfoxide
DNA	Deoxyribonucleic acid
DPBS	Dulbecco's phosphate buffered saline
DTT	Dithiothreitol
dTTP	Deoxythymidine triphosphate
EDTA	Ethylenediamine tetraacetic acid
ER	Endoplasmic reticulum
FBS	Fetal bovine serum
G418	Geneticin sulphate
kDa	kilo Dalton
MATE	Multidrug and toxin extrusion proteins
MDCK	Madin Darby canine kidney cell line II
MDR1	Multidrug resistance protein 1
MEM	(Eagles) Minimum essential medium
mRNA	Messenger ribonucleic acid
MRP	Multidrug resistance protein
NBD	Nucleotide binding domain

OAT	Organic anion transporters
OATP	Organic anion transporting polypeptides
OCT	Organic cation transporters
PBST	Phosphate buffered saline tween
PCR	Polymerase chain reaction
qPCR	Quantitative real-time polymerase chain reaction
RNA	Ribonucleic acid
RNAse	Ribonuclease
RT-PCR	Reverse transcription polymerase chain reaction
SDS	Sodium dodecyl sulfate
SLC	Solute carrier transporter superfamily
sscDNA	Single stranded complementary deoxyribonucleic acid
TAE	Tris-Acetate-EDTA
TEMED	N,N,N',N'-Tetramethylethylendiamin
TMD	Transmembrane domain
TRIS	Tris(hydroxymethyl)-aminomethane
UGT	UDP-glucuronosyltransferase
UDPGA	Uridine diphosphate glucuronic acid
UV	Ultraviolet light
X-β-Gal	5-bromo-4-chloro-3-indolyl-β-D-galactopyranoside

1. INTRODUCTION

Absorption and disposition (distribution, metabolism and excretion) affect pharmacokinetics and toxicity of drugs and thus they are in focus of drug development studies (Caldwell et al. 1995; Ruiz-Garcia et al. 2008). One important factor affecting absorption of an orally administered drug molecule is permeability (Amidon et al. 1995). In addition, permeability affects the metabolism and distribution of a drug molecule (Wu and Benet 2005). After entering the human body, drug molecules could undergo metabolism and are excreted as metabolites or as unchanged molecules (Caldwell et al. 1995). Generally, high permeable drugs are metabolized more extensively than low permeable drugs that are more prone to excretion without metabolism (Wu and Benet 2005). In addition, metabolism and permeability affects both the extent of absorption and the excretion route of drug molecules (Caldwell et al. 1995; Benet et al. 2011).

Drug metabolism is divided into two major classes, oxidative metabolism and conjugative metabolism (Di 2014). Cytochrome P450 enzymes (CYP) are mainly responsible for the oxidative metabolism whereas UDP-glucuronosyltransferases (UGT) are the main enzymes responsible for the conjugative metabolism. A drug molecule could be a substrate for a single enzyme of one class of enzymes or for multiple enzymes in one class of enzymes or for several enzyme classes. Oxidative metabolism does not substantially affect lipophilicity of drugs (Smith and Dalvie 2012). On the other hand, conjugated metabolites such as glucuronic conjugates are generally hydrophilic and thus low permeable. These drug metabolites are particularly prone to enterohepatic circulation, when excreted to bile, or to enteric recirculation, when excreted in intestinal lumen (Wakabayashi et al. 1994; Fagerholm 2008; Zhang et al. 2013). This is caused by deconjugation of a drug metabolite in the intestine and reabsorption of the parent drug. Enterohepatic circulation and enteric recirculation can substantially affect pharmacokinetics of a drug (Gregus and Klaassen 1987; Fagerholm 2008).

Highly permeable drugs and drug metabolites can enter and exit cells and human body by passive diffusion but low permeable drugs and drug metabolites need usually active transport by transporter proteins (Wu and Benet 2005). Especially conjugated drug metabolites are excreted out of the cells via efflux transporters leading to excretion into

feces or urine (Jeong et al. 2005; Shi and Li 2014). Drug transporters are classified as the uptake and efflux transporters (Giacomini et al. 2010; Hillgren et al. 2013). Uptake transporters transport compounds into cells and efflux transporters transport compounds out of the cells such as enterocytes and hepatocytes. The major classes of uptake transporters are organic anion transporting polypeptides (OATPs), organic anion transporters (OATs) and organic cation transporters (OCTs). On the other hand, the major class of efflux transporters is ABC transporters, which include among others multidrug resistance protein 1 (MDR1), breast cancer resistance protein (BCRP) and multidrug resistance proteins (MRPs). Especially MRP2 and MRP3 are known to be involved in transport of conjugative metabolites such as glucuronides (Zamek-Gliszczynski et al. 2006a; Zamek-Gliszczynski et al. 2014).

Methods for *in vivo* prediction of drug metabolism and excretion are not fully standardized and they lack correlation between *in vitro* and *in vivo* situation (Lavé et al. 2009; Pellegatti 2012; Di 2014). Before clinical studies, data of drug metabolism and excretion are acquired *in vivo* and *in vitro* animal studies and *in vitro* human studies. Because *in vivo* animal models are mostly used to predict human pharmacokinetics and toxicokinetics, more reliable human *in vitro* models are needed. Firstly, *in vivo* animal studies are expensive and possess ethical consideration compared to *in vitro* studies (Lavé et al. 2009; Pellegatti 2012). Secondly, preclinical animal studies do not result in comprehensive correlation between animal and human *in vivo* situations.

The aim of this study was to develop new cell models expressing human efflux transporters (MRPs) and conjugative drug metabolizing enzymes (UGTs) to study metabolism and excretion of drug molecules *in vitro*. Madin Darby canine kidney cell line (MDCK) was chosen to express human proteins, because this cell line is widely established for *in vitro* drug metabolism and transport studies (Fahrmayr et al. 2012; Fahrmayr et al. 2013; Brouwer et al. 2013). In addition, this cell line does not express proteins of human origin and forms *in vitro* a polarized monolayer, which allows vectorial transport studies of drug molecules and their metabolites.

2. LITERATURE REVIEW

2.1 Glucuronidation

Most of the drugs undergo biotransformation before they are excreted out of body (Williams et al. 2004; Di 2014). Ten years ago, approximately 75 % of top 200 prescribed drugs were metabolized before excretion. Cytochrome P450 enzymes (CYP) which catalyze oxidation reactions are the most important primary clearance way for drugs that are metabolized. However, conjugation reaction with glucuronic acid (glucuronidation) plays a key role in drug metabolism besides CYPs. Now, it is estimated that 35 % of current drugs are inactivated by glucuronidation (Guillemette et al. 2014). Drugs could undergo also sulfotransferase-catalyzed conjugation with sulfate, but this does not play a key role in drug metabolism compared to glucuronidation (Williams et al. 2004; Di 2014).

Glucuronidation could occur in molecules that contain hydroxyl-, carboxylic acid- or amine-groups (Rowland et al. 2013). The amine group could be located in either heterocycle ring or aliphatic chain. In rare cases, glucuronidation could occur in thiol groups or in acidic carbon. UDP-glucuronosyltransferases (UGT) catalyze the reaction between uridine diphosphate glucuronic acid (UDPGA) and a molecule undergoing glucuronidation. This glucuronidation reaction results in glucuronic acid metabolite of drugs, called glucuronides. Figure 1 presents a representative glucuronidation reaction of SN-38, the active metabolite of irinotecan in humans (Hanioka et al. 2001).

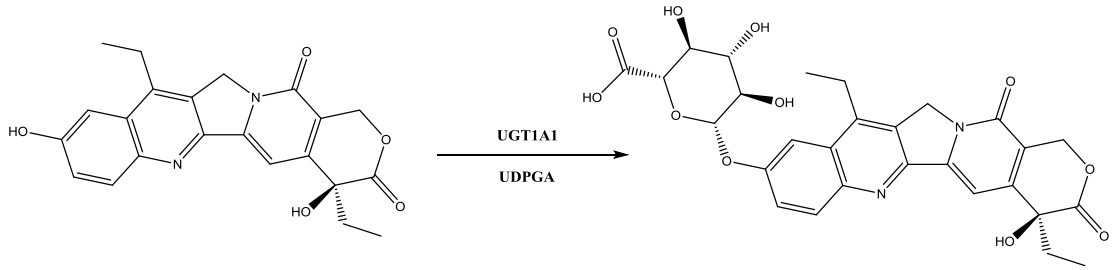

Figure 1. A representative scheme of glucuronidation reaction representing glucuronidation of SN-38 (active metabolite of irinotecan) resulting to SN-38-glucuronide. UGT1A1 = Uridine 5'-diphospho-glucuronosyltransferase 1A1 and UDPGA = uridine diphosphate glucuronic acid.

2.1.1 UDP-glucuronosyltransferases

UGTs are located in the endoplasmic reticulum (ER) of cells and they are structured in N- and C-terminal domains (Laakkonen and Finel 2010). In addition, they contain an envelope helix between the C-terminal domain and the transmembrane segment forming proteins of approximately 530 amino acids length. Interestingly, almost the entire protein localizes inside ER, which means that molecules undergoing glucuronidation and the source of glucuronic acid, UDPGA, need to permeate ER before glucuronidation. In addition, molecules have to first permeate inside cells before glucuronidation, which means that highly glucuronidated molecules have good permeation and thus are highly lipophilic (Wu and Benet 2005; Rowland et al. 2013).

There are 19 different isozymes, which catalyze glucuronidation reactions, in the superfamily of UGTs (Rowland et al. 2013). Based of sequence similarities, they are divided into subfamilies 1A, 2A and 2B. These subfamilies consist of UGT1A1, UGT1A3-10, UGT2A1-3, UGT2B4, UGT2B7, UGT2B10-11, UGT2B15, UGT2B17 and UGT2B28. However, UGT1A5, UGT2A1-3, UGT2B11 and UGT2B28 are thought not to be involved in drug metabolism (Guillemette et al. 2014; Stingl et al. 2014; Oda et al. 2015). In addition, expression of UGT1A7 protein is not detected in liver, small intestine or kidney and its mRNA expression is low in these tissues, so it seems that it does also not contribute to drug metabolism (Ohno and Nakajin 2009; Court et al. 2012; Sato et al. 2014). Interestingly, 10 % of Caucasian people carry UGT2B17 deletion and even 30 % have no or only little expressed protein, which might also affect its contribution to drug metabolism (Gallagher et al. 2007; Fallon et al. 2013).

All UGTs involved in drug metabolism are expressed in all three major drug metabolizing tissues; liver, intestine and kidney but with tissue specific expression pattern and highly variable expression levels between different isozymes (Ohno and Nakajin 2009; Court et al. 2012; Fallon et al. 2013; Sato et al. 2014;). Relative expression of UGTs involved in drug metabolism in liver, kidney and intestine tissues are presented in Table 1. The highest expressed UGT in liver is UGT2B7, expression of which is two times higher than that of UGT1A1. On the other hand, UGT1A1 is expressed approximately two times higher than UGT2B7 in intestine, although UGT2B17 possess superior expression in this

tissue. Only three UGTs are expressed in kidney; UGT1A9, UGT2B7 and UGT1A6. In addition, UGT1A10 is highly expressed in intestine but not in liver.

Table 1. Relative protein expression levels of UGTs involved in drugs metabolism in liver, intestine and kidney. In addition, expression of the UGTs in selected other tissues is presented. Relative expression levels in liver according to Harbourt et al. 2012, Ohtsuki et al. 2012, Fallon et al. 2013, Achour et al. 2014, Sato et al. 2014 and Oda et al. 2015. Relative expression levels in small intestine and kidney according to Sato et al. 2014. Expression of UGT1A8 in small intestine and expression of other UGTs in selected other tissues according to Ohno and Nakajin 2009 and Court et al. 2012. N.D. = not detected.

UGT	**Relative protein expression**			**Expression in selected other tissues**
	Liver	**Small Intestine**	**Kidney**	
UGT1A1	3	24	N.D.	-
UGT1A3	2	1	N.D.	-
UGT1A4	3	1	N.D.	-
UGT1A6	2	N.D.	1	Stomach, trachea, nasal and adrenal
UGT1A8	N.D.	low	N.D.	-
UGT1A9	2	N.D.	12	Adrenal
UGT1A10	N.D.	10	N.D.	Colon, nasal and trachea
UGT2B4	3	N.D.	N.D.	Hearth, prostate and testis
UGT2B7	6	10	7	Colon, pancreas and uterus
UGT2B10	1	N.D.	N.D.	-
UGT2B15	3	N.D.	N.D.	Breast, trachea, prostate and testis
UGT2B17	1	56	N.D.	Colon, breast, cervix, nasal and adipose

2.1.2 UDP-glucuronosyltransferases in detoxification of xenobiotics

General properties of substrates for UGTs are quite well understood, because these enzymes accept compounds containing free hydroxyl, amine or carboxylic acid groups. Even very small molecules like ethanol could be glucuronidated (Schwab and Skopp 2014). However, compounds that are glucuronidated normally have molecular weight of 100-600 Da representing well typical drug molecules (Obach et al. 2008; Stingl et al. 2014). Especially, small phenol containing compounds are good substrates for UGTs (Ethell et al. 2002). In many cases, the substrate specificity of individual UGTs is overlapping and it is not possible to predict substrate specificity of a single isozyme (Miners et al. 2004; Dong et al. 2012). Despite, there are some typical features of

compounds glucuronidated by some isozymes: UGT1A4 and UGT2B10 seem to be the only isoforms catalyzing efficient glucuronidation reactions of different amines (Kaivosaari et al. 2011). On the other hand, UGT1A6 glucuronidates rather small phenol containing molecules (Ethell et al. 2002; Dong et al. 2012).

Because UGTs accept small molecules with certain properties, substrates for them include a wide variety of molecules including endogenous compounds, drugs and other xenobiotics such as flavonoids and related plant derived molecules, industrial chemicals and carcinogenic compounds (Nowell et al. 1999; King et al. 2000; Wu et al. 2011; Guillemette et al. 2014; Gramec Skledar et al. 2014; Stingl et al. 2014). In addition, products of oxidative metabolism, that introduce hydroxyl group(s) in drug molecules, could be also substrates for UGTs (Anderson et al. 2009; Kamdem et al. 2010; Chen et al. 2012). However, glucuronidation of oxidative metabolites of drugs is only rarely well characterized on the level of individual UGTs.

Glucuronidation of endogenous compounds and xenobiotics is mostly considered as inactivation reaction that mediates subsequent excretion of compounds out of the human body (Rowland et al. 2013). However, there are examples of glucuronidation reactions, which actually activate compounds pharmacologically, toxicologically or as for perpetrators of drug interactions (Table 2).

For example, glucuronide conjugates could undergo oxidative metabolism and/or subsequently inhibit CYPs. Gemfibrozil glucuronide inhibits CYP2C8 (Delaforge et al. 2005; Baer et al. 2009). The same enzyme is also known to oxidize estradiol-17-glucuronide (Shitara et al. 2004). In some cases, UGTs might affect carcinogenic activation of compounds. Benzidine and its metabolites are conjugated to N-glucuronides that are excreted to urine (Zenser et al. 1998). However, it is speculated that glucuronidation actually promotes activation of procarcinogenic benzidine in bladder because N-glucuronides are acid label and are cleaved under the low pH of the urine. This will subsequently release benzidine for carcinogenic activation in bladder.

Acyl glucuronides, that are glucuronide conjugates of carboxylic acids, have been in high interest because they are chemically rather unstable (Sallustio et al. 2000). In some cases, it is shown that acyl glucuronides could act as nucleophiles and subsequently react covalently with proteins. This might cause toxic effects in tissues, especially in liver, and

be related to adverse drug effects. For example, it is shown that diclofenac-glucuronide forms protein adducts in livers of human and mouse (Aithal et al. 2004).

It is widely known that oxidative metabolism could lead in many cases to active drug metabolites (Obach 2013). On the other hand, it is rare that conjugative metabolism leads to pharmacologically active metabolite. However, a well-known example of a pharmacologically active glucuronide is presented in the case of morphine-6-glucuronide that was found considerably more potent than morphine itself (Paul et al. 1989).

Table 2. Selected examples of glucuronides that have pharmacological activity. [1]Delaforge et al. 2005, [2]Baer et al. 2009, [3]Zenser et al. 1998, [4]Aithal et al. 2004, [5]Paul et al. 1989.

Glucuronide	**Physiological consequence of glucuronidation**
Estradiol-17-glucuronide 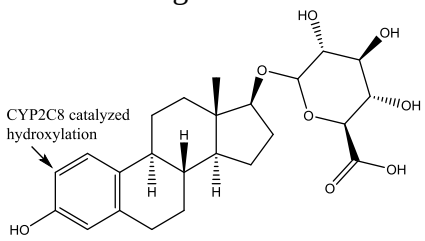	Substrate for CYP2C8 that catalyzes oxidation of estradiol-17-glucuronide to 2-hydroxy-estradiol-17-glucuronide.[1]
Gemfibrozil-glucuronide 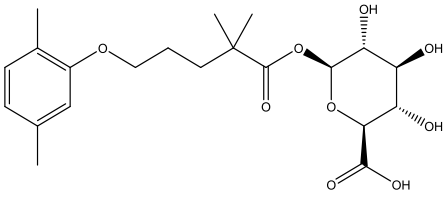	Irreversible inhibition of CYP2C8.[2]
Benzidine-glucuronide 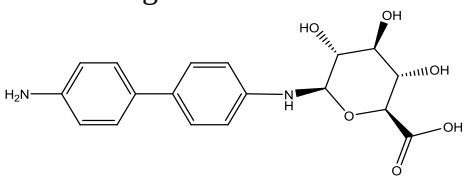	Deglucuronidation of benzidine-glucuronide in urine bladder and subsequent activation of benzidine by oxidative metabolism to carcinogenic compound.[3]
Diclofenac-glucuronide 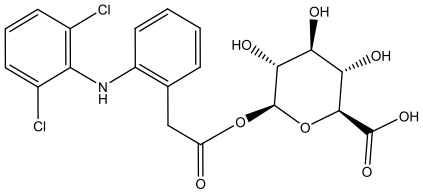	Chemically unstable glucuronide that forms protein adducts.[4]

Morphine-6-glucuronide

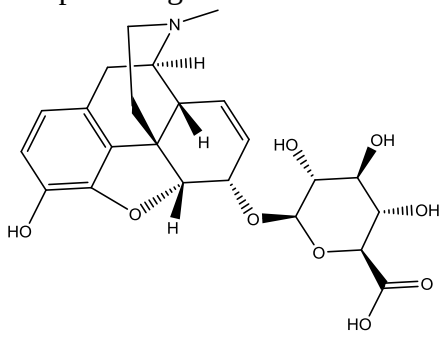

>100 fold analgesic potency compared to morphine.[5]

2.1.3 UDP-glucuronosyltransferases in metabolic clearance of drugs

Glucuronidation plays a key role in the detoxification of drugs, but also in deactivation of endogenous compounds. The most prominent function known for UGTs is detoxification of bilirubin, which is catalyzed by UGT1A1 (Bosma et al. 1994). Bilirubin is the endproduct of hemoglobin catabolism. It is extensively glucuronidated and subsequently excreted by efflux transporter MRP2 to bile and feces (Keppler 2014). In addition, glucuronidation is an important regulation mechanism for the homeostasis of active androgens and estrogens (Raftogianis et al. 2000; Bélanger et al. 2003; Gauthier-Landry et al. 2015). Nevertheless, conjugation reactions with glucuronic acid play a major role in drug metabolism and thus here are presented some examples (Table 3).

Paracetamol is extensively conjugated with glucuronic acid and subsequent paracetamol-glucuronide is excreted via urine (McGill and Jaeschke 2013). The main UGTs involved in paracetamol glucuronidation are UGT1A6 and UGT1A9, which are highly expressed in liver (Court et al. 2001). Especially UGT1A6 plays a key role in glucuronidation of paracetamol (Miners et al. 2011). A drug that is extensively conjugated in intestine and has a bioavailability only of few percent is raloxifene (Morello et al. 2003; Jeong et al. 2004; Sun et al. 2013). UGT1A10 and both UGT1A1 and UGT1A9 are mainly responsible for glucuronidation of raloxifene in intestine and liver, respectively. Entacapone is highly conjugated in human with glucuronic acid (Wikberg et al. 1993; Lautala et al. 2000). Conjugation takes place in liver and UGT1A9 is mainly responsible for it. UGT2B7 is responsible for high rate conjugation of zidovudine, morphine and codeine, which are excreted via urine almost completely as glucuronide conjugates (Hoskin and Hanks 1990; Vree et al. 1992; Veal and Back 1995; Court et al. 2003). On

the other hand, ezetimibe is almost solely excreted via feces and the glucuronide metabolite is majorly responsible for circulating metabolites (Kosoglou et al. 2005). UGT1A1 and UGT1A3 are responsible for the glucuronidation of ezetimibe in intestine and liver (Ghosal et al. 2004).

Table 3. Selected examples of drugs, which are metabolized primary via glucuronidation. Site of glucuronidation is indicated with slash-lined circle in the compound. In addition, primary UGTs responsible for the glucuronidation of the compound, primary tissue for the glucuronidation, excretion route of the glucuronide and amount of the glucuronidation of total metabolism is presented. [1]Court et al. 2001, [2]Miners et al. 2011, [3]McGill and Jaeschke 2013, [4]Jeong et al. 2004, [5]Sun et al. 2013, [6]Morello et al. 2003, [7]Lautala et al. 2000, [8]Wikberg et al. 1993, [9]Court et al. 2003, [10]Vree et al. 1992, [11]Hoskin and Hansk 1990, [12]Veal and Back 1995, [13]Ghosal et al. 2004, [14]Kosoglou et al. 2005.

Drug	**UGTs**	**Primary tissue for glucuronidation**	**Excretion route and amount of glucuronidation**
Paracetamol 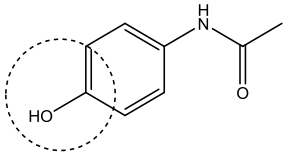	**1A6**, 1A9[1,2]	Liver[3]	Urine, 60 %[3]
Raloxifene 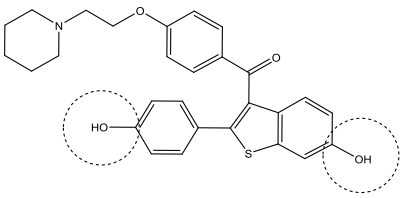	**1A10**, 1A1[4,5]	Intestine/liver[4,5]	Feces, 98 %[6]
Entacapone 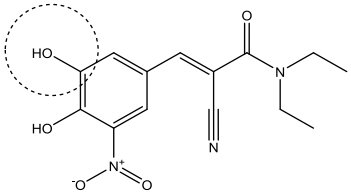	1A9[7]	Liver[7,8]	Feces, 95 %[8]
Codeine 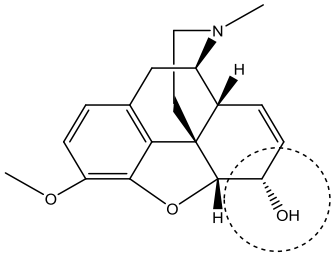	2B7, 2B4[9]	Liver[9,10]	Urine, 80 %[10]

Morphine 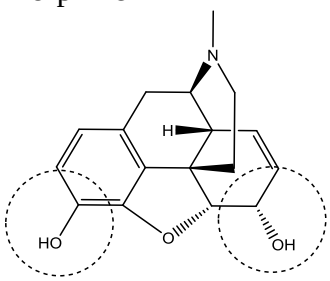	**2B7,** 2B4[9]	Liver[11]	Urine, 90%[11]
Zidovudine 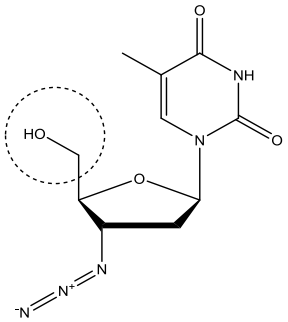	2B7[9]	Liver[12]	Urine, 70 %[12]
Ezetimibe 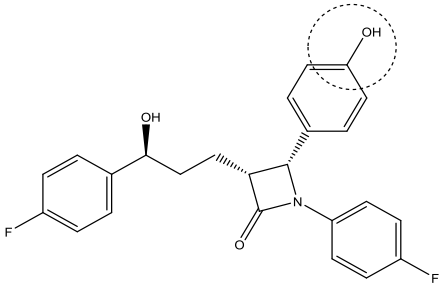	**1A1,** 1A3[13]	Intestine/ Liver[13, 14]	Feces, 90 %[14]

2.1.4 UDP-glucuronosyltransferases and their significance for drug metabolism

The selected examples in Table 3 show that glucuronidation is involved in metabolism of clinical highly significant drugs. Stingl and coworkers (2014) reviewed literature and searched for drugs that are directly or their metabolites are significantly eliminated via glucuronidation. This data was further analyzed by Guillemette and coworkers (2014). It was concluded that UGT2B7, UGT1A9, UGT1A3, UGT1A4 and UGT1A1 had 19 %, 14 %, 13 %, 11% and 11 % contribution, respectively, to glucuronidation of the all drugs presented by Stingl and coworkers (2014). When looking for the protein expression data of these enzymes in liver and intestine (Table 2), it is clear that UGT2B7 and UGT1A1 have the highest contribution for the glucuronidation of drugs. On the other hand, UGT1A3 and UGT1A4 are expressed also in both tissues but at lower level than UGT2B7 in liver or lower level than UGT2B7 and UGT1A1 in intestine. In addition, UGT1A9 is

highly expressed only in liver.

Considering the above and results in Table 3, it could be stated that UGT1A1 and UGT2B7 are highly significant in view of drug development. Actually, European Medicines Agency (EMA) and U.S. Food and Drug Administration (FDA) recommend to determinate clearance of new investigational drugs via UGTs and especially examine contribution of UGT1A1 and UGT2B7 (EMA 2012; FDA 2012).

2.2 Drug transporting proteins

Most of the known xenobiotic efflux transporters are part of the adenosine triphosphate (ATP) binding cassette (ABC) superfamily (Schinkel and Jonker 2003; Giacomini et al. 2010; König et al. 2013). There are 49 different proteins in seven subfamilies of ABC-superfamily (Vasiliou et al. 2009). The subfamilies ABCB, ABCC and ABCG include transporters that are known to be involved in drug disposition (Borst and Elferink 2002; Schinkel and Jonker 2003; Giacomini et al. 2010; König et al. 2013). The most important proteins in the superfamiliy of ABC-transporters for drug transport are multidrug resistance protein 1 (MDR1, P-glycoprotein/*ABCB1*), breast cancer resistance protein (BCRP/*ABCG2*) and multidrug resistance proteins 2-4 (MRP2-4 /*ABCC2-4*).

The second superfamily of drug transporters is the superfamily of solute carrier (SLC) transporters (Giacomini et al. 2010; Hediger et al. 2013; König et al. 2013). This superfamily of transporters includes 52 families and about 400 different transport proteins. The most important proteins of SLC transporters in drug disposition are organic anion transporting polypeptides (OATP/*SLC21*), organic anion transporters (OAT/*SLC22*), organic cation transporters (OCT/*SLC22*) and multidrug and toxin extrusion proteins (MATE/*SLC47A*) (Damme et al. 2011; Roth et al. 2012). OATPs, OCTs and OATs are mainly involved in uptake of drug molecules into enterocytes, hepatocytes and kidney cells. On the other hand, MATEs are efflux transporters expressed in liver and in kidney. SLC transporters do not contain nucleotide binding domains (NBD) and their mechanism of transport is mainly based on ion gradients over the cell membrane. For example, MATEs use an inward-directed proton gradient over the plasma membrane

to transport their substrates out of the cells (Damme et al. 2011).

Both uptake and efflux transporters play important roles in the absorption of orally administered drugs and elimination of drug molecules and their metabolites (Giacomini et al. 2010; Hillgren et al. 2013; König et al. 2013; Zamek-Gliszczynski 2014). The focus will be here only on the efflux transporters MRP2-4, BCRP and MDR1. These transporters are the best-characterized efflux transporters in the view of disposition of drug molecules and their metabolites. Especially, substrate specificity of MRP2-3 will be presented here in more detail because they are known to be involved in transport of conjugative drug metabolites (Zamek-Gliszczynski 2006a). However, bile salt efflux protein (BSEP), MATEs, MRP5 and MRP6 are likely also to be involved in disposition of drug molecules and their metabolites, but these proteins need still characterization and further research of their significance in disposition of drugs and their metabolites (Hillgren et al. 2013).

2.2.1 Structure and mechanism of ATP-binding cassette transporters

MDR1, BCRP and MRP2-4 are located in the plasma membrane of polarized cells such as enterocytes, hepatocytes and renal proximal tubule cells, where they can be localized either at the blood side (basolateral) or at the luminal side (apical) (Schinkel and Jonker 2003). These transporters actively transport compounds out of cell using energy released by hydrolysis of ATP. Because the transport process is active, ABC-transporters can transport against a concentration gradient.

ABC transporters involved in drug disposition are normally formed of two transmembrane domains (TMD), each consists of six transmembrane α-helical segments (Schinkel and Jonker 2003). In addition, these transporters also consist of two NBDs, which are located intracellularly and are responsible for the hydrolysis of ATP. NBDs are highly conserved because they are critical for energy-dependent transport and they form the signature protein sequence that is specific for ABC-transporters (Deeley et al. 2006). In addition, NBDs do not affect substrate specificity of a transporter. The substrate specificity is controlled by TMDs and especially by amino acids located near to, or in the

substrate binding site.

BCRP, MRP2 and MRP3 differ in the number of TMDs and NBDs compared to MDR1 and MRP4. BCRP is formed only by one NBD and one TMD and is so called a "half-transporter", it is 655 amino acids of size compared to other drug ABC transporters, which are 1300-1500 amino acids of size (Schinkel and Jonker 2003). On the other hand, MRP2 and MRP3 contain one additional aminoterminal transmembrane segment consisting of five transmembrane helices.

Transmembrane domains of ABC-transporters fold towards each other in cell membrane, forming a pore between them (Deeley et al. 2006; Sharom 2008; Rees et al. 2009). In addition, nucleotide binding domains fold towards each other and work co-operatively during the transport process. Simplified transport mechanism of ABC transporters involves binding of the compound to one or two sites of TMD, mainly from the cytoplasm but in some cases also through cell membrane. Binding of the substrate is followed by binding and hydrolysis of one or two ATPs. Hydrolysis of ATP to adenosine diphosphate (ADP) and free phosphate drives a conformation change of the protein and throws the molecule through the pore inside of the protein out of a cell. This is followed by release of ADP and recover of the original conformation of the transporter and readiness to transport a new molecule.

2.2.2 Multidrug resistance protein 1, breast cancer resistance protein and multidrug resistance proteins 2-4

MDR1, BCRP and MRP2-4 were all cloned from human cancer cell lines that showed resistance against multiple cancer drugs (Chen et al. 1986; Taniguchi et al. 1996; Kool et al. 1997; Doyle et al. 1998). In addition, rat Mrp2 was earlier cloned from rat strain the (TR^-) that has chronic conjugated hyperbilirubinemia and defective bile excretion of organic anions (Paulusma et al. 1996). Multidrug resistant cancer cell lines overexpress an efflux transporter or pattern of transporters, which causes multifold resistance to certain cancer drug molecules when compared to same cancer cell line without any overexpression. Expression of above transporters was found to cause *in vitro* resistance against multiple cancer agents such as doxorubicin, etoposide, vincristine and

methotrexate (Gottesman et al. 2002). Because of that, function of these transporters was mainly considered only from the perspective of the cause for multidrug resistance in the beginning, although MRP2 was known to be involved in excretion of organic anionic compounds. However, later their contribution to absorption and disposition of drug molecules and their metabolites were recognized (Suzuki and Sugiyama 2000).

Besides cancer tissues, MDR1, BCRP and MRP2-4 are expressed in important tissues in the view of drug metabolism, namely in intestine, liver and kidney (Figure 2). Enterocytes, hepatocytes and kidney proximal tubule epithelial cells are polarized cells, which form a barrier between two compartments. Transporters could be expressed in either side of membrane. Figure 2 presents localization of each of these transporters in liver, intestine and kidney tissue. In addition, MRP4 might be localized in the basolateral membrane of human enterocytes, because it is was shown to be localized in the basolateral membrane of human epithelial colorectal adenocarcinoma cells (Caco-2) (Ming and Thakker 2010). MRP3 was shown to be expressed also in the basolateral membranes of the distal convoluted tubules in kidney (Scheffer et al. 2002).

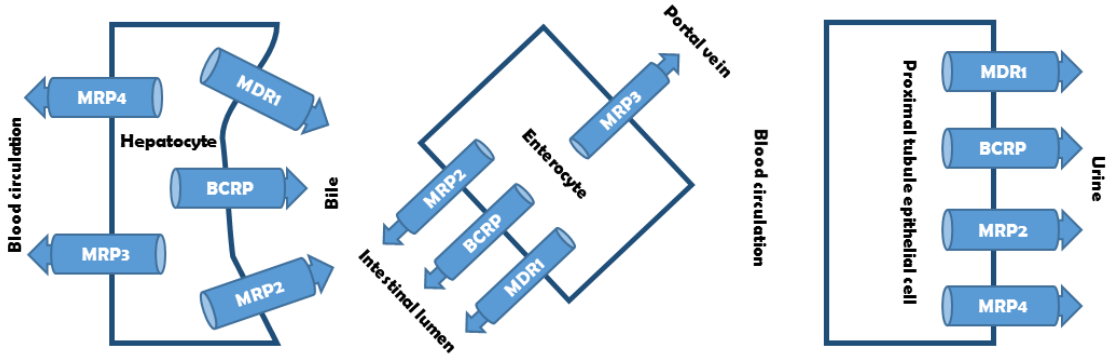

Figure 2. Localization of MDR1, BCRP and MRP2-4 in liver, intestine and kidney cells. Localization of MRP3 in enterocytes is based on human colon cells and rat small intestine (Rost et al. 2002; Scheffer et al. 2002). Localization of MRP2, BCRP, MDR1, and MRP3 in other tissues, is based on human samples (Thiebaut et al. 1987; Mayer al. 1995; Kartenbeck et al. 1996; König et al. 1999a; Fromm et al. 2000; Maliepaard et al. 2001; Scheffer et al. 2002; Van Aubel et al. 2002; Rius et al. 2003; Huls et al. 2008).

In addition to the different localization in plasma membranes, these proteins show also different expression patterns and protein levels in tissues (Table 4). MRP2 has the highest expression compared to other MRPs in liver but in small intestine its expression is almost equal to MRP3 (Drozdzik et al. 2014; Wang et al. 2015). Interestingly, in colon MRP3 is

highly expressed compared to MRP2 (Drozdzik et al. 2014). MDR1 and MRP4 show high expression in kidney, whereas MRP2 has moderate and MRP3 has minor expression in kidney (Hilgendorf et al. 2007). In addition to kidney, MRP4 is highly expressed in prostate where it localizes to the basolateral membrane (Rius et al. 2005). Thrombocytes also show high expression of MRP4 (Jedlitschky et al. 2004). It is notable that only MDR1, BCRP and MRP4 have significant expression in human brain microvessels that are present in the blood brain barrier (Shawahna et al. 2011; Uchida et al. 2011). Relative expression levels of MDR1, BCRP and MRP2-4 in kidney, small intestine and liver are presented in Table 4.

Table 4. Relative expression of MDR1, BCRP and MRP2-4 in liver, small intestine and kidney. Relative expressions are based on protein expression (liver and small intestine) or mRNA expression (kidney and MRP4 in small intestine). In addition, expressions in selected other tissues is presented. [1]Wang et al. 2015, [2]Ohtsuki et al. 2012, [3]Drozdzik et al. 2014 [4]Hilgendorf et al. 2007, [5]Shawahna et al. 2011, [6]Uchida et al. 2011, [7]Sugawara et al. 1998, [8]Maliepaard et al. 2001, [9]Kool et al. 1997, [10]König et al. 1999a, [11]Scheffer et al. 2002, [12]Lee et al. 1998, [13]Rius et al. 2005, [14]Jedlitschky et al. 2004

Transporter	**Relative expression**			**Other tissues**
	Liver	**Small Intestine**	**Kidney**	
MDR1	14[1, 2]	2[3]	High[4]	Human brain microvessels[5,6], colon[3], adrenal gland[7], placenta[7]
BCRP	4[1, 2]	1[3]	Low[4]	Human brain microvessels [5,6], colon[3,8], placenta[8]
MRP2	22[1, 2]	3[3]	High[4]	Colon[3]
MRP3	11[1, 2]	2[3]	Low[4]	Colon[3,9,10,11], pancreas[10,11] adrenal gland[10,11]
MRP4	1[2]	Low[3, 4]	High[4]	Human brain microvessels [5,6] Colon[3], prostate[12,13] thrombocytes[14]

2.2.3 *In vitro* substrate specificity of multidrug resistance protein 1, breast cancer resistance protein and multidrug resistance proteins 2-4

MDR1, BCRP and MRP2-4 show quite distinctive substrate specificities even sometimes overlapping. MDR1 is mainly involved in transport of lipophilic drug molecules that

contain a cationic charge or no charge (Oude Elferink et al. 1995; Seelig 1998; Ambudkar et al. 1999; Stouch and Gudmundsson 2002; Ambudkar et al. 2003; Fromm 2004; Hoffmann and Kroemer 2004). However, there are some reports that MDR1 might transport also anionic drugs including olmesartan and fexofenadine and glucuronide conjugates of estradiol and telmisartan (Huang et al. 1998; Cvetkovic et al. 1999; Yamada et al. 2007; Ishiguro et al. 2008). MRP2-4 were reported to be mainly transporters of anionic drugs, and especially anionic drug conjugates such as glucuronides, sulfates and glutathiones (König et al. 1999b; Zamek-Gliszczynski 2006a; Borst et al. 2007; van der Schoor et al. 2015). On the other hand, substrate specificity of BCRP seems to be mixed between substrate specificity of MRPs and MDR1 (Ni et al. 2010; Szafraniec et al. 2014; Mao and Unadkat 2015). BCRP has an overlapping substrate specificity with MDR1 by transporting neutral, cationic, lipophilic and aromatic rings containing drug molecules. In addition, BCRP is able to transport anionic molecules and even sulfate and glucuronide conjugates (Zamek-Gliszczynski 2006a; van de Wetering et al. 2009a; Han et al. 2010; Mao and Unadkat 2015). Actually, BCRP prefers sulfate conjugates over glucuronide conjugates and it is recognized as a transporter of sulfate conjugates (Suzuki et al. 2003; Mizuno et al. 2007; Mao and Unadkat 2015; Mutsaers et al. 2015). Because BCRP, and especially MDR1, are not mainly considered as transporters for glucuronide conjugates, they are no further discussed here.

2.2.4 Considerations in substrate specificity determination for multidrug resistance proteins *in vitro*

In vitro assays for the identification of substrates for efflux transporters could be classified in direct and indirect assays. Direct assays use inside-out oriented membrane vesicles prepared from cell lines and tissues overexpressing a transporter of interest (Glavinas et al. 2008; Brouwer et al. 2013). In addition, cell lines overexpressing a transporter of interest could be used for direct transport assays, if the permeability of a compound is high enough (Brouwer et al. 2013). On the other hand, determination of cytotoxicity produces indirect evidence of substrates for transporters (Xia et al. 2007). For cytotoxicity determinations, a compound is incubated in transporter-transfected and non-transfected cell lines and cytotoxicity is compared between these two cell lines. In addition, indirect

measurement of transport are also inhibition studies in which a compound is tested to modulate transport of a probe substrate by the transporter of interest in inside-out oriented membrane vesicles or in cell lines (Brouwer et al. 2013).

Different assay techniques could yield discrepancies in characterization of the substrate specificity of the transporter. For example, cytotoxicity assays do not reveal which transporter causes the resistance, because cell lines could overexpress multiple different transporters (Kool et al. 1997). In addition, if transport of a radiolabeled compound is studied in a cell line overexpressing a single transporter and only total radioactivity is measured, it is impossible to draw conclusions if the compound or its metabolites are actually transported. Most of the pioneer work in the area of MRPs was done by utilizing cytotoxicity assays or using radiolabeled compounds in whole cell based assays without proper analytical tools. Especially, most of the neutral lipophilic cancer agents considered as substrates for MRPs were investigated in these assays. For example, MRP1 was shown to cause resistance against doxorubicin and vincristine, but vesicle transport assays with the same compounds did not show active transport by MRP1 (Grant 1994; Jedlitschky et al. 1996; Loe et al. 1996). Interestingly, Priebe and coworkers (1998) found that glutathione conjugates of doxorubicin and daunorubicin inhibiting transport of leukotriene C_4 by MRP1, which might indicate that they are the actual substrates, but not the parent compounds. In addition, glutathione itself was also identified as a substrate for MRP2 but not for MRP3 in whole cell based assays (Kool et al. 1999; Paulusma et al. 1999; Evers et al. 2000; Wortelboer et al. 2003). However, this could not be shown in vesicle studies (Paulusma et al. 1999).

In addition, it is shown that cell lines used for overexpression of efflux transporters (*e.g.* HeLa, MDCK, LLC-PK1, CHO-K1, COS-7) have also capability for the metabolic reactions (Hao et al. 1994; Evers et al. 1998; Ryu et al. 2000; Ji et al. 2002; Ng et al. 2003; Imai et al. 2003; Wortelboer et al. 2003; Zamek-Gliszczynski et al. 2006b; Lo et al. 2007). These reactions include sulfation, glucuronidation and glutathione transferase activity. Because all above disruptive factors, only inside-out oriented membrane vesicle assays or cell line assays with modern analytical techniques such as liquid chromatography should be considered as the gold standard for *in vitro* transporter substrate specificity determination.

2.2.5 Substrates of multidrug resistance proteins 2-3

Table 5 presents substrates and their kinetic constants, if available, for MRP2 and MRP3 based on literature review. Substrates are further classified in glutathione conjugates, glucuronide conjugates, sulfate conjugates, and sulfite or phosphonate or carboxyl containing substrates and neutral compounds. Substrate specificity of MRP2 and MRP3 is quite highly overlapping. In addition, glucuronide conjugates and carboxylic acid containing compounds seem to be the major classes of substrates for both transporters. Sulfate, sulfite and phosphonate containing compounds are also anionic and partly transporterted by MRP2 and MRP3. On the other hand, neutral molecules are not readily transporterted by MRP2 or MRP3. Affinity (K_m-value) varies also quite much between substrates, being over 10 000 fold different between the highest affinity and the lowest affinity compounds. However, if the affinity of the compound for both transporters is available, differences between them are not high. Selected examples of structures of MRP2 and MRP3 substrates are presented in Figure 3.

Table 5. Substrates for MRP2 and MRP3 and their K_m-values if available. + = is a substrate, - = is not a substrate, N.A. = not available. [1]Smitherman et al. 2004, [2]Wortelboer et al. 2003, [3]Evers et al. 1998, [4]Zeng et al. 2000, [5]Cui et al. 1999, [6]Bakos et al. 2000, [7]Paumi et al. 2003, [8]Ji et al. 2002, [9]Kamisako et al. 1999, [10]Lee et al. 2004, [11]Krumpochova et al. 2012, [12]van de Wetering et al. 2009b, [13]Gerk et al. 2007, [14]Chu et al. 2004, [15]Zelcer et al. 2001, [16]Hirouchi et al. 2009, [17]Chu et al. 2009, [18]Zelcer et al. 2006, [19]Leslie et al. 2001, [20]van de Wetering et al. 2007, [21]Patel et al. 2013, [22]Matsunaga et al. 2014, [23]van de Wetering et al. 2009a, [24]Vasilyeva et al. 2015, [25]Ishiguro et al. 2008, [26]Wittgen et al. 2012, [27]Zelcer et al. 2003 [28]Kopplow et al. 2005, [29]Han et al. 2010, [30]Akita et al. 2002, [31]Letschert et al. 2005, [32]Oleschuk et al. 2003, [33]Imaoka et al. 2007, [34]Ray et al. 2006, [35]Cui et al. 2001, [36]Pratt et al. 2006, [37]Seelheim et al. 2013, [38]de Waart et al. 2012, [39]Ferslew et al. 2014, [40]Matsushima et al. 2008, [41]Zeng et al. 2001, [42]Yamada et al. 2007, [43]Leier et al. 2000, [44]de Waart et al. 2006, [45]Evers et al. 2000, [46]van Aubel et al. 2005, [47]Baltes et al. 2007, [48]Minematsu et al. 2008, [49]Li et al. 2008a, [50]Marchetti et al. 2008, [51]Huisman et al. 2002, [52]Tong et al. 2014, [53]Yu et al. 2013, [54]Takusagawa et al. 2013, [55]Chu et al. 2007

SUBSTRATE	**MRP2**	**MRP3**
Glutathione conjugates		
Chlorambucil	10 µM[1]	N.A.
Curcumin	+[2]	N.A.
Dinitrophenyl	7 µM[3]	6 µM[4]
Ethacrynic acid	+[3]	N.A.
Leukotriene C_4	1 µM[5]	5 µM[4]
N-ethylmaleimide	+[6]	N.A.
Prostaglandin J_2	N.A.	3 µM[7]
4-hydroxynonenal	+[8]	N.A.
Glucuronide conjugates	**MRP2**	**MRP3**
Bilirubin (mono- and bis-glucuronides)	1 µM[9]	+[10]

Enterodiol	+[11]	5 µM[12]
Enterolactone	+[11]	2 µM[12]
Equol	N.A.	6 µM[12]
Estradiol (3-glucuronide)	130 µM[13]	N.A.
Estradiol (17-glucuronide)	7 µM[5]	26 µM[4]
Ethinylestradiol (3-glucuronide)	25 µM[14]	9 µM[14]
Etoposide	N.A.	11 µM[15]
E3040 (6-hydroxy-5,7-dimethyl-2-methylamino-4-(3-pyridymethyl)benzothiazole)	+[16]	+[16]
Gaboxadol	-[17]	N.A.
Gemfibrozil	+[16]	+[16]
Genistein	N.A.	8 µM[12]
Glycitein	N.A.	14 µM[12]
Hyocholate	N.A.	40 nM[18]
Hyodeoxycholate	N.A.	700 nM[18]
(methylnitrosamino)-1-(3-pyridyl)-1-butanol	+[19]	N.A.
Morphine	50 µM[20]	+[20]
Mycophenolic acid (acyl glucuronide)	-[21]	N.A.
Mycophenolic acid (phenol glucuronide)	300 µM[22]	270 µM[22]
Resveratrol	22 µM[23]	14 µM[23]
Secoisolariciresinol	+[11]	6 µM[12]
Sorafenib	24 µM[24]	190 µM[24]
Telmisartan	+[25]	N.A.
Troglitazone	+[16]	+[16]
7-hydroxycoumarin	-[26]	190 µM[26]
Sulfate conjugates	**MRP2**	**MRP3**
Dehydroepiandrosterone	-[27]	46 µM[10]
Estrone (3-sulfate)	+[28]	N.A.
Ethinylestradiol (3-sulfate)	-[29]	-[29]
Taurolithocholate (3-sulfate)	N.A.	+[30]
Enterodiol-glucuronide	0.75 µM[11]	N.A.
Enterolactone-glucuronide	0.6 µM[11]	N.A.
Cholecyctokinin octapeptide (CCK-8)	8 µM[31]	N.A.
Sulfite containing compounds	**MRP2**	**MRP3**
Taurocholate	-[13]	+[32]
Tauroursodeoxycholate	+[13]	N.A.
Phosphonate containing compounds	**MRP2**	**MRP3**
Adefovir	-[33]	N.A.
Cidofovir	-[33]	N.A.
Tenofovir	-[34]	N.A.
Carboxyl containing compounds	**MRP2**	**MRP3**
Bromosulfophthalein	12 µM[35]	N.A.
Carboxydichlorofluorescein	20 µM[36]	11 µM[37]
Cefadroxil	+[38]	2.5 mM[38]
Enalaprilat	N.A.	-[39]
Fexofenadine	+[40]	N.A.
Folic acid	N.A.	2 mM[41]
Glycocholate	N.A.	250 µM[4]
Leucovorin	N.A.	1.7 mM[41]

Methotrexate	3 mM[6]	620 µM[41]
Mycophenolic acid	-[21]	N.A.
Olmesartan	15 µM[42]	N.A.
Para-aminohippurate	900 µM[43]	N.A.
Prostaglandin E_2	+[44]	-[44]
Sulfinpyrazone (acidic carbon)	+[45]	N.A.
Uric acid	-[46]	N.A.
Valproic acid	-[47]	N.A.
Zonampanel	-[48]	N.A.
Neutral compounds	**MRP2**	**MRP3**
Belotecan	+[49]	N.A.
Enalapril	N.A.	-[38]
Erlotinib	-[50]	N.A.
Gaboxadol	-[16]	N.A.
Indinavir	+[51]	-[51]
Lenalidomide	-[52]	-[52]
Liensinine	-[53]	N.A.
Mirabegron	-[54]	N.A.
Ritonavir	+[51]	-[51]
Saquinavir	+[51]	-[51]
Sitagpliptin	-[55]	N.A.
Topotecan	+[49]	N.A.

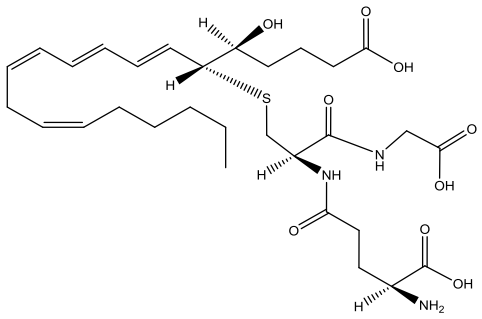

Leukotriene C4

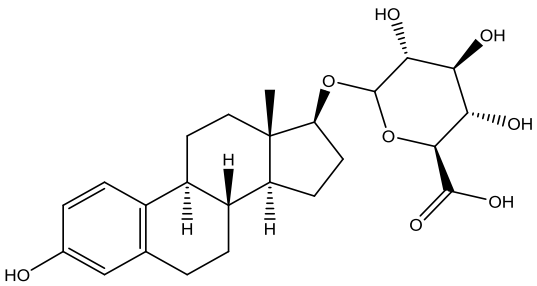

Estradiol-17-glucuronide

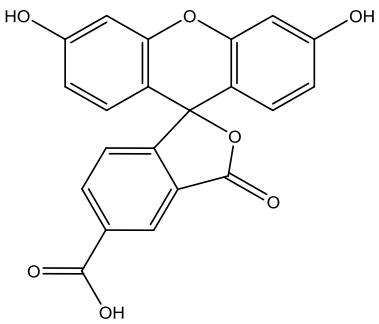

Carboxydichlorofluorescein

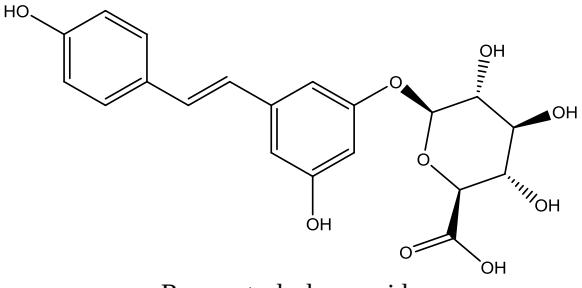

Resveratrol-glucuronide

Figure 3. Selected examples of structures of substrates for MRP2 and MRP3.

2.3 Integrating glucuronidation and drug efflux tranporters

Drug molecules that undergo extensive metabolism have good permeability and passive diffusion plays a key role in the permeation of these compounds into cells (Wu and Benet 2005; Benet et al. 2011). Substrates for UGTs are generally lipophilic and thus have sufficient properties for good cell membrane permeability (Lin and Wong 2002; Smith et al. 2003; Rowland et al. 2013). On the other hand, conjugation of drug molecules with glucuronic acid leads generally to more hydrophilic compounds that are any more able to cross cell membranes by passive diffusion (Jeong et al. 2005; Zamek-Gliszczynski et al. 2006a; Smith and Dalvie 2012; Shi and Li 2014).

Glucuronidation takes place in the main drug metabolizing tissues including intestine, liver and kidney (Jeong et al. 2005; Rowland et al. 2013; Di 2014). During absorption of orally administered drug, it could go through first pass biotransformation in intestine and liver (Caldwell et al. 1995). Subsequent distribution phase will expose drug molecules for biotransformation in all three main tissues that metabolize drugs, namely in liver, intestine and kidney.

Because glucuronides, and other conjugates, are hydrophilic and could not cross cell membrane by passive diffusion, they are actively transported out of cells by efflux transporters (Jeong et al. 2005; Zamek-Gliszczynski et al. 2006a; Smith and Dalvie 2012; Shi and Li 2014). As is presented in section 2.2.5, glucuronides are good substrates for MRP2 and MRP3. Conjugation and subsequent excretion of glucuronides from tissues are together regarded as interplay of conjugation and efflux transport (Shi and Li 2014).

Generally, disposition of lipophilic drugs is dependent on metabolism and especially conjugation because they have high reabsorption from renal tubule, bile ducts and intestine and thus could not be easily eliminated from the body directly (Fagerholm 2007; Fagerholm 2008, Varma et al. 2009 and Varma et al. 2012). On the other hand, glucuronidation and subsequent efflux transport mediate excretion of drugs from human body via bile to feces or via blood circulation to urine (Jeong et al. 2005). However, questions remain to answer in this interplay (Jeong et al. 2005; Shi and Li 2014; Zamek-Gliszczynski et al. 2014):

1. When will a glucuronide conjugate of a drug eliminated via urine or feces?
2. Is efflux transport the limiting step of elimination of glucuronide conjugates and could it affect bioavailability or toxicity of drugs, or cause drug-drug interactions?

2.3.1 Disposition of glucuronides

MRP2 is highly expressed in liver and small intestine, and to lesser extent in kidney (see section 2.2.2). It excretes glucuronides to bile and subsequently to intestinal lumen. In intestine, it transports glucuronides into intestinal lumen. In addition, it contributes to the excretion of locally formed glucuronides and to vectorial transport and subsequent active secretion of glucuronides in kidney. MRP4 has tissue specific localization; it is localized in apical membrane of kidney contrary to liver where it is localized in basolateral membrane (see section 2.2.2). In addition, it has an expression equal or even higher than MRP2 in kidney (Nishimura and Naito 2005; Hilgendorf et al. 2007). Therefore, it contributes, as MRP2, to active secretion and vectorial transport of glucuronides in kidney.

Excretion of glucuronides via bile could lead to enterohepatic circulation, which will lead to prolonged residence time of drug molecule in the human body (Gregus and Klaassen 1987; Fagerholm 2008). Enterohepatic circulation means deconjugation of glucuronides, excreted to intestine via bile, by intestinal β-glucuronidases and subsequent reabsorption of the parent drug molecule. MRP2 might be solely responsible for the biliary excretion of glucuronides even BCRP and MDR1 have comparable expression levels and localization in liver (see seaction 2.2.2). Beside liver, MRP2 might affect local enteroenteric circulation in intestine (Jeong et al. 2004). This means that glucuronides formed in intestine are excreted to intestinal lumen, deconjugated and subsequently reabsorbed (Wakabayashi et al. 1994; Jeong et al. 2005; Xia et al. 2012; Zhang et al. 2013).

MRP3 is localized in basolateral membranes of liver, intestine and kidney. In addition, MRP4 is localized in basolateral membrane of liver and probably in basolateral membrane of human intestine (see section 2.2.2). However, expression of MRP4 in

normal liver is much lower than the expression of MRP3 or MRP2 (Ohtsuki et al. 2012). In addition, in small intestine MRP4 is expressed less than MRP3, which is expressed at similar level to MRP2 (Hilgendorf et al. 2007). Based on expression levels, it is unknown if MRP4 contributes to the transport of glucuronides in liver and/or intestine. On the other hand, MRP3 has a high expression level in these tissues and contributes to the efflux of glucuronides. However, MRP3 has low expression in kidney and its contribution to reabsorption and excretion of glucuronides to blood circulation in kidney is unknown.

Processes of interplay between glucuronidation and efflux transporters in liver and small intestine are summarized in Figure 4.

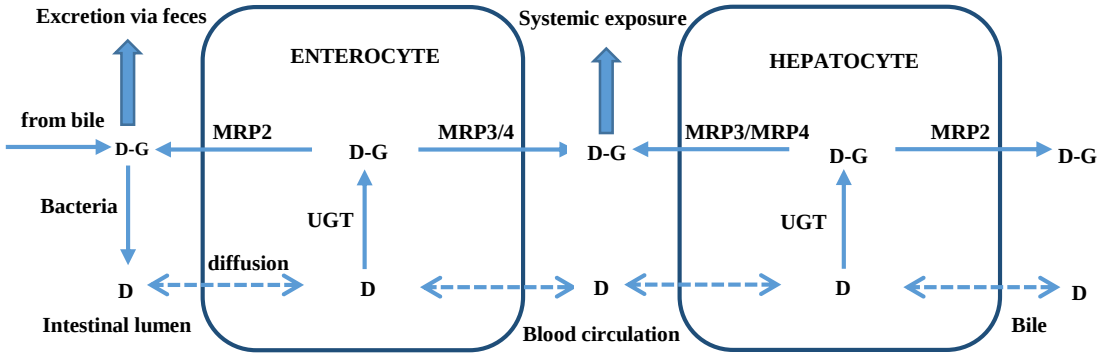

Figure 4. Scheme of interplay between glucuronidation and efflux transport in small intestine and liver. D = drug and D-G = glucuronide conjugate of drug.

2.3.2 Studying of the interplay between glucuronidation and efflux transport

Lack of specific MRP2-4 inhibitors and difficult bile sampling from humans causes difficulties in studies of the interplay between glucuronidation and efflux transport *in vivo* in humans (Gregus and Klaassen 1987; Ghibellini et al. 2006; Brouwer et al. 2013; Hillgren et al. 2013). Samples of feces and urine are available for biotransformation studies in man, but feces samples represent unabsorbed and unconjugated drug or metabolites but not actual metabolites excreted via bile and/or enterocytes. In addition, tissue sampling (*e.g.* kidney and liver) in humans is not routinely possible. Because of these limitations, *in vivo* animal studies and especially several different transporter-knockout mice models are widely used for studying the interplay between glucuronidation and efflux transport *in vivo* (Xia et al. 2007; Zamek-Gliszczynski et al. 2013; Zamek-Gliszczynski et al. 2014).

There are also several cell lines that express transporters of human origin and thus allow studying of efflux and uptake in same cell-based system in *in vitro* (Xia et al. 2007; Brouwer et al. 2013). However, there are only few cell lines reported that co-overexpress both metabolizing enzymes and efflux transporters (Fahrmayr et al. 2012; Kwatra et al. 2012; Neve et al. 2013 Quan et al. 2015). In addition, intestinal and hepatic cell lines (such as Caco-2 and hepatocytes) express several metabolizing enzymes, uptake and efflux transporters and thus cannot be used for detailed studies, because there are no specific inhibitors of transporters or metabolizing enzymes (Xia et al. 2007; Brouwer et al. 2013; Hillgren et al. 2013).

Several rat strains lack functional Mrp2 and thus they could be used as models to study the *in vivo* significance of the transporter (Oude Elferink et al. 1995). These rat strains are GY/TR$^-$ and Eisai hyperbilirubinemic mutant rats (EHBR). *In vivo* studies with these rat strains have proved the most important *in vivo* function of Mrp2; biliary excretion of conjugated bilirubin, which is almost absent in these strains and leads to highly elevated plasma levels of bilirubin glucuronides. However, later more defined animal models have become available, namely knockout mice (Xia et al. 2007). The advantage of these models is that they are well defined by silencing specifically a gene and allow combining different knockout strains. Knockout mice of Mrp2-4 are available including different combined strains such as Mrp2$^{-/-}$/Mrp3$^{-/-}$ and Mrp3$^{-/-}$/Mrp4$^{-/-}$ (Leggas et al. 2004; Belinsky et al. 2005; Chu et al. 2006; van de Wetering et al. 2007).

Because of species differences, the animal models might not be fully representative for the human situation. Two main reasons contribute to discrepancies: differences in substrate specificity of transporters and differences in protein expression of transporters between species. There are comparative *in vitro* studies between human and animal transporters such as MRP2 and Mrp2 (Ishizuka et al. 1999; Akita et al. 2002; Li et al. 2008b; Yasunaga et al. 2008; Herédi-Szabó 2009). However, these studies suggest that there are no substantially differences in substrate specificities of the same transporters between species. On the other hand, protein amounts of transporters in different species seem to explain more of variability between species (Ninomiya et al. 2005; Li et al. 2009). For example, Mrp2 is highly expressed in livers of rats and mice but less in humans, dogs and monkeys (Ninomiya et al. 2005; Kamiie et al. 2008; Li et al. 2009; Wang et al. 2015). On the other hand, Mrp3 was hardly detectable in livers of rats, but was expressed quite

comparable to human MRP3 in livers of monkey and dogs (Wang et al. 2015). However, Mrp3 is highly expressed in mice (Kamiie et al. 2008). In addition to transporters, it is important to know that there are interspecies differences in drug metabolizing enzymes such as UGTs (Komura and Iwaki 2011).

There are also reports that dog and rats have lower molecular weight threshold for anionic compounds that are excreted to bile compared to humans (Yang et al. 2009; Yang et al. 2010). This cut-off value was 400 Da for dogs and rats and 475 Da for humans. Therefore, prediction of biliary excretion of drugs in humans based on animal studies is not straightforward and does not give reliable results (Mahmood 2005; Ghibellini et al. 2006; Fagerholm 2008). Nevertheless, knockout animal studies represent good models for mechanistic understanding of interplay between glucuronidation and efflux transporters even if translating their data to human is challenging (Zamek-Gliszczynski et al. 2013). For this purpose, some examples are presented in the next sections.

2.3.3 *In vivo* contribution of multidrug resistance protein 2-4 to disposition of glucuronides in liver

Paracetamol is extensively conjugated with glucuronic acid and subsequently excreted via urine in human and mouse (Zamek-Gliszczynski et al. 2006c; McGill and Jaeschke 2013). Knockout of Mrp2 in mice led to no changes of biliary clearance of paracetamol glucuronide (Zamek-Gliszczynski et al. 2006c). Interestingly, basolateral clearance of paracetamol glucuronide was three times higher in $Mrp2^{-/-}$ mice. On the other hand, it is known that protein levels of basolateral efflux transporters Mrp4 and Mrp3 are elevated in $Mrp2^{-/-}$-mice seven and one and half times, respectively (Chu et al. 2006; Nezasa et al. 2006). This might affect the interpretation of the results, when Mrp2 is absent. However, knockout of Mrp3 in mice led to a substantial change of the basolateral excretion and intracellular concentration of paracetamol glucuronide (Manautou et al. 2005). 20 times more of paracetamol glucuronide accumulated in livers of $Mrp3^{-/-}$ mice compared to control mice. At the same time, plasma excretion of paracetamol glucuronide was decreased 10 times and cumulative biliary excretion increased 10 times. Zamek-Gliszczynski and coworkers (2006c) also found that $Mrp3^{-/-}$ mice accumulated six times

more paracetamol glucuronide in liver and had 25 times lower basolateral clearance of it compared to control mice. In addition, biliary clearance was not changed but cumulative excretion of paracetamol glucuronide in bile was 10 times higher. Mrp4$^{-/-}$ mice was also used in the same study, but pharmacokinetics of paracetamol glucuronide stayed similar compared to wild type mice.

Morphine is rapidly metabolized to two glucuronides (M3G and M6G) in humans (Hoskin and Hansk 1990). On the other hand, mice are able only to form M3G (Zelcer et al. 2005). Mrp3$^{-/-}$ mice had almost abolished urinary excretion of M3G and very low plasma concentrations of it compared to wild type mice. In addition, hepatic concentrations of M3G were over five times higher and biliary excretion was the main route of M3G compared to wild type mice. In summary, knockout of Mrp3 changed the predominant excretory route from urine to bile and subsequently to feces compared to wild type mice and this was caused mainly by impaired basolateral excretion of morphine-glucuronide from liver. van de Wetering and coworkers (2007) further characterized pharmacokinetics of M3G in Mrp2$^{-/-}$ and Mrp2$^{-/-}$/Mrp3$^{-/-}$ double knockout mice and found that both mouse strains lacked almost fully biliary excretion of M3G, which was around 30 % in Mrp3$^{-/-}$ and wild type mice. In addition, Mrp2$^{-/-}$ mice had higher plasma concentrations of M3G compared to wild type mice. Mrp3$^{-/-}$/Mrp4$^{-/-}$ mice was also compared to Mrp3$^{-/-}$ mice, but there was no difference in plasma concentration of M3G between these two strains indicating that Mrp4 does not play role in basolateral efflux of morphine glucuronide.

Etoposide is partly metabolized via glucuronidation in human (D'Incaici et al. 1986). Mrp2$^{-/-}$ mice excrete 20 % of administered etoposide to urine compared to less than 5 % excreted by wild type mice (Lagas et al. 2010a). In addition, plasma concentration of etoposide glucuronide was two times higher when Mrp2 was absent and the intrahepatic concentration was slightly decreased. Interestingly, absence of Mrp3 did not change plasma or intrahepatic levels of etoposide glucuronide but Mrp2$^{-/-}$/Mrp3$^{-/-}$ mice had substantially higher intrahepatic concentrations but no change in plasma concentrations of etoposide glucuronide. Based on these results, it seems that in some cases Mrp2 and Mrp3 could compensate each other when one is absent, but when both are absent the glucuronide will accumulate inside the tissue where it is formed. In addition, upregulation of Mrp3 in Mrp2$^{-/-}$ mice might complicate interpretation of results.

Sorafenib is partly metabolized via glucuronidation (Zimmerman et al. 2012). Pharmacokinetics of sorafenib-glucuronide was studied in Mrp2$^{-/-}$, Mrp3$^{-/-}$, Mrp4$^{-/-}$ and Mrp3$^{-/-}$/Mrp4$^{-/-}$ mice and compared to wild type mice (Vasilyeva et al. 2015). Absence of Mrp2 resulted in 350 fold higher plasma levels and three times higher liver concentrations of sorafenib-glucuronide compared to wild type mice. However, urinary excretion of sorafenib-glucuronide was practically unchanged but biliary excretion decreased 12 fold compared to wild type. Interestingly, when Mrp3$^{-/-}$, Mrp4$^{-/-}$ and Mrp3$^{-/-}$/Mrp4$^{-/-}$ mice were compared to wild type, no differences in liver accumulation or plasma levels of sorafenib-glucuronide was seen. These results indicate that Mrp2 excretes efficiently sorafenib-glucuronide to bile and Mrp3$^{-/-}$ and Mrp4$^{-/-}$ can compensate the absence of Mrp2. However, when Mrp2 is present, the absence of Mrp3$^{-/-}$ and Mrp4$^{-/-}$ does not affect pharmacokinetics of sorafenib-glucuronide, but there has to be other transporter(s) for basolateral efflux because knockout of Mrp3 and Mrp4 did not decrease basal levels of sorafenib-glucuronide in plasma.

2.3.4 *In vivo* contribution of multidrug resistance protein 2-4 to disposition of glucuronides in small intestine

4-methylumbelliferone (4-MU) is extensively conjugated with glucuronide acid (Nagy et al. 2015). Zamek-Gliszczynski and coworkers (2006c) showed that the glucuronide of 4-MU accumulated three times more in livers of Mrp3$^{-/-}$ mice, but not in livers of Mrp4$^{-/-}$ mice, compared to wild type mice. In addition, basolateral clearance was five times lower and biliary clearance two times higher in Mrp3$^{-/-}$ mice compared to wild type mice. When 4-MU was administered orally to Mrp3$^{-/-}$ and wild type mice, the wild type mice had four times lower plasma levels of 4-MU-glucuronide (Hirouchi et al. 2009). Perfused segments of small intestine from Mrp3$^{-/-}$ and wild type mice revealed that along the whole small intestine, basolateral efflux of 4-MU-glucuronide was 2-4 lower in the absence of Mrp3 (Kitamura et al. 2010). However, apical efflux or intracellular concentrations of 4-MU-glucuronide did not change.

Resveratrol is highly glucuronidated (Walle et al. 2004). When resveratrol was administered orally to Mrp3$^{-/-}$ and wild type mice, the knockout mice had 10 times lower

plasma levels of resveratrol glucuronide compared to wild type mice (van de Wetering et al. 2009). In addition, urinary excretion of resveratrol glucuronide was markedly reduced but accumulation in liver was only minor affected when Mrp3 was absent. The excretion pathway of total resveratrol changed from urine to feces in $Mrp3^{-/-}$ mice compared to wild type mice.

Zamek-Gliszczynski and coworkers (2011) studied the effect of Mrp2 knockout in mice on plasma concentrations of ethinylestradiol-glucuronide. When ethinylestradiol was administered orally, 46 times higher exposure of ethinylestradiol-glucuronide was detected in the absence of Mrp2.

Diclofenac was administered orally to $Mrp2^{-/-}$ and wild type mice and plasma levels of diclofenac-glucuronide were measured (Lagas et al. 2010b). In the absence of Mrp2, plasma levels of diclofenac-glucuronide were eight times higher compared to wild type mice. Biliary excretion was decreased two fold but no change in hepatic concentrations was seen. In addition, the effect of single and double knockout mice, $Mrp3^{-/-}$ and $Mrp2^{-/-}$ /$Mrp3^{-/-}$, was studied after parenteral administration of diclofenac. Plasma levels of diclofenac-glucuronide were only minorly decreased in both strains compared to wild type mice, but no change was seen in intrahepatic concentration. However, when 15 times higher diclofenac dosage was administered in another study to $Mrp3^{-/-}$ mice, a nine fold decrease in diclofenac-glucuronide plasma level was found compared to wild type mice (Scialis et al. 2015). However, biliary excretion or intrahepatic concentrations were not increased. These results indicate that Mrp2 transports diclofenac-glucuronide to the intestinal lumen and into bile. In addition, Mrp3 compensates the absence of Mrp2, when a high amount of glucuronide is produced. However, in both studies basal levels of basolateral and apical excretion of diclofenac-glucuronide was found, although Mrp3 or/and Mrp2 were absent. This indicates that there are other transporters capable to transport diclofenac-glucuronide.

2.3.5 Summary of *in vivo* animal studies of interplay between glucuronidation and efflux transport

Based on *in vivo* mice studies (2.3.3 and 2.3.4), it is quite clear that Mrp2 and Mrp3 contribute significantly to apical and basolateral efflux of glucuronides, respectively. Together Mrp2 and Mrp3 restrict the accumulation of glucuronides in drug metabolizing tissues, namely in liver and intestine. In addition, they can compensate for each other, when one is absent or if high intracellular glucuronide levels are present. However, contribution of Mrp4 to excretion of glucuronides seems to be currently unclear.

2.4 Background and aims of this study

UGTs and MRPs play key roles in the detoxification and disposition of various endogenous and exogenous compounds, and drugs. Because they work together and form interplay, it is important to study them in the same system. However, best tools at present to study this interplay are only tools to study both individual processes *in vitro* or have a mechanistic understanding of the interplay *in vivo*. These include *in vitro* glucuronidation and transport assays with human originated material or recombinant material. On the other hand, *in vivo* studies are conducted only in preclinical animals and are mainly restricted to transporter knockout models of mice.

However, there are only few reported *in vitro* based systems for studying the glucuronidation-efflux transport interplay. Quan and coworkers (2015) established transfected HeLa-cells with UGT1A1 and studied excretion of chrysin-glucuronide in the presence of MRP and BCRP inhibitors or by knocking down BCRP, MRP1, MRP3 or MRP4 with short hairpin RNA. However, because there are not specific inhibitors for these transporters and knocking down with short hairpin RNA does not fully silence expression of transporters, this system does not allow for specific determination of transporters contributing to glucuronide efflux. HeLa-cells also do not express MRP2 and expression levels of other transporters might differ substantially compared to liver or intestine tissues. In addition, difference in basolateral and apical efflux is not possible to study in this system because HeLa-cells do not form polarized monolayers.

Fahrmayr and coworkers (2012) established more advanced systems based on triple-transfected MDCK-cells expressing OATP1B1, UGT1A1 and MRP2. This cell line was used to study vectorial transport of ezetimibe. Interestingly, increased amount of ezetimibe-glucuronide was transported to the apical compartment, when MRP2 was present in the cell lines compared to control cell line expressing only OATP1B1 and UGT1A1. However, these cell models do not allow studying basolateral efflux of glucuronides. In addition, these cell lines express uptake-transporter that complicates the handling of the cell lines and usually highly metabolized drugs have high passive permeability. Actually, in that study the expression of OATP1B1 did not affect the accumulation of ezetimibe inside cells.

Prediction of biotransformation reactions of drugs and subsequent metabolites in humans is routinely done in drug development and is based on *in vitro* assays (Vermeir et al. 2005; Ruiz-Garcia et al. 2008; Di 2014). However, understanding of disposition of metabolites is still poor and better tools are needed, especially for the prediction and understanding of human circulating metabolites (Anderson et al. 2009; Dalvie et al. 2009; Smith and Dalvie 2012; Loi et al. 2013). In addition, preclinical animal *in vivo* models are not sufficient to predict human metabolism (Lavé et al. 2009; Pellegatti 2012; Zamek-Gliszczynski et al. 2013). Futhermore, European Medicines Agency (EMA) and U.S. Food and Drug Administration (FDA) demand preclinical toxicological studies for all metabolites that are present in humans but not in preclinical animals or human exposure of metabolites exceeds significantly animal exposure (FDA 2008; EMA 2009). Because of these factors, better tools are needed to understand and predict systemic and tissues exposure and excretory routes for drug metabolites.

The main objective of this study was to establish cell lines expressing human UGT1A1 or UGT2B7 and both MRP2 and MRP3, because these enzymes and transporters play a key role in glucuronidation of drugs and excretion of glucuronides from intestine or liver to blood circulation or to bile and intestinal lumen (see sections 2.1-2.3). The MDCK-cell line was chosen to express human proteins because this cell line is well established in drug metabolism studies and it forms polarized monolayer that allows studying vectorial transport of drug molecules (Fahrmayr et al. 2012; Brouwer et al. 2013). Newly established cell lines would allow studying glucuronidation of drugs and subsequent disposition of glucuronides. In addition, it could allow a better prediction of human

metabolism of drugs that are metabolized by UGT1A1 or UGT2B7. These cell lines could also be used to identify inhibitors of UGT1A1, UGT2B7, MRP2 and MPR3 and study the effect of inhibitors to glucuronidation-efflux transport interplay.

For this purpose, the following aims were set:

- Clone the *UGT2B7* cDNA, construct a mammalian expression vector of the *UGT2B7* cDNA and express UGT2B7 in MDCK cells expressing MRP2 or MRP3.

- Clone the *ABCC3* cDNA encoding MRP3, construct a mammalian expression vector of this cDNA and express MRP3 in MDCK cells expressing UGT2B7 or UGT1A1 and MRP2.

- Establish MDCK-UGT1A1 and MDCK-UGT1A1-MRP2 cell lines.

- Characterize newly established cell lines regarding the level of mRNA and protein expression of UGT1A1, UGT2B7 and MRP3.

3. MATERIALS AND METHODS

All materials and devices used in this study are presented in this section. In addition, all methods are described in detail. Solutions and buffers are described in detail in Appendices 1 and 2.

3.1 Materials

All commercially acquired reagents and materials used in this study are presented in Table 6 (Cell culturing) and Table 7 (Molecular biology). All materials used for molecular biology applications or cell culturing were used sterile (provided by manufacturer or

autoclaved in-house). Water used for all reactions was molecular biology quality (Table 7). Ion exchanged and 0.2 µm -filtered water was used only for preparation of solutions and buffers (see Appendices 1 and 2 for recipes). In addition, certain materials are not presented here (for example pipette tips and glass pipettes), but they were from commercial origins and were autoclaved in-house before use.

Table 6. Cell culturing materials and reagents. **A** = Greiner-Bio-One GmbH (Frickenhausen, Germany); **B** = Carl Roth GmbH + Co. KG (Karlsruhe, Germany); **C** = Sarstedt AG & Co (Nümbrecht, Germany); **D** = Life Technologies GmbH (Darmstadt, Germany); **E** = Merck KGaA (Darmstadt, Germany); **F** = Becton, Dickinson and Company (NJ, USA); **G** = QIAGEN GmbH (Hilden, Germany)

MATERIAL	**CATALOGUE NUMBER OF THE SUPPLIER**	**SUPPLIER**
Cell culture flask, 25 cm^2	83.3910.002	C
Cell culture flask, 75 cm^2	83.3911.002	C
Cell culture multiwell plate, 24 wells	662160	A
Cell culture dish, 10 cm	664160	A
DMSO	4720.2	B
DPBS	14190-094	D
FBS	10270-106	D
G418 sulfate	11811-031	D
MEM	31095-029	D
Penicillin (10 000 U/ml) – Streptomycin (10 000 µg/ml) solution	15140-122	D
Serological pipettes: 2 ml	86.1252.001	C
5 ml	86.1253.001	C
10 ml	86.1254.001	C
25 ml	86.1685.001	C
50 ml	86.1689.001	C
Sodium butyrate	8.17500.0100	E
Sterile syringe filter, 0.2 µm pore size	83.1826.001	C
Syringe, 20 ml	300296	F
Tube, 2 ml, cryogenic	5000-0020	D
Tube, 15 ml	62.554.502	C
Tube, 50 ml	62.547.254	C
Transfection reagent, Effectene	301425	G
Trypsin (0.05 %)-EDTA (0.5 mM), phenol red solution	25300-062	D
Zeocin, 100 mg/ml solution	R250-01	D

Table 7. Molecular biology materials and reagents. **A** = Greiner-Bio-One GmbH (Frickenhausen, Germany); **B** = Carl Roth GmbH + Co. KG (Karlsruhe, Germany); **C** = Sarstedt AG & Co (Nümbrecht, Germany); **D** = Life Technologies GmbH (Darmstadt, Germany); **E** = Merck KGaA, Darmstadt, Germany; **F** = Becton, Dickinson and Company (NJ, USA); **G** = QIAGEN GmbH (Hilden, Germany); **H** = New England Biolabs GmbH (Frankfurt, Germany); **I** = Agilent Technologies Sales & Services GmbH & Co.KG (Waldbronn, Germany); **J** = Bio-Rad Laboratories GmbH (München, Germany); **K** = Promega GmbH (Mannheim, Germany); **L** = Roche Diagnostics GmbH (Mannheim, Germany); **M** = Genaxxon BioScience GmbH (Ulm, Germany); **N** = Sigma-Aldrich Chemie GmbH (Schelldorf, Germany); **O** = Abcam plc (Cambridge, UK); **P** = Dianova GmbH (Hamburg, Germany); **Q** = GE Healthcare Life Sciences (Buckinghamshire, UK); **R** = A. Hartenstein GmbH (Würzburg, Germany); **S** = Medicell Membranes Ltd (London, UK); **T** = VWR International GmbH (Erlangen, Germany); **U** = Clontech Laboratories, Inc. (CA, USA); **V** = MACHEREY-NAGEL GmbH & Co. KG, (Düren, Germany); **W** = AppliChem GmbH (Darmstadt, Germany); **X** = Institute of Experimental and Clinical Pharmacology and Toxicology, Friedrich-Alexander-Universität Erlangen-Nürnberg (Erlangen, Germany)

MATERIAL	CATALOGUE NUMBER OF SUPPLIER	SUPPLIER
Acetic Acid	3738.1	B
Acrylamide/bis-acrylamide solution, 30 %, 2,7 % cross-linker	161-0158	J
Agarose, genetic technology quality	6352.2	B
Agarose, LE	M3044.0500	M
Ampicillin, sodium salt	K029.2	B
Antibody, Anti-β-actin, mouse monoclonal	A5441	N
Antibody, Anti-UGT1A1, rabbit polyclonal	Ab62600-100	O
Antibody, Goat Anti-Mouse IgG -Horseradish Peroxidase conjugated, polyclonal	115-035-062	P
Antibody, Goat Anti-Rabbit IgG -Horseradish Peroxidase conjugated	RPN4301	Q
Ammonium peroxydisulfate	9178.1	B
Blotting paper, 0.35 mm thickness	GB58	R
Bromophenol blue	B0126	N
cDNA, liver	In-house synthesis	X
cDNA synthesis kit, iScript	170-8891	J
Cell culture dishes 100x20 mm	664160	A
Cell scraper	83.1830	C
Chemiluminescent detection reagent, Amersham ECL Western Blotting Detection Reagent	RPN2209	Q
Competent cells, One Shot TOP10	C404003	D
Competent cells, XL10-Gold ultracompetent	200315	I
Competent cells, XL1-Blue supercompetent	200519-4 (mutagenesis kit)/ 200236	I

Cuvette, semi-micro acrylic	67.740	C
Dialysis tubing, molecular weight cut off 12-14 000 Da	DTV.12000.02.30	S
Dimethylformamide	T921.1	B
DNA ladder, 1 kb, 0.5 mg/ml	25-2030	T
DNA ladder, 2-log, 1 mg/ml	N3200S	H
DNA ladder, 2-log, tridye, 100 µg/ml	N3270S	H
DNA ligase T4, 400 u/µl	M0202S	H
DNA ligase T4 reaction buffer, 10X	B0202S	H
DNA quick ligase T4, 2 000 u/µl	M2200S	H
DNA quick ligase T4 reaction buffer, 2X	B2200S	H
DNA polymerase, Advantange cDNA polymerase mix	639105	U
DNA polymerase, iTaq	170-8870	J
DPBS, powder	21600-044	D
DTT	6908.2	B
EDTA, disodium salt dihydrate	8043.3	B
Ethanol	9065.4	B
Ethidium bromide	7870.2	B
Gel loading dye, Blue, 6X	B7021S	H
Gel loading dye, Purple, 6X	B7024S	H
Glycerin	3783.1	B
Glycin	3908.3	B
Hydrochloric acid, 32 %	P074.1	B
Isopropanol	6752.4	B
LB-Agar, (Luria/Miller)	X969.1	B
LB-Medium, (Luria/Miller)	X968.1	B
LightCycler Capillaries, 20 µl	04929292001	L
LightCycler reaction mix	03515885001	L
Lysozyme, 20 000 u/mg	8259.1	B
Methanol	8388.6	B
Milk powder	T145.2	B
Mutagenesis kit, QuickChange II site-directed	200523-5	I
Mutagenesis kit, QuickChange multi-site-directed	200515-5	I
N,N,N',N'-Tetramethylethylendiamin	A1148.0025	W
Nucleotides for PCR: dATP, dCTP, dGTP, dTTP	N0440S, N0441S, N0442S, N0443S	H
Petri dishes	632180	A
Phosphatase, Antarctic, 5 u/µl	M0289S	H

Phosphatase reaction buffer, 10X	B0289S	H
Plasmid Miniprep System, PureYield	A1222	K
Ponceau S	5938.1	B
Protease inhibitor cocktail tablets, Complete Mini	04693124001	L
Protein Assay Kit, BCA Pierce	23225	D
Protein ladder, 10 to 250 kDa PageRuler Plus Prestained	26619	D
Restriction enzyme, *Apa*I, 50 u/µl	R0114S	H
Restriction enzyme, *Bam*HI-HF, 20 U/µl	R3136S	H
Restriction enzyme, *Bst*XI, 10 u/µl	R0113S	H
Restriction enzyme, *Eco*RI-HF RE-Mix, 10X	R5101S	H
Restriction enzyme, *Kpn*I, 10 u/µl	R0142S	H
Restriction enzyme, *Not*I-HF, 20 u/µl	R3189S	H
Restriction enzyme, *Pst*I, 20 u/µl	R0140S	H
Restriction enzyme reaction buffer, CutSmart Buffer, 10X	B7204S	H
Restriction enzyme reaction buffer, NEBuffer 1, 10X	B7001S	H
Restriction enzyme reaction buffer, NEBuffer 2, 10X	B7002S	H
Restriction enzyme reaction buffer, NEBuffer 3, 10X	B7003S	H
Restriction enzyme reaction buffer, NEBuffer 4, 10X	B7004S	H
Restriction enzyme reaction BSA, 10 mg/ml, 100X	B9001S	H
Reverse transcriptase, M-MLV, RNase H Minus + 5x reaction buffer	M368B	K
Ribonuclease A, 90 u/mg	7156.1	B
RNA, liver and kidney, Human Total RNA Master Panel II	636643	U
RNase inhibitor, 40 u/µl	N251B	H
RNA isolation kit, NucleoSpin RNA Plus	740984.50	V
Saccharose	1.07653.1000	E
SDS	2326.2	B
S.O.C. Medium	15544-034	D
Sodium Acetate trihydrate	6779.2	B
Stripping reagent for western blot	21059	D
Topo TA Cloning Kit	450641	D
Transfer membrane	NC02	R

TRIS-Base	4855.3	B
TRIS-HCl	9090.2	B
Triton X 100	3051.2	B
Tube, 13 ml	62.515.006	C
Tube, PCR, 0.2 ml	82-0620-A	T
Tube, micro, 1.5 ml	72.690.001	C
Tube, micro, 1.5 ml with assembled cap	72.692.005	C
Tube, micro, 2 ml	72.695.500	C
Trichloroacetic acid	8789.1	B
Tween 20	9127.1	B
Water, for molecular biology	T143.3	B
X-β-Gal	2315.2	B

3.1.1 Devices

Devices used in this study for cell culturing work or molecular biology work are presented in Table 8 and Table 9, respectively.

Table 8. Devices used in cell culturing work.

DEVICE	**MODEL**	**MANUFACTURER**
Biosafety cabinet, class II	Biowizard KR-130	Kojair Tech Oy (Vilppula, Finland)
Cell counting chamber, 0.100 mm depth, 0.0025 mm^2	Neubauer	Paul Marienfeld GmbH & Co. KG (Lauda-Königshofen, Germany)
Centrifuge	Z400	HERMLE Labortechnik GmbH (Wehingen, Germany)
Freezing container	5100-0001	Thermo Fisher Scientific Inc. (MA, USA)
Incubator	Heracell 150	Thermo Fisher Scientific Inc. (MA, USA)
Microscope	CKX41	Olympus Co. (Tokyo, Japan)
Water bath	1004	GFL - Gesellschaft für Labortechnik GmbH (Burgwedel, Germany)

Table 9. Devices used in molecular biology work.

DEVICE	MODEL	MANUFACTURER
Autoclave	2540 EL	Systec GmbH (Linden, Germany)
Centrifuge, microtube	5424	Eppendorf AG (Hamburg, Germany)
Centrifuge, cooling	5810R with rotor F45-30-11 (microtubes) or with rotor A-4-62 (15 ml tubes)	Eppendorf AG (Hamburg, Germany)
Electrophoresis system with 1 mm glass and 10 well comb	Mini-PROTEAN 3 Cell	Bio-Rad Laboratories (CA, USA)
Electrophoresis power supply	PowerPac 1000	Bio-Rad Laboratories (CA, USA)
Gel electrophoresis cell, large	Sub-Cell GT	Bio-Rad Laboratories (CA, USA)
Gel electrophoresis cell, small	Mini-Sub Cell GT	Bio-Rad Laboratories (CA, USA)
Gel electrophoresis power supply	PowerPac Basic	Bio-Rad Laboratories (CA, USA)
Heating block	MC-01N	UniEquip Laborgerätebau- und Vertriebs GmbH, (Planegg, Germany)
Incubator	IH50	Incutec GmbH (Mössingen, Germany)
Lightcycler	2.0	Roche Diagnostics GmbH, (Mannheim, Germany)
Lightcycler centrifuge adapters	1909312	Roche Diagnostics GmbH, (Mannheim, Germany)
Microcentrifuge	[1]Rotilabo	Carl Roth GmbH + Co. KG (Karlsruhe, Germany)
Mixer, rotating	RM 5-40	Ingenieurbüro CAT M. Zipperer GmbH (Staufen, Germany)
Molecular Imager	ChemiDoc XRS System	Bio-Rad Laboratories (CA, USA)
pH-meter	CyberScan pH310	Thermo Fisher Scientific Inc. (MA, USA)
Protein blotting system	Mini Trans-Blot Cell	Bio-Rad Laboratories (CA, USA)
Scale, 0.01-120 g	TB-124A	Sartorius Corporation (NY, USA
Scale, 0.5-2200 g	TB-2202A	Sartorius Corporation, NY, USA)
Shaker	K15-500	Incutec GmbH (Mössingen, Germany)

Spectrophotometer	Genesys 10S UV-Vis	Thermo Fisher Scientific Inc. (MA, USA)
Spectrophotometer cell, quartz, 10 mm path	-	Bio-Rad Laboratories (CA, USA)
Thermocycler	Labcycler 48	Sensoquest GmbH (Göttingen, Germany)
UV imaginer	Intas UV systeme	INTAS Science Imaging Instruments GmbH (Göttingen, German)y
Vacuum manifold	Vac-Man Laboratory Vacuum Manifold, 20 sample capacity	Promega Corporation (WI, USA)
Vacuum pump for manifold	2522C-02	Welch (IL, USA)
Vortex mixer	ZX3	VELP Scientifica (Usmate, Italy)
Water bath	1004	GFL - Gesellschaft für Labortechnik GmbH (Burgwedel, Germany)
Water purification with 0.2 µm filter	TKA GenPure UF/UV, 08.2204	Thermo Fisher Scientific Inc. (MA, USA)

3.1.2 Primers

All primers used in this study and their applications are presented in Table 10. Oligo(dT)$_{18}$, oMRP3-RT-F, oMRP3-RT-R, oUGT2B7-seq1, oUGT2B7-seq2, oUGT2B7-R, oUGT1A1-seq1, oUGT1A1-RT-F and oUGT1A1-RT-R primers were ordered from Sigma-Aldrich Chemie GmbH (Schnelldorf, Germany). All the other primers were from biomers.net GmbH (Ulm, Germany). Primers used for mutagenesis reactions were acquired as high-pressure liquid chromatography (HPLC) purified from the manufacturer. Other primers were standard quality provided by manufacturer without additional purifications.

Table 10. Primers used in this study and their DNA sequence. Added restriction site is indicated by bold letters.

NAME OF THE PRIMER	**USED FOR**	**DNA SEQUENCE**
T7-promoter	Sequencing	5’-taatacgactcactataggg-3’
BGH-reverse	Sequencing	5’-tagaaggcacagtcgagg-3’
M13-reverse	Sequencing	5’-caggaaacagctatgac-3’

Oligo(dT)$_{18}$	cDNA synthesis	5’-ttttttttttttttttt-3’
oβ-actin-F	qPCR, PCR	5’-tgacggggtcacccacactgtgcccatcta-3’
oβ-actin-R	qPCR, PCR	5’-ctagaagcatttgcggtggacgatggaggg-3’
oMRP3-F	Cloning PCR	5’-gcctcggccccatggacg-3’
oMRP3-R	Cloning PCR	5’-ggccaggaggaaatctcagg-3’
oMRP3-*Xba*I-F	Cloning PCR	5’-**tctaga**cgcgcctcggccc-3’
oMRP3-Clone-R	Cloning PCR	5’-ggccccgatgacgtggtcaaa-3’
oMRP3-Clone-F	Cloning PCR	5’-ccaagcgctaccagcagact-3’
oMRP3-Clone-R2	Cloning PCR	5’-ccaggaaaggccaggaggaaatctc-3’
oMRP3-Clone-F2	Cloning PCR	5’-gctagctgacctggagatgctgcctg-3’
oMRP3-RT-F	qPCR, PCR	5’-ggaccctgcgcatgaacctg-3’
oMRP3-RT-R	Cloning PCR, qPCR, PCR	5’-aggcaagtccagcatctctgg-3’
oMRP3-seq1	Sequencing	5’-ccacagctgctcagcatcct-3’
oMRP3-seq2	Sequencing	5’-ggtgagctccagctgctgc-3’
oMRP3-seq3	Sequencing	5’-cgctcgccacagtccttctt-3’
oMRP2-RT-F	qPCR	5’-cttcggaaatccaagatcctgg-3’
oMRP2-RT-R	qPCR	5’-tagaattttgtgctgttcacattct-3’
oUGT2B7-F	Cloning PCR	5’-caccaggatgtctgtgaaatgg-3’
oUGT2B7-R	Cloning PCR	5’-actgaatgagtctcacctatcag-3’
oUGT2B7-Clone-R	Cloning PCR	5’-ccagcttcaaatctcagatataac-3’
oUGT2B7-seq1	Sequencing	5’-tgaagttctaggaagacccact-3’
oUGT2B7-seq2	Sequencing	5’-ttcaacacaatgtcgagtacaga-3’
oUGT2B7-Mut-F	Mutagenesis	5’-caactgtgatatttatcgtcacaaaatgttgtctgttttgttctgg-3’
oUGT2B7-Mut-R	Mutagenesis	5’-ccagaaacaaaacagacaacattttgtgacgataaatatcacagttg-3’
oUGT1A1-seq1	Sequencing	5’-gcagcgggtgaagaacatgc-3’
oUGT1A1-RT-F	qPCR	5’-gttacaaggagaacatcatgcg-3’
oUGT1A1-RT-R	qPCR	5’-cccacccacttctcaatggg-3’

3.1.3 Plasmids

Plasmids used in this study were from either commercial origin or in-house established (Table 11). In addition, Table 11 presents plasmids generated within this study. Charts of the plasmids are presented in Appendix 3. Charts include restrictions sites used in this study, primer binding sites and sites of antibiotic resistance genes, the cytomegalovirus

promoter and the insert.

Table 11. Plasmids used in this study and their origin of source and literature reference if available.

NAME OF THE PLASMID	CATALOGUE NUMBER OF THE MANUFACTURER OR THE LITERATURE REFERENCE AND ORIGIN OF SOURCE
pcDNA3.1/Hygro(-)	V875-20, Life Technologies GmbH (Darmstadt, Germany)
pcDNA3.1/Zeo(-)	V86520, Life Technologies GmbH (Darmstadt, Germany)
pCR2.1-TOPO	450641, Life Technologies GmbH (Darmstadt, Germany)
pcDNA3.1/Zeo(-)-UGT1A1	Institute of Experimental and Clinical Pharmacology and Toxicology, Friedrich-Alexander-Universität Erlangen-Nürnberg (Erlangen, Germany), *(Fahrmayr et al. 2012)*
pcDNA3.1/Zeo(-)-UGT2B7(1575T)	Institute of Experimental and Clinical Pharmacology and Toxicology, Friedrich-Alexander-Universität Erlangen-Nürnberg (Erlangen, Germany)
pcDNA3.1/Hygro(-)-MRP3	This study
pMA-MRP3	Dr. Markus Keiser, University of Greifswald (Greifswald, Germany), *(Commercially produced by Life Technologies GmbH, Darmstadt, Germany)*
pGEM-T-UGT2B7(802C)	Institute of Experimental and Clinical Pharmacology and Toxicology, Friedrich-Alexander-Universität Erlangen-Nürnberg (Erlangen, Germany)
pCR2.1-TOPO-MRP3-part	Institute of Experimental and Clinical Pharmacology and Toxicology, Friedrich-Alexander-Universität Erlangen-Nürnberg (Erlangen, Germany)
pCR2.1-TOPO-MRP3	This study
pCR2.1-TOPO-MRP3-3‘-part	This study

3.1.4 Cell lines

Table 12 describes all cell lines used in this study. MDCK-VC cell line is transfected with the empty pcDNA3.1/G418(-)-vector and does not overexpress any protein. This cell line was used as control for immunoblot analysis.

Table 12. Cell lines used in this study, their origin of source and literature reference if available.

NAME OF THE CELL LINE	CATALOGUE NUMBER OF THE MANUFACTURER OR THE LITERATURE REFERENCE AND ORIGIN OF SOURCE
MDCK-II parental cell line	LGC Standards (Teddington, UK), CRL-2936
MDCK-MRP2	Institute of Experimental and Clinical Pharmacology and Toxicology, Friedrich-Alexander-Universität Erlangen-Nürnberg (Erlangen, Germany), (*Cui et al. 1999)*
MDCK-VC G418 (transfected with the empty pcDNA3.1/G418)	Institute of Experimental and Clinical Pharmacology and Toxicology, Friedrich-Alexander-Universität Erlangen-Nürnberg (Erlangen, Germany), (*Cui et al. 1999)*
MDCK-UGT1A1	This study

3.2 Methods

All methods used in this study are described below. Reagents used in methods are presented in Table 6 and Table 7. In addition, description of solutions and buffers are presented in Appendices 1 and 2.

3.2.1 Cell culturing

MDCK-cells were cultured in MEM-medium supplemented with 1 % penicillin, 1% streptomycin and 10 % heat-inactivated FBS and were incubated under moisture atmosphere containing 5 % of CO_2. Cells were grown as monolayers in 25 cm^2 cell culture flasks containing 8 ml appropriate media. Depending on cell line, the medium was supplemented with additional 0.8 mg/ml G418 (MDCK-VC and MDCK-MRP2), 0.5 mg/ml zeocin (MDCK-UGT1A1) or both 1 mg/ml zeocin and 0.8 mg/ml G418 (MDCK-UGT1A1-MRP2). Detailed recipes for media are presented in Appendix 1.

Cells were split and subcultured two times a week. During day 3-4 of post-splitting, cells reached confluence in 25 cm^2 flasks. Splitting was conducted according to following

protocol: Medium was aspirated and cell monolayer was washed with 2 ml DPBS. Subsequently, 1.5 ml trypsin-solution was applied to cell monolayer and the flask was incubated 15-30 minutes at 37 °C in the cell incubator. After cells were detached from the surface, cell suspension was transferred with 5 ml of appropriate media to 15 ml tubes and centrifuged for 3 minutes at 500 g. Supernatant was removed and the cell pellet was suspended in 5 ml appropriate media and 0.4-0.8 ml of this suspension, corresponding a subdilution of 1:13 or 1:6, was subcultured as described above.

All media, DPBS and trypsin solution applied to cells were warmed to 37 °C before use in any cell culture method.

3.2.2 Transfection of MDCK-cells

$1x10^6$ parental MDCK or MDCK-MRP2 cells were cultured in 10 cm cell culture dishes containing 10 ml of appropriate medium for 24 hours before the stable transfection with the vector containing *UGT1A1* cDNA (pcDNA3.1/Zeo(-)-UGT1A1). Cells reached approximately 40 % confluency before the transfection. Transfection was done according to protocol of the manufacturer of the transfection reagent. Briefly, 2 µg of the plasmid DNA was mixed with Buffer EC in a total volume of 300 µl. Furthermore, 16 µl of Enhancer-solution was added to the mixture and it was vortexed for one second followed by incubation for 5 minutes at room temperature. Following incubation, 60 µl of Effectene-solution was added to the mixture, vortexed for 15 seconds and further incubated 10 minutes at room temperature. Before applying the transfection mixture to the cells, medium was aspirated from the cell culturing dish, cells were washed with 5 ml DPBS and supplemented with 8 ml of the appropriate medium. After 10 minutes incubation of the transfection reagent mixture, it was first mixed with 2 ml of the appropriate medium and then transferred to the cells and mixed gently by shaking the dish.

After 24 hours of transfection, the medium was aspirated, cells were washed with 5 ml of DPBS and 10 ml fresh pre-warmed medium was added. 48 hours after transfection, medium was aspirated, cells were washed with 5 ml DPBS and trypsinized with 1 ml

trypsin solution for 20 minutes at 37 ˚C. After the cells were detached, they were transferred with 5 ml of appropriate media to 15 ml tubes and centrifuged 3 minutes at 500 g. The supernatant was aspirated and the pellet was suspended with 10 ml of appropriate media containing the selection antibiotic zeocin. This suspension was transferred in dilutions of 1:5, 1:10 and 1:20 to cell culture dishes in a total volume of 10 ml of appropriate media containing 0.5 mg/ml of zeocin to give the first passage of MDCK-UGT1A1 or MDCK-UGT1A1-MRP2 cells.

The media were changed two times a week. Subsequent passages were done according to same protocol as above. Instead of dilutions used for the first passage, higher dilutions were used for the subsequent passages; 1.25-200 µl of 5 ml cell suspension was subcultured. Dilution factors and number of the passages are presented in the *Results* section. In addition, zeocin concentration was changed from 0.5 mg/ml to 1 mg/ml in the case of MDCK-UGT1A1-MRP2 cells after the first passage.

Single colonies were isolated by using blotting paper size of approximately 0.25 cm^2. First, media were aspirated and cells were washed with 5 ml DBPS. A piece of blotting paper was drowned in trypsin solution and subsequently pressed onto a colony and transferred into a well of 24 well plate containing 1 ml media. The plate was incubated at 37 °C in cell incubator and medium was changed two times a week until cells reached 50-80 % confluency. Finally, cells from one well were transferred to a 25 cm^2 cell culture flask. For the transfer, medium was aspirated, cells were washed with 1 ml DPBS and 300 µl trypsin was applied to the cells. Trypsinization was carried out for 30-60 minutes in 37 °C incubator, after which the suspension was diluted with 1 ml appropriate medium and transferred to 25 cm^2 cell culture flask containing 7 ml of the same medium to give the first passage for a clone. Cells were cultured 3-11 days and the medium was changed two times a week. After cells reached 80-100 % confluency, they were split, as described in 3.2.1, and subcultured.

3.2.3 Storage cell culture

MKDC-UGT1A1 clones 4 and 7 were grown to 100 % confluence in two 75 cm^2 cell culture flasks during 4 days after 2:5 subdilution from 25 cm^2 cell culture flasks. After reaching confluence, cells were washed with 3 ml DPBS, trypsinized with 2 ml trypsin solution for 30 minutes, transferred to 15 ml tubes with 5 ml MEM-PS-Zeo-medium and centrifuged 3 minutes at 500 g. Supernatants were removed and both pellets were suspended and combined in a total volume of 7.2 ml MEM-PS-Zeo medium. This suspension was divided into 0.9 ml aliquots in 2 ml cryogenic tubes. Tubes were filled with 0.9 ml media containing 20 % DMSO, 40 % FBS and 40 % MEM-PS-Zeo-medium to a total volume of 1.8 ml. Tubes were frozen in freezing container at -80 °C for 24 hours, after which they were stored in liquid nitrogen.

3.2.4 RNA isolation

MDCK-UGT1A1 and MDCK-UGT1A1-MRP2 cells were cultured in a cell culture dish with a dilution of 1:5-3:5 from 25 cm^2 flask, in a total volume of 8 ml appropriate medium. After culturing for 72 hours, medium was changed to fresh medium containing 10 mM sodium butyrate to induce protein expression (Cui et al. 1999). After 24 hours of the induction, RNA was isolated by NucleoSpin RNA Plus kit according to the procedure of the manufacturer. Briefly, medium was aspirated from the cell culture dish and 350 µl lysis buffer was applied, spread over the entire surface and incubated for a couple of minutes at room temperature. The cell suspension was harvested with cell scraper, homogenized with pipette and centrifuged through the first column of the kit. 100 µl of binding solution was added to the filtrate and mixed with a pipette. The entire solution was centrifuged through the second column of the kit. This column was further washed with 200 µl wash buffer 1 and 600 µl and 250 µl wash buffer 2. RNA was eluted two times with 30 µl water provided by the kit.

3.2.5 sscDNA synthesis using total RNA of MDCK cells

sscDNA was synthesized using total RNA of MDCK cells using the iScript cDNA synthesis kit according to the protocol of the manufacturer. Briefly, the reaction contained 1 µg of total RNA, 4 µl iScript reaction mix, 1 µl reverse transcriptase and water, provided by the kit, added to a total reaction volume of 20 µl. Reaction was prepared in a PCR-tube and run in the thermocycler according to the parameters in Table 13.

Table 13. Thermocycler parameters for sscDNA synthesis using total RNA of MDCK-cells.

TEMPERATURE	TIME
25 ˚C	5 minutes
42 ˚C	30 minutes
85 ˚C	5 minutes
4 ˚C	Until sample was analyzed

sscDNA synthesis was evaluated by PCR amplification of a 660 base pair fragment of β-actin using iTaq DNA polymerase according to the protocol provided by the manufacturer. Briefly, reaction was prepared in a PCR tube and contained 2 µl 10X PCR buffer, 1.5 mM magnesium chloride, 200 µM of each nucleotide (dATP, dCTP, dGTP and dTTP), 0.5 U DNA polymerase, 1 µl of cDNA preparation, 0.4 µM oβ-actin-F and oβ-actin-R and water added to a final volume of 20 µl. Reaction was run in the thermocycler according to the parameters in Table 14.

Table 14. Thermocycler parameters for amplification of a 660 base pair fragment of β-actin for analysis of sscDNA synthesis.

TEMPERATURE	TIME	
95 ˚C	3 minutes	
95 ˚C	30 seconds	40X
62 ˚C	30 seconds	
72 ˚C	1 minute	
72 ˚C	10 minutes	
4 ˚C	Until sample was analyzed	

3.2.6 Quantitative PCR (Lightcycler)

LightCycler was used for qPCR-analysis of *UGT1A1*, *ABCC2* and *β-actin* mRNA expression. Reactions were prepared in LightCycler 20 µl capillaries on precooled LightCycler centrifuge adapters according to the protocol provided by the manufacturer with slight modifications. Briefly, reactions were prepared in volumes of 10 µl containing 1 µM reverse primer, 1 µM forward primer, 1 µl sscDNA template and 2 µl DNA polymerase, reaction buffer and fluorescence dye mixture diluted with water to a total volume. Capillaries were centrifuged briefly and qPCR was run in LightCycler according to the parameters in Table 15. Primers used for specific amplifications of cDNA fragment are presented in Table 16.

Table 15. LightCycler parameters for qPCR amplification of ssCDNA fragments.

TEMPERATURE	TIME	
95 ˚C	10 minutes	
95 ˚C	10 seconds	45 cycles
64 ˚C	10 seconds	
72 ˚C	30 seconds	
95 ˚C	10 seconds	
60 ˚C	10 seconds	0.1˚C/min
95 ˚C	-	
25 ˚C	Until sample was analyzed	

Table 16. Primers used for amplification of cDNA fragments in qPCR.

ANALYZED cDNA	FORWARD PRIMER	REVERSE PRIMER
UGT1A1	oUGT1A1-RT-F	oUGT1A1-RT-R
ABCC2	oMRP2-RT-F	oMRP2-RT-R
β-actin	oβ-actin-F	oβ-actin-R

3.2.7 Protein isolation and determination of protein concentration for immunoblotting

MDCK-UGT1A1 cells were cultured on a cell culture dish by dilution of 2:5 from a 25 cm^2 culture flask in a total volume of 8 ml. Cells were incubated at 37 °C in the cell incubator for 24 hours after the medium was changed to medium containing 10 mM

sodium butyrate to induce protein expression (Cui et al. 1999). After 24 hours incubation, medium was aspirated and cells were washed with 5 ml DPBS. 10 ml DPBS was added to the dish and cells were incubated for 5 minutes at 37 °C. After the incubation, cells were harvested with a cell scraper, transferred to a 15 ml tube and centrifuged 10 minutes at 400 g and 4 °C. The supernatant was removed and the pellet was suspended in 100 µl cold 0.2 % SDS solution containing protease inhibitors (one tablet dissolved in 7 ml 0.2 % SDS). This suspension was stored for 24 hours at -20 °C.

Protein concentrations of protein homogenates were measured by commercially available BCA Protein Assay Kit according to the protocol of the manufacturer. Briefly, all the samples were diluted by a factor of 1:5 with 0.2 % SDS solution to a total volume of 25 µl in 1.5 ml micro tubes. 500 µl mixture containing 49 parts of solution A and 1 part of solution B, was mixed with the samples. In addition, standards were prepared by the same procedure using 0.2 % SDS stock solutions of standards containing 0, 100, 250, 500 and 1000 µg/ml BSA (diluted from BSA provided by the kit). Samples were incubated 30 minutes at 37 °C in water bath and subsequently the absorbance was measured at 560 nm wavelength in the spectrophotometer. The protein concentration of samples were calculated based on absorbance of the standard samples.

3.2.8 Protein electrophoresis, blotting and immunostaining

A two segment gel was used for protein electrophoresis. This gel was casted in two phases: Firstly, a 10 % running gel was casted between isopropanol rinsed glass plates and covered finally by isopropanol after the casting. Secondly, after 45 minutes incubation of the running gel at room temperature, 1 cm of 4 % stacking gel was casted and a 10 well comb was installed at the head of the glass plate. The gel was stored over night between wet paper towels and packed inside aluminium folio.

For the protein electrophoresis, 15 µg of total protein of every sample was diluted with 5 µl of 4X loading buffer and water to a total volume of 20 µl. Samples were incubated 5 minutes at 95 °C and subsequently cooled down on ice. The entire volume of the samples were applied into the wells of the gel. In addition, 8 µl of the protein ladder was applied

(see Figure 5 for protein bands in the ladder). The gel was run in running buffer for 90 minutes using 130 V.

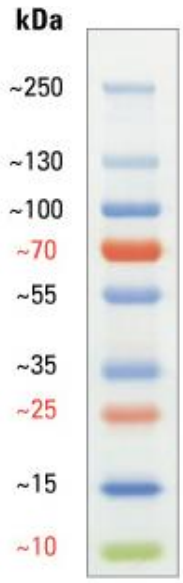

Figure 5. Sizes of marker proteins in the protein ladder used in this study (www.thermoscientific.de).

After separation of the proteins, the gel was blotted onto transfer membrane (nitrocellulose) between three blotting papers on each side in blotting buffer for 90 minutes at 100 V. The system was cooled with ice during the entire blotting procedure. After the blotting, the membrane was stained with protein staining solution for 5 minutes, washed once with water and photographed under visible light to ensure proper protein separation.

The membrane was further washed with PBST solution for 10 minutes. After PBST washing, the membrane was blocked with 5 % milk for 1 hour. Primary antibody staining was done overnight at 4 °C by placing the membrane inside a 50 ml tube containing 5 ml of 1:400 UGT1A1-antibody dilution in 0.5 % milk. On the next day, the membrane was washed twice for 10 minutes with PBST. Secondary antibody staining was done for 45 minutes at room temperature by placing the membrane inside a 50 ml tube containing 5 ml of 1:10 000 Anti-rabbit-antibody dilution in 5 % milk. The staining was followed by four washes of the membrane with PBST, each for 15 minutes. Luminescence reaction was induced by staining the membrane for approximately 2 minutes with 4 ml of a mixture containing 1:1 dilution of solutions 1 and 2 provided by chemiluminescent detection reagent kit. The membrane was photographed under visible light and luminescence was detected by exposing the membrane five times for 20 seconds. The final picture was merged from all five pictures and the visible light picture.

For β-actin immunostaining, the membrane was stripped of the previous antibodies by incubating it 15 minutes at 37 °C with 10 ml stripping reagent. The membrane was subsequently washed two times for 10 minutes with PBST. Primary antibody staining was done by placing the membrane inside a 50 ml tube containing 5 ml of 1:15 000 dilution of β-actin-antibody in 5 % milk. This reaction was incubated 90 minutes at room temperature. After the incubation, membrane was handled as described above, but instead of the Anti-rabbit-antibody, Anti-mouse-antibody was used in a 1:2 000 dilution.

A vertical mixer was used for all washing steps and protein stainings. For primary and secondary antibody stainings, a roll mixer was used. In addition, all antibodies and their dilutions are presented in Table 17.

Table 17. Antibodies used in this study, their dilutions, incubation temperatures and time.

PRIMARY ANTIBODY	SECONDARY ANTIBODY
Anti-UGT1A1, 1:400 in 0.5 % milk, incubated at 4 °C for overnight	Goat Anti-rabbit IgG, 1:10 000 in 5 % milk incubated at RT for 45 minutes
Anti-β-actin, 1:15 000 in 5 % milk, incubated at RT for 90 minutes	Goat Anti-mouse IgG, 1:2000 in 5 % milk incubated at RT for 45 minutes

3.2.9 sscDNA synthesis using total RNA of liver or kidney

For the synthesis of liver and kidney sscDNA, 1 µg of total RNA of liver or kidney was supplemented with 14 U RNase inhibitor and 1 µg of Oligo$(dT)_{18}$ in a total volume of 14 µl in a PCR-tube. This reaction was incubated at 70 °C for five minutes in the thermocycler and subsequently cooled down on ice for 5 minutes. After this incubation, 5 µl 5X reaction buffer, 1 µl (200 U) reverse transcriptase and final concentration of 500 µM of each nucleotide (dATP, dCTP, dGTP and dTTP) were added. Water was added to a total volume of 25 µl. The reaction was incubated in the thermocycler for 10 minutes at 40 °C, 50 minutes at 55 °C and finally cooled down on ice.

3.2.10 PCR for cloning of cDNA fragments

PCR for cloning of *ABCC3* and *UGT2B7* cDNAs and cDNA fragments is described here. The Advantage cDNA polymerase mix was used for amplification reactions according to instructions of the manufacturer. Briefly, 5 µl 10X reaction buffer, 2 µl liver or kidney sscDNA, 1 µl DNA polymerase mixture, 0.4 µM final concentration of both forward and reverse primers and 200 µM final concentration of each nucleotide (dATP, dCTP, dGTP and dTTP) were mixed in a PCR-tube. Water was added to final volume of 50 µl and the reaction was carried out as presented in Table 18. When pGEM-T-UGT2B7(802C) or non-linearized pMA-MRP3 -plasmids were used as the templates, 4 pg of the plasmid was used for amplification reaction. In the case of *Not*I linearized pMA-MRP3, 20 pg of

the plasmid was used for amplification reaction. Control reactions were carried out as cloning reactions, but the reaction volume was reduced to a volume of 20 µl. Table 19 presents primers used for all cloning PCR amplifications in this study.

Table 18. Thermocycler parameters for PCR amplifications of *ABCC3* and *UGT2B7* cDNAs and cDNA fragments. Panel A describes conditions for all other PCR amplifications but two-step PCR for *ABCC3* cDNA amplification is described in panel B.

A

TEMPERATURE	TIME	
94 ˚C	60 seconds	
94 ˚C	30 seconds	40-45 cycles
60-64 ˚C	30 seconds	
72 ˚C	60 seconds/ 1 kilobase of the target sequence	
72 ˚C	10 minutes	
4 ˚C	Until sample was analyzed	

B

TEMPERATURE	TIME	
94 ˚C	60 seconds	
94 ˚C	30 seconds	30-40 cycles
68 ˚C	3 minutes	
68 ˚C	3 minutes	
4 ˚C	Until sample was analyzed	

Table 19. Primers used for PCR amplification of cDNA fragments.

cDNA fragment	FORWARD PRIMER	REVERSE PRIMER
UGT2B7	oUGT2B7-F	oUGT2B7-R (sscDNA)/ oUGT2B7-Clone-R (for pGEM-T-UGT2B7(802C))
UGT2B7 control	oUGT2B7-seq2	oUGT2B7-R
ABCC3	oMRP3-F	oMRP3-R
ABCC3 (pMA-MRP3)	oMRP3-F	oMRP3-RT
ABCC3 3'-part	oMRP3-*Xba*I-F	oMRP3-Clone-R
ABCC3 5'-part	oMRP3-Clone-F	oMRP3-R
ABCC3 5'-part (two step PCR)	oMRP3-Clone-F2	oMRP3-Clone-R2
ABCC3 control	oMRP3-RT-F	oMRP3-RT-R
β-actin	oβ-actin-F	oβ-actin-R

3.2.11 Cloning of PCR amplified fragments

PCR amplified cDNA fragments were cloned into the pCR2.1-TOPO-vector using both PCR reaction and gel electrophoresis purified cDNA fragments. The Topo TA Cloning

Kit was used for this purpose according to the instructions of manufacturer. Briefly, 4 µl of a PCR-reaction or 4 µl of a gel purified cDNA fragment was mixed with 1 µl salt-solution and 1 µl pCR2.1-TOPO in a 2 ml micro tube. Reaction was incubated 5-30 minutes at room temperature. 3 µl of the reaction was transformed in One Shot TOP10 -cells as described in 3.2.15. White colonies were further analysed by isolation and restriction analysis of plasmids (see 3.2.12 and 3.2.19).

3.2.12 Plasmid restrictions

Plasmid restrictions were used for three different purposes in this study: For subcloning of the *UGT2B7* cDNA or the *ABCC3* cDNA into expression vectors pcDNA3.1/Hygro(-)- or pcDNA3.1/Zeo(-), for restriction analysis of subclonings of the *UGT2B7* cDNA and the *ABCC3* cDNA and restriction analysis of cloning of PCR amplified fragments. In addition, pMA-MRP3 was restricted to aid PCR amplification of the full-length *ABCC3* cDNA.

For the restriction of pMA-MRP3, 1 µg of pMA-MRP3 was incubated with 20 U of *Not*I in a reaction containing 5 µl of 10X SmartCut buffer and water added to a total volume of 50 µl. This reaction was incubated 80 minutes at 37 °C.

Reactions that were set up for subcloning of the *UGT2B7* cDNA into pcDNA3.1/Hygro(-)-vector, contained 4-9 µg of vectors pGEM-T-UGT2B7(802C) or pcDNA3.1/Hygro(-), 100-150 U of *Apa*I or 30 U of *Bst*XI or 20-40 U of *Not*I and 5 µl 10X CutSmart buffer for *Apa*I and *Not*I or 5 µl 10X NEBuffer 3 supplemented with 5 µg of BSA for *Bst*XI. Total volume of reactions were 50 µl and they were incubated overnight at 37 °C for *Bst*XI and *Not*I or at 25 °C for *Apa*I reactions.

Reactions that were set up for subcloning of the *UGT2B7* cDNA into pcDNA3.1/Zeo(-)-vector, contained 3-7 µg of vectors pGEM-T-UGT2B7(802C) or pcDNA3.1/Hygro(-)-vector, 50-250 U of *Apa*I or 20-100 U of *Pst*I and 5 µl 10X CutSmart buffer for *Apa*I or 5 µl 10X NEBuffer 3 supplemented with 5 µg of BSA for *Pst*I in a total volume of 50 µl. Reactions were incubated 9 hours or overnight at 37 °C.

For subcloning of *ABCC3* cDNA, 3.5 µg of pcDNA3.1/Hygro(-) was restricted with 40

U of *Not*I and 45 U of *Kpn*I for 4.5 hours at 37 °C. *Not*I restriction contained 5 µl 10X CutSmart buffer and *Kpn*I restriction contained 5 µl 10X NEBuffer 1 supplemented with 5 µg of BSA. 5 µg of pCR2.1-TOPO-MRP3 was restricted with 5 U of *Not*I, 15 U of *Kpn*I and 5 µl 10X NEBuffer 2 supplemented with 5 µg of BSA. This reaction was incubated for 6 hours at 37 °C. Reaction volumes were 50 µl in both cases.

For the analysis of clonings of PCR amplifications, 9 µl of plasmid isolation was restricted with 1 µl of 10X *Eco*RI-HF Re-Mix in a total volume of 10 µl at 37 °C for 30-90 minutes.

All other restriction analysises were performed with 1-2 µg of plasmid DNA in a reaction with either *Eco*RI or *Bam*HI. 1-2 µl of *Eco*RI-HF RE-Mix was used for *Eco*RI restrictions in a total volume of 10-20 µl. *Bam*HI restrictions were supplemented with 10-20 U of the enzyme and 1-2.5 µl 10X SmartCut buffer in a total volume of 10-25 µl.

3.2.13 DNA dephosphorylation

To avoid religations in subcloning reaction of the *UGT2B7* cDNA into *Not*I restricted pcDNA3.1/Hygro(-)-vector, the vector was dephosphorylated. The dephosphorylation reaction was conducted by addition of 6 µl 10 X Antarctic phosphatase reaction buffer and 5-20 U of Antarctic phosphatase directly to the *Not*I restriction of the vector. The reaction was incubated 15-20 minutes at 37 °C and the phosphatase was heat-inactivated subsequently for 5 minutes at 65 °C.

3.2.14 DNA ligation

Before ligation, gel-purified cDNA fragments and the respective expression vectors were analysed by agarose gel electrophoresis and concentrations of both were estimated. In all ligation reactions, the concentration of the vector and the insert cDNA varied between 20-60 ng and 20-100 ng, respectively. Total concentration of DNA in ligation reactions varied between 40-120 ng of DNA. Ratios between expression vector and insert were 1:2-

1:4 and 1:2-1:9 for the *ABCC3* cDNA and the *UGT2B7* cDNA ligation reactions, respectively. In addition, control ligation reactions were occasionally added by excluding insert from the ligations reaction to check religations.

Two different ligation methods were used in this study: T4 DNA quick ligase and T4 DNA ligase. Ligations with T4 DNA quick ligase were conducted in the reaction volume of 20 µl containing 10 µl 2X of quick ligase reaction buffer, appropriate amount of DNA diluted with water in a volume of 10 µl and 1 µl quick T4 ligase corresponding to 2 000 U. Ligations were incubated 5-10 minutes at 25 °C and after the incubation, the reactions were cooled down on ice. T4 DNA ligase reactions contained 2 µl 10X reaction buffer, appropriate amount of DNA diluted with water to a total volume of 18 µl and 1 µl of T4 DNA ligase corresponding to 400 U. Reactions were incubated overnight at 16 °C and subsequently heat-inactivated for 10-15 minutes at 65 °C and cooled down on ice.

Ligation reactions for *ABCC3* cDNA into pcDNA3.1/Hygro(-) or for *UGT2B7* cDNA into pcDNA3.1/Zeo(-) were transformed to XL-1 Blue supercompetents cells (see 3.2.15). All the other ligation reactions were transformed to XL-10-Gold ultracompetent cells (see 3.2.15).

3.2.15 Plasmid transformation

Three different competent cells were used in this study: One Shot TOP10, XL-10-Gold ultracompetent and XL-1 Blue supercompetent. The TOP10 cells were used only for transformations of PCR amplifications cloned into the pCR2.1-TOPO-vector. The other two competent cells were used for transformations of mutagenesis and ligation reactions.

PCR amplifications cloned in the pCR2.1-TOPO-vector were transformed into One Shot TOP10 cells according to the instructions of the manufacturer. Briefly, 3 µl of the cloning reaction was transferred to tube containing 50 µl of competent cells that were thawed on ice. Transformation reaction was incubated 30 minutes on ice and heat-shocked for 30 seconds at 42 °C in water-bath. After the heat-shock, the transformation was cooled down for 2 minutes on ice and subsequently 250 µl of S.O.C.-medium (room temperature) was added into the tube. The transformation reaction was further incubated 1 hour at 37 °C.

A 100 µl aliquot and the rest of the transformation reaction was plated onto agar plates supplemented with 100 µg/ml ampicillin and pre-warmed to 37 °C. In addition, plates were spread beforehand with 40 µl of 40 mg/ml X-β-Gal DMF-solution, corresponding to 1.6 mg of X-β-Gal per plate, for α-complementation test. Plates were incubated at 37 °C for 20-24 hours.

Transformations into XL-10-Gold ultracompetent cells were done according to the instructions of the manufacturer with slight modifications. Briefly, 50 µl of the cells were thawed on ice and transferred to a 13 ml pre-cooled tube. 2 µl of the β-mercaptoethanol mixture was transferred to the cells and tubes were gently shaked every two minutes for 10 minutes during incubation on ice. 2 µl of the ligation or 1.5 µl of the mutagenesis reaction was transferred to the cells, shaked gently and incubated 30 minutes on ice. Transformation reaction was subsequently heat-shocked 30 seconds at 42 °C in water-bath, cooled down on ice for 2 minutes and 450 µl of preheated (42 °C) S.O.C.-medium was applied to the cells. Transformation reaction was incubated 1 hour at 37 °C. A 100 µl aliquot and the rest of the transformation reaction was plated onto 37 °C pre-warmed agar plates supplemented with 100 µg/ml ampicillin. Plates were incubated for 16-20 hours at 37 °C.

Tranformations into XL-1 Blue supercompetent cells were done according to the instructions of the manufacturer with slight modifications. Briefly, 50 µl of the cells were thawed on ice and transferred to a 13 ml pre-cooled tube on ice. 0.85 µl of the β-mercaptoethanol mixture was transferred to the cells and tubes were gently shaked every two minutes for 10 minutes during incubation on ice. 5 µl of ligation reaction was transferred to the cells, shaked gently and incubated further 30 minutes on ice. Transformation reaction was heat-shocked 45 seconds at 42 °C in water-bath, cooled down on ice for 2 minutes and 450 µl of preheated (42 °C) S.O.C.-medium was applied to the cells. Transformation reaction was incubated 1 hour at 37 °C. A 100 µl aliquot and the rest of the transformation reaction was plated onto 37 °C pre-warmed agar plates supplemented with 100 µg/ml ampicillin. Plates were incubated for 20-24 hours at 37 °C.

3.2.16 Site-directed mutagenesis

For the correction of base pair exchange in the vector pcDNA3.1/Zeo(-)-UGT2B7(1575T), two commercial mutagenesis kits were used: QuickChange multi-site-directed kit with XL-10-Gold ultracompetent cells (Kit I) and QuickChange II site-directed kit with XL-1 Blue supercompetent cells (Kit II). Three reactions (I-III) were conducted with Kit I and nine reactions (I-IX) and one control reaction with Kit II.

Mutagenesis reactions with Kit I were prepared according to instructions of the manufacturer. Three different experimental setups were carried out with Kit I. Reactions I and II consisted of 100 ng of the pcDNA3.1/Zeo(-)-UGT2B7(1575T)-vector, 100 ng of oUGT2B7-Mut-F-primer, 2.5 µl 10 X QuickChange Multi reaction buffer, 0.5 µl QuickSolution, 1 µl deoxynucleotide mix, 1 µl QuickChange Multi enzyme blend and water added to total reaction volume of 25 µl in a PCR-tube. Reaction III was same as reactions I and II, but consisted of 50 ng of the pcDNA3.1/Zeo(-)-UGT2B7(1575T)-vector, 150 ng of oUGT2B7-Mut-F-primer and DMSO was added to final concentration of 10 %. Reactions were run in the thermocycler as described in Table 20. After the thermocycler reaction, 1 µl of *Dpn*I was added to the reactions and reaction I and II were incubated for 1 hour and the reaction III for 1.5 hours at 37 °C. 1.5 µl of every reaction was transformed into XL-10-Gold ultracompetent cells as described in 3.2.15. 100 µl and 250 µl aliquots of the transformation reaction were plated onto agar plates supplemented with 100 µg/ml ampicillin.

Table 20. Thermocycler parameters for mutagenesis reactions with Kit I. Panel A describes parameters for reactions I and II and panel B describes parameters for reaction III.

A

TEMPERATURE	TIME	
95 ˚C	60 seconds	
95 ˚C	60 seconds	30 cycles
55 ˚C	60 seconds	
65 ˚C	14 minutes	
65 ˚C	5 minutes	

B

TEMPERATURE	TIME	
98 ˚C	90 seconds	
98 ˚C	90 seconds	30 cycles
65 ˚C	15 minutes	
65 ˚C	5 minutes	

4 ˚C	Until sample was analyzed	4 ˚C	Until sample was analyzed

Mutagenesis reactions with Kit II were prepared according to instructions of the manufacturer. Briefly, reactions consisted of 5 µl of 10X reaction buffer, 5-150 ng of pcDNA3.1/Zeo(-)-UGT2B7(1575T)-vector, 125-200 ng of both oUGT2B7-Mut-F- and oUGT2B7-Mut-R-primers, 1 µl deoxynucleotide mix, 1 µl PfuUltra High-Fidelity DNA polymerase and water was added to a final reaction volume of 50 µl in a PCR-tube. Together nine different reactions were performed (Table 21). Reaction conditions for each reaction are described in Table 21. Reactions were run in the termocycler according to parameters in Table 22. After the thermocycler reaction, reactions were incubated with 1 µl *Dpn*I for 1 hour or 1.5 hours (reactions VII and IX) at 37 °C. Reactions were transformed into XL-1 Blue supercompetent cells as described in 3.2.15 and Table 21. Transformations of reactions I-VII were not incubated for 10 minutes with β-mercaptoethanol mixture, because this step was not included in the mutagenesis protocol provided by the manufacturer. 100-500 µl aliquots of the transformation reactions were plated onto agar plates supplemented with 100 µg/ml of ampicillin.

The control reaction was performed according to instructions of the manufacturer.

Table 21. Reaction setups for Kit II –mutagenesis reactions.
*Reaction was precipitated according to 3.2.21 before the transformation. #Reaction was transformed in XL-10-Gold ultracompetent cells according to 3.2.15.

REACTION	**I**	**II**	**III**	**IV**	**V**	**VI**	**VII**	**VIII**	**IX**
Amount of the template	5 ng	20 ng	150 ng	5 ng	25 ng	50 ng	50 ng	25 ng	25 ng
Amount of each primer	125 ng	125 ng	125 ng	125 ng	125 ng	125 ng	125 ng	150 ng	200 ng
Final concentration of DMSO	0 %	0 %	0 %	0 %	0 %	0 %	5 %	10 %	10 %
Amount of transformed	1 µl and 30 µl*	1 µl and 30 µl*	3 µl, 4 µl and 36 µl*	1 µl	1 µl	4 µl and 36 µl*	4 µl and 45 µl#	50 µl*	50 µl*

Table 22. Thermocycler parameters for mutagenesis reactions with Kit II. Panel A describes parameters for reactions I-VI and panel B describes parameters for reaction VII-IX. *In reaction IX 45 seconds and 16 cycles was used instead of 30 seconds and 12 cycles.

A

TEMPERATURE	TIME	
95 ˚C	30 seconds	
95 ˚C	30 seconds	12 cycles
55 ˚C	60 seconds	
68 ˚C	7 minutes	
4 ˚C	Until sample was analyzed	

B

TEMPERATURE	TIME	
98 ˚C	30 seconds*	
98 ˚C	45 seconds	12* cycles
68 ˚C	8 minutes	
4 ˚C	Until sample was analyzed	

3.2.17 Bacterial cultures

For preparation of plasmids, a single colony was picked with a pipette tip from agar plates and transferred to 13 ml tubes containing 5 ml LB-medium supplemented with 50 µg/ml ampicillin. The culture was incubated overnight at 37 °C with shaking. In the case of over day incubation, 2 ml of the respective media were used instead of 5 ml and incubation was carried out for 6-8 hours.

3.2.18 Permanent bacterial culture

For permanent bacterial cultures, a fresh overnight bacterial culture was established by transferring approximately 10 µl of an appropriate bacterial culture to 5 ml of fresh LB-medium supplemented with 50 µg/ml ampicillin. The culture was incubated overnight at 37 °C. After the incubation, 600 µl of culture was supplemented with 400 µl of sterile glycerol in 1.5 ml micro tube with assembled cap, vortex mixed and stored at -80 °C.

3.2.19 Plasmid isolation

Two different plasmid isolation procedures were used in this study; a commercially available plasmid extraction kit (PureYield Plasmid Miniprep System) and the plasmid extraction method described by Holmes and Quigley (1981). The former was used when plasmid was prepared for sequencing, transfection or cloning reactions. The latter was used for analysis of cloning reactions or mutagenesis.

The PureYield Plasmid Miniprep System plasmid extraction kit was used according to instructions of the manufacturer. Briefly, 3 ml (in two 1.5 ml aliquots) of overnight bacterial culture was centrifuged at 20 000 g for 30 seconds in 1.5 ml micro tube. The supernatant was removed and the pellet suspended in 600 µl of water. 100 µl of lysis buffer was added to the suspension and mixed gently turning up and down the tube three times. This was followed by addition of 350 µl of neutralization solution and inverting the tube 6-10 times. The tube was centrifuged at 20 000 g for 3 minutes and the resulting supernatant was loaded onto column and eluted in vacuum manifold. The column was washed with 200 µl of endotoxin removal solution and 400 µl of wash solution. This was followed by 1 minute centrifugation of the column at 20 000 g. DNA was eluted with 32 µl of water by incubating 1 minute at room temperature and 15 seconds centrifugation at 20 000 g.

For plasmid isolations according to Holmes and Quigley (1981), 1.5 ml of overnight culture was centrifuged 5 minutes at 2 000 g in 1.5 ml micro tube. The supernatant was removed and the pellet was suspended in 200 µl of STETL-solution. The tube was incubated in boiling water for 35 seconds and centrifuged 10 minutes at 16 000 g. The resulting cell debris was removed by a toothpick and 200 µl of isopropanol was added to precipitate plasmid DNA. The precipitation was centrifuged at 4 °C and at 18 000 g for 30 minutes. After the centrifugation, the supernatant was removed, the pellet was airdried at room temperature for 10-20 minutes and dissolved in 50 µl of water containing 1.8 U/ml of ribonuclease A.

3.2.20 DNA and RNA concentration measurement

2 µl of DNA or RNA was diluted by a factor of 40 with water into a total volume of 80 µl. This solution was transferred to quartz cuvette and UV absorbance was measured at 260 nm and 280 nm in spectrophotometer. Water was used as a blank sample for all measurements. Concentration of DNA or RNA was based on the absorbance at 260 nm. Purity of DNA or RNA was evaluated based on ratio of absorbance at 260 nm and 280 nm.

3.2.21 DNA purification

DNA-fragment purification was performed after gel electrophoresis of PCR amplified cDNA fragments or restriction reactions. In addition, when sequential restrictions were done and one buffer was not compatible for both reactions, DNA-fragments were purified.

cDNA fragments or restricted plasmids of interest were cut out of the agarose gel with a scalpel and transferred into dialysis tubing and filled with 200-600 µl of 1X TAE-buffer. Tubing was sealed at both ends and placed in the gel electrophoresis cell containing 1X TAE. The gel inside the tube was placed at the edge near the cathode of the electrophoresis cell to aid transfer of DNA out of the gel into buffer. Dialysis was run for 60 minutes at 60 V. After the run, the solution was transferred to 1.5 ml micro tube and DNA was precipitated by adding 1/10 of total volume of 3 M sodium acetate pH 4.8 and absolute ethanol 3 times of a total volume. The precipitation was incubated at least 30 minutes at -20 °C but also incubations over night or over weekend were conducted. The incubation was followed by 21 000 g centrifugation at 0 °C for 30 minutes. Finally, the supernatant was removed, the pellet was washed by up and down pipetting 200 µl of 70 % ethanol and dried at room temperature. The pellet was dissolved in appropriate volume of water before use for next reaction.

3.2.22 DNA sequencing

Samples for DNA sequencing were prepared in 1.5 ml microtubes and contained 800 ng of the plasmid of interest, 1.4 µM final concentration of the primer used for sequencing and water added to total volume of 14 µl. Samples were sequenced by LGC Genomics GmbH (Berlin, Germany).

3.2.23 Agarose gel electrophoresis

Gel electrophoresis analysis of DNA fragments was performed in 0.8 % or 1.5 % agarose gels. 1.5 % agarose gels were used only for the analysis of qPCR-reactions. A typical sample volume loaded onto gel was 12 µl per well and it contained appropriate amount of DNA (typically 400-600 ng), a restriction or a plasmid isolation and 2 µl 6X gel loading dye. In the case of DNA purifications, larger volumes were loaded onto the gel. These volumes were in the range of 15-30 µl and contained 1/6 of a total volume 6X gel loading dye. In addition, 10 µl DNA marker, corresponding to 1 µg of DNA, was loaded onto every gel. The length of bands and amount of DNA per band in DNA markers are presented in Figure 6. Gels were run in electrophoresis chamber filled with 1X TAE-buffer for 40-100 minutes at 100 V, or at 120 V in the case of larger gel. After the run, gel was stained for 3-4 minutes with ethidium bromide water solution. Staining was followed by one brief and a second 6-10 minutes wash with tap water. Gels were visualized under UV-light of 312 nm and digitally photographed.

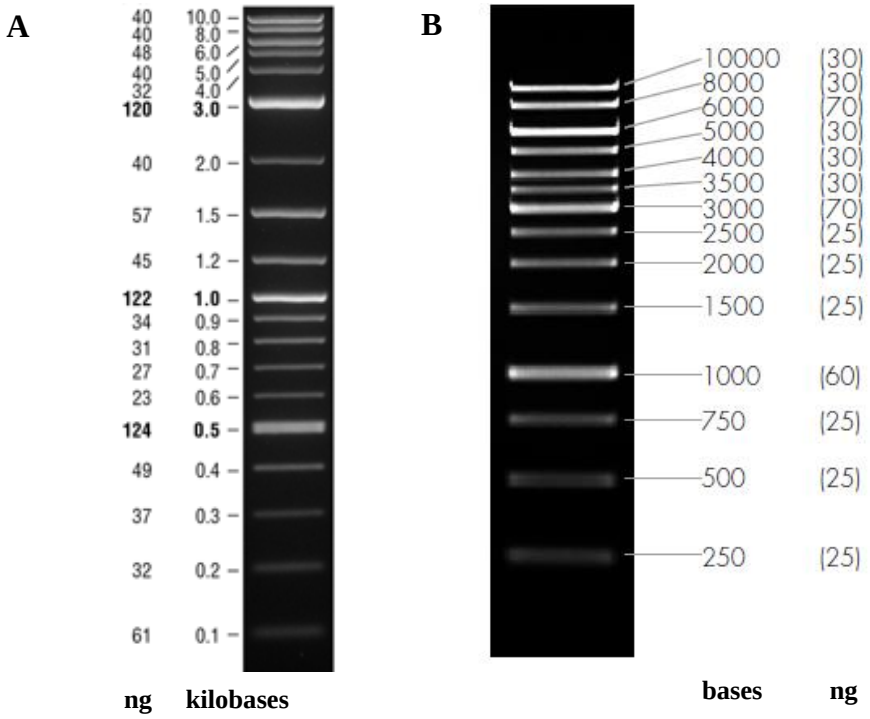

Figure 6. Length and amount of DNA fragments of 2-log (A) and 1 kb (B) DNA ladder (www.neb.com; www.peqlab.de).

4. RESULTS

4.1 Cloning of the human *UGT2B7* cDNA

To establish a stable expression of a human protein in mammalian cells, an expression vector containing the cDNA encoding the protein of interest has to be generated. For this purpose, the cDNA has to be cloned, sequenced (and corrected if it contains base pair exchanges) and subsequently subcloned into expression vector. Here, mammalian expression vectors pcDNA3.1/Hygro(-) and pcDNA3.1/Zeo(-) were chosen for the expression of *UGT2B7* cDNA. For the amplification of the *UGT2B7* cDNA, kidney and liver sscDNAs were used (4.1.1). In addition, in-house generated vectors pGEM-T-UGT2B7(802C) and pcDNA3.1/Zeo(-)-UGT2B7(1575T) were available. However, both vectors contained a base pair exchange compared to reference sequence of *UGT2B7*. Because of that, they had to be corrected before using them for the expression

of UGT2B7 (4.1.5). In addition, pGEM-T-UGT2B7(802C) is a subcloning vector and is suitable only as a source for the *UGT2B7* cDNA that has to be cloned in one of the expression vectors before transfecting mammalian cells (4.1.3-4). However, *UGT2B7* cDNA could be amplified using pGEM-T-UGT2B7(802C) as the template and subsequently subcloned into another cloning vector such as the pCR2.1-TOPO, which would allow to use multiple different cloning strategies compared to pGEM-T-UGT2B7(802C)-vector (4.1.2).

4.1.1 Amplification of the *UGT2B7* cDNA using liver or kidney sscDNA as the template

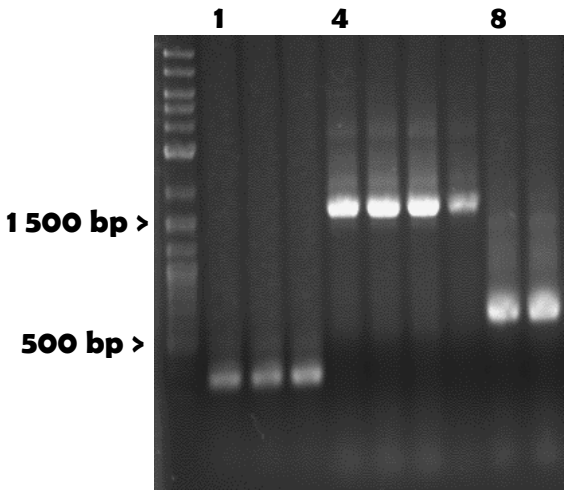

Figure 7. Amplification of the *UGT2B7* cDNA fragments and the *β-actin* cDNA fragment using kidney sscDNA as the template. The amplified cDNA fragments are the control fragment of *UGT2B7* (lanes 1-3), the *UGT2B7* (lanes 4-7) and the *β-actin* fragment (lanes 8-9).

UGT2B7 is expressed in intestine, liver and kidney (Sato et al. 2014). Therefore, total RNA of all these tissues could be used as a template for the amplification of the 1690 bp protein coding sequence of the *UGT2B7* cDNA. Attempts to amplify the *UGT2B7* cDNA from liver sscDNA did not succeed, although the β-actin control reaction gave an amplification product (results not shown). However, the amplification of the *UGT2B7* cDNA fragment was successful when using kidney sscDNA (Figure 7). In addition, two control reactions were included in the same experiment; amplification of the β-actin cDNA fragment (661 bp) and amplification of the 393 bp control fragment of the *UGT2B7* cDNA (Figure 7). The amplified 1600 bp cDNA fragment of *UGT2B7* was subcloned into the pCR2.1-TOPO-vector and 32 transformants were analyzed after the transformation (results not shown). Restriction analysis was further conducted with *Bam*HI and *Eco*RI for two transformants.

The *UGT2B7* cDNA contains an internal restriction site for both enzymes (Appendix 3). In addition, pCR2.1-TOPO contains an internal *Bam*HI restriction site and two internal *Eco*RI restriction sites at the both ends of the cloned PCR fragment. Restriction analysis of pCR2.1-TOPO-UGT2B7 with *Bam*HI should result in 1210 bp and 4370 bp fragments. On the other hand, *Eco*RI digestion of the plasmid should result in 309 bp, 1360 bp and 3910 bp fragments.

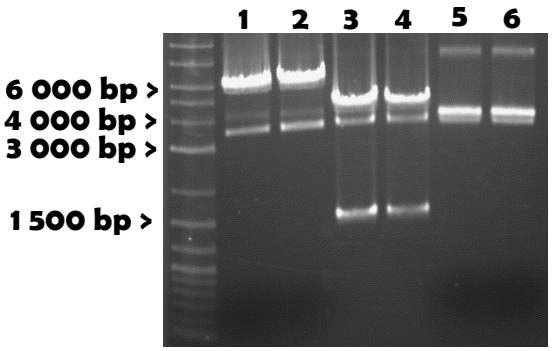

Figure 8. Restriction analysis of pCR2.1-TOPO-UGT2B7 transformants 1 and 2. The *UGT2B7* cDNA was cloned using kidney sscDNA as the template. Lane 1 and 2 are *Bam*HI restriction analyses of transformant 1 and 2, respectively. Lane 3 and 4 are *Eco*RI restriction analyses of transformant 1 and 2, respectively. Lanes 5 and 6 are unrestricted plasmids 1 and 2, respectively.

The results of the restriction analysis are shown in Figure 8. *Bam*HI digestions of both transformants resulted in a 6000 bp fragment and *Eco*RI digestions resulted in 4000 bp and 1500 bp fragments. These results are not in agreement with the expected fragment lengths (see above). In addition, both transformants were sequenced (T7-promoter-primer) including sequencing of transformant 1 also with oUGT2B7-seq1-primer. No sequence could be detected for the sequencing with the oUGT2B7-seq1, which indicates absence of the *UGT2B7* cDNA. Even though two other sequencing analyses gave same results, no *UGT2B7* cDNA was observed in this sequence. An alignment of the sequence corresponded with the sequence between bp 922-1989 in the expression vectors pcDNA3.1/Zeo(-) and pcDNA3.1/Hygro(-). Cloning was repeated and 20 additional transformants were analyzed. Similar results were obtained with the restriction analysis and no positive clones could be generated (results not shown)

4.1.2 Amplification of the *UGT2B7* cDNA using pGEM-T-UGT2B7(802C) as the template

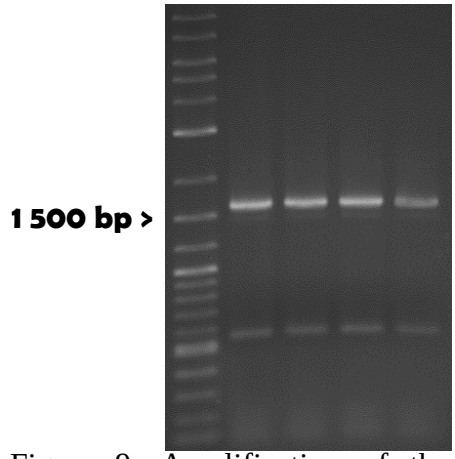

Figure 9. Amplification of the *UGT2B7* cDNA using pGEM-T-UGT2B7(802C)-plasmid as the template. 1700 bp bands correspond to the length of the *UGT2B7* cDNA.

Because the amplification of the *UGT2B7* cDNA was not successful when using liver or kidney sscDNA as the template, attempts were made to amplify it using in-house available pGEM-T-UGT2B7(802C)-vector as the template. Although this cDNA contains a base pair exchange compared to reference sequence, it could be corrected when the cDNA is subcloned into the expression vector.

The amplification was successful only in one experiment (Figure 9). The amplified fragment was subsequently cloned into pCR2.1-TOPO and 10 transformants were analyzed with *Eco*RI restriction analysis (Figure 10).

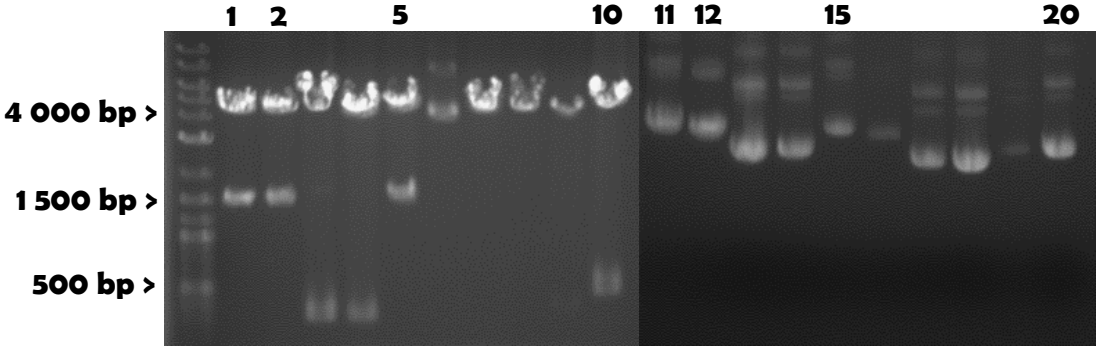

Figure 10. *Eco*RI restriction analysis of transformant from the cloning of PCR amplified *UGT2B7* cDNA. Lanes 1-10 and Lanes 11-20 are *Eco*RI restriction analyzed and unrestricted transformants, respectively. Lanes 1 and 11 and lanes 2 and 12 are transformants 1 and 2, respectively.

The *UGT2B7* cDNA contains an internal *Eco*RI restriction site and two *Eco*RI restriction sites are located at the both ends of the cloned cDNA fragment in the pCR2.1-TOPO-plasmid (Appendix 3). Therefore, *Eco*RI digestion of pCR2.1-TOPO-UGT2B7 is expected to result in 309, 1360 and 3910 bp fragments. Even the shortest fragment was not visible in the restriction analysis, longer fragments showed the correct lengths in the

case of three transformants (lanes 1, 2 and 5 in Figure 10). Transformants 1 and 2 were sequenced using T7-promoter-primer. Interestingly, both sequences were same and identical with sequences obtained using kidney sscDNA as the template (see 4.1.1).

4.1.3 Cloning of the *UGT2B7* cDNA from the pGEM-T-UGT2B7(802C) into expression vector pcDNA3.1(-)-Hygro

After unsuccessful amplifications of the *UGT2B7* cDNA, the cloning strategy was changed to restrict *UGT2B7* cDNA from the vector pGEM-T-UGT2B7(802C), ligate it into expression vector pcDNA3.1 and correct the base pair exchange. For the first strategy, the expression vector pcDNA3.1(-)-Hygro was used, which contains same unique restrictions sites as pGEM-T-UGT2B7(802C) (Appendix 3). These restriction sites, *Apa*I and *Bst*XI, allow ligation of the *UGT2B7* cDNA in the right orientation into expression vector, when both vectors are restricted with them.

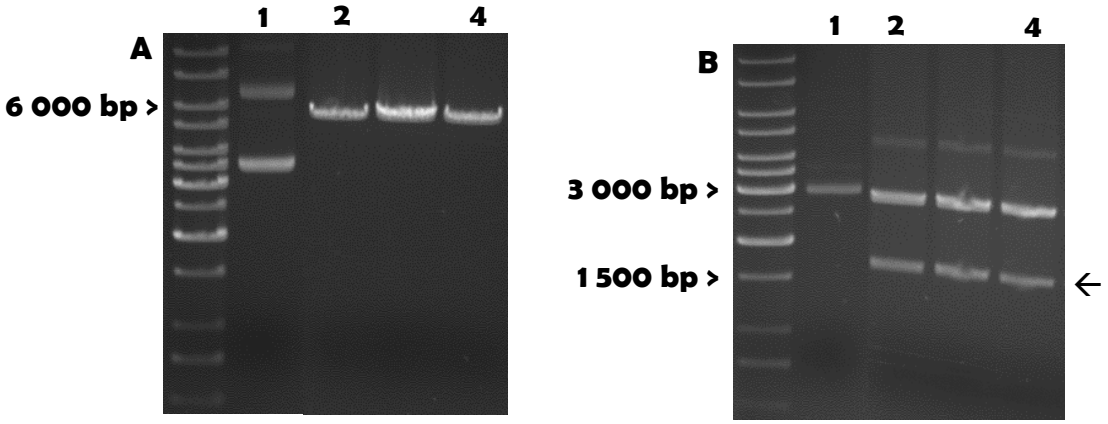

Figure 11. *Apa*I and *Bst*XI restrictions of the vectors pcDNA3.1(-)-Hygro (panel A) and pGEM-T-UGT2B7(802C) (panel B). Lanes 1 and 2-4 are unrestricted and restricted vectors, respectively. The arrow indicates the 1600 bp cDNA fragment of the *UGT2B7*.

Figure 11 shows *Apa*I and *Bst*XI restrictions of the vectors pcDNA3.1(-)-Hygro and pGEM-T-UGT2B7(802C). The correct length band, 1630 bp, corresponding to the *UGT2B7* cDNA was obtained (the arrow in Figure 11B). In addition, the restriction of pcDNA3.1(-)-Hygro showed the correct length of the vector, 5600 bp. Both DNA fragments were purified and ligated. Subsequent 100 transformants of the cloning

reaction were analysed by plasmid isolation and agarose gel electrophoresis analysis of plasmids. A representative analysis is shown in Figure 12. None of the analysed transformants showed significantly longer plasmids than the empty pcDNA3.1(-)-Hygro-vector. The cloning reaction was repeated and additional 60 transformants were analysed with the similar result (results not shown).

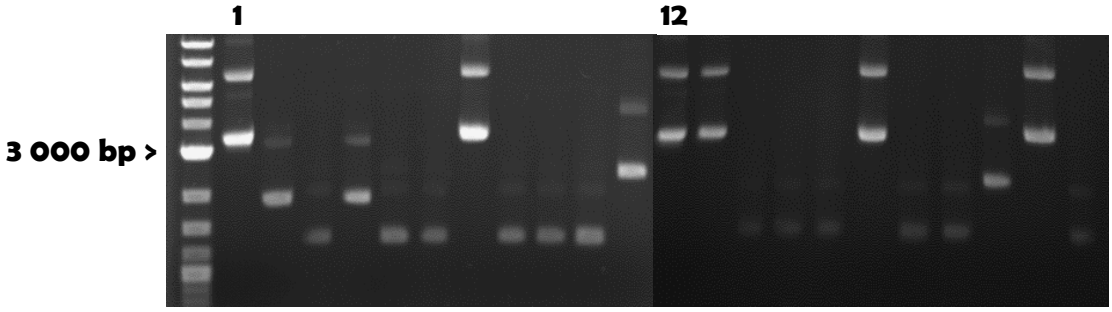

Figure 12. Agarose gel electrophoresis analysis of 20 transformants isolated from the cloning of the *UGT2B7* cDNA into pcDNA3.1(-)-Hygro. Lanes 1 and 12 are the empty vector pcDNA3.1(-)-Hygro.

As the second strategy, pGEM-T-UGT2B7(802C) and pcDNA3.1(-)-Hygro vectors were restricted with *Not*I that is not a unique restriction site for them. Because of that, the ligation reaction could result in two different orientations of the *UGT2B7* cDNA in pcDNA3.1(-)-Hygro and thus is less favorable than the first strategy with *Apa*I and *Bst*XI restrictions. A representative agarose gel electrophoresis analysis of transformants from the cloning reaction of *Not*I restricted *UGT2B7* cDNA into *Not*I restricted pcDNA3.1(-)-Hygro-vector is presented in Figure 13. This cloning reaction was repeated four times and all together 350 transformants were analysed. Interestingly, seven transformants showed similar length as transformant 11 and were longer in length than the empty vector pcDNA3.1/Hygro(-) (Figure 13). Because this cloning strategy could lead in two different orientations of the *UGT2B7* cDNA in the expression vector, restriction analysis was conducted. All the seven transformants were analysed with restriction analysis using *Eco*RI and *Bam*HI. In the correct orientation, the start codon of the *UGT2B7* cDNA locates after the cytomegalovirus promoter and the restriction analysis should result in fragments of 297, 1360 and 4170 bp, and 534 and 6730 bp for *Eco*RI and *Bam*HI restrictions, respectively (Appendix 3). On the other hand, if the orientation of the *UGT2B7* cDNA in the expression vector is the wrong, the restriction analysis with *Eco*RI

should result in the same fragments but *Bam*HI restriction should result in fragments of 1240 and 6030 bp.

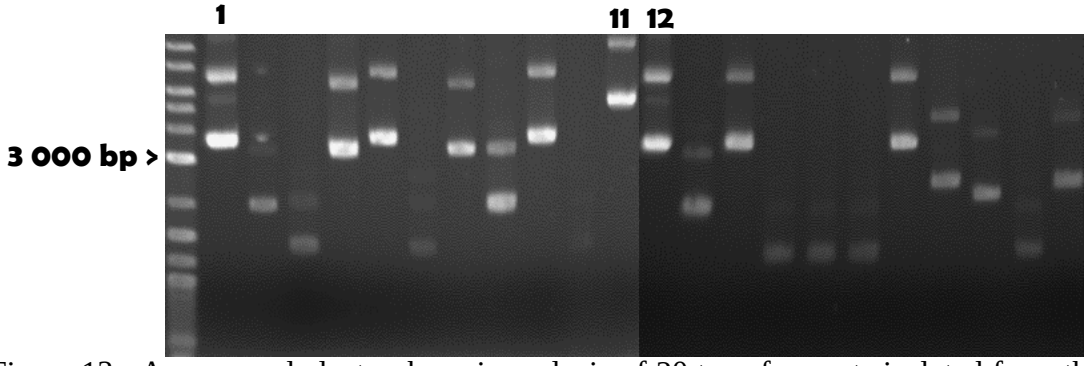

Figure 13. Agarose gel electrophoresis analysis of 20 transformants isolated from the cloning of the *UGT2B7* cDNA into pcDNA3.1(-)-Hygro using *Not*I restriction. Lanes 1 and 12 are the empty pcDNA3.1/Hygro(-)-vectors.

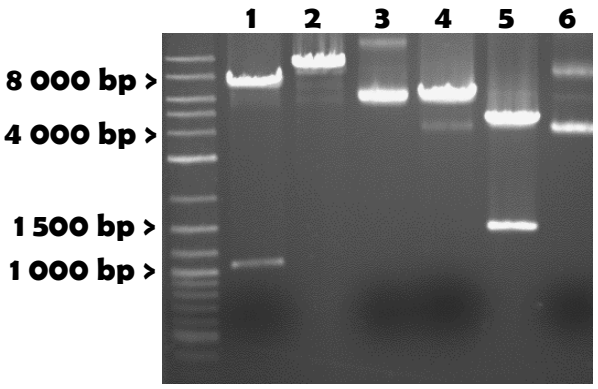

Figure 14. Restriction analysis of the empty pcDNA3.1(-)-Hygro-vector and transformant 11 (see Figure 13). Lanes 1-3 are, *Bam*HI, *Eco*RI and unrestricted transformant 11, respectively. Lanes 3-6 are *Bam*HI, *Eco*RI and unrestricted empty vector pcDNA3.1(-)-Hygro, respectively.

A representative agarose gel electrophoresis analysis of *Bam*HI and *Eco*RI restriction analysed transformant 11 and the empty vector pcDNA3.1/Hygro(-) is presented in Figure 14. *Eco*RI restriction linearized transformant 11 and did not show 1360 bp length fragment (lane 2 in Figure 14). However, the 1360 bp fragment was released when the empty vector pcDNA3.1(-)-Hygro was restricted with *Eco*RI (lane 5 in Figure 14). This result indicates that the transformant did not contain either pcDNA3.1(-)-Hygro-vector or the *UGT2B7* cDNA. Finally, two transformants were sequenced with T7-promoter-primer but in both cases, no clear DNA sequence could be detected. The fluorograms showed overlay of different sequences (results not shown).

4.1.4 Cloning of the *UGT2B7* cDNA from the pGEM-T-UGT2B7(802C) into expression vector pcDNA3.1(-)-Zeo

Because the subcloning of the *UGT2B7* cDNA into vector pcDNA3.1(-)-Hygro was not successful, another expression vector was chosen for the next attempt. pcDNA3.1(-)-Zeo contains unique restriction sites for *Apa*I and *Pst*I, which were not available in the vector pcDNA3.1(-)-Hygro (Appendix 3). In addition, the same restrictions sites are in the vector pGEM-T-UGT2B7(802C) and thus could be used for the subcloning of the *UGT2B7* cDNA into pcDNA3.1(-)-Zeo.

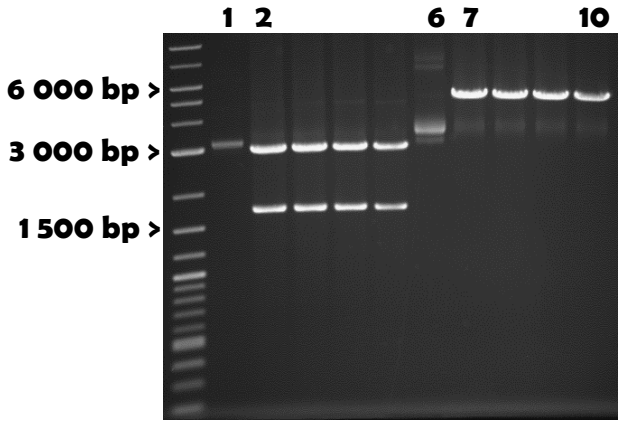

Figure 15. *Apa*I and *Pst*I restricted vectors pGEM-T-UGT2B7(802C) and pcDNA3.1/Zeo(-). Lane 1 and 6 are unrestricted pGEM-T-UGT2B7(802C) and pcDNA3.1/Zeo(-), respectively. Lanes 2-5 and lanes 7-10 are restricted pGEM-T-UGT2B7(802C) and pcDNA3.1/Zeo(-), respectively.

Figures 15 presents *Apa*I and *Pst*I restricted vectors pGEM-T-UGT2B7(802C) and the pcDNA3.1/Zeo(-). Restriction of the pGEM-T-UGT2B7(802C) resulted in 1700 bp fragment corresponding to the length of the *UGT2B7* cDNA (lanes 2-5 in Figure 15). In addition, *Apa*I and *Pst*I restriction of the pcDNA3.1/Zeo(-)-vector resulted in a 5000 bp fragment corresponding to the length of the vector (Lanes 7-10 in Figure 15). The DNA fragments were purified and subsequently ligated. Figure 16 shows a representative agarose gel electrophoresis analysis of 20 transformants isolated from the transformation. Altogether, 200 transformants were analyzed after all cloning attempts. All analyzed plasmids were of the same length as the empty pcDNA3.1/Zeo(-)-vector, but one transformant showed an insert in the vector (Lane 6 in Figure 16). This transformant was further analyzed with restriction analysis and sequencing.

Figure 17 presents restriction analysis of transformant 6 and the empty pcDNA3.1/Zeo(-)-vector with *Eco*RI and *Bam*HI. *Eco*RI and *Bam*HI restrictions of pcDNA3.1/Zeo(-)-UGT2B7 should result in fragments of 5010, 1360 and 277 bp, and 6170 and 480 bp,

respectively (Appendix 3). On the other hand, *Bam*HI and *Eco*RI are unique restriction sites of the empty pcDNA3.1/Zeo(-)-vector and the restrictions with them linearizes the vector and subsequently result in a 5000 bp fragment.

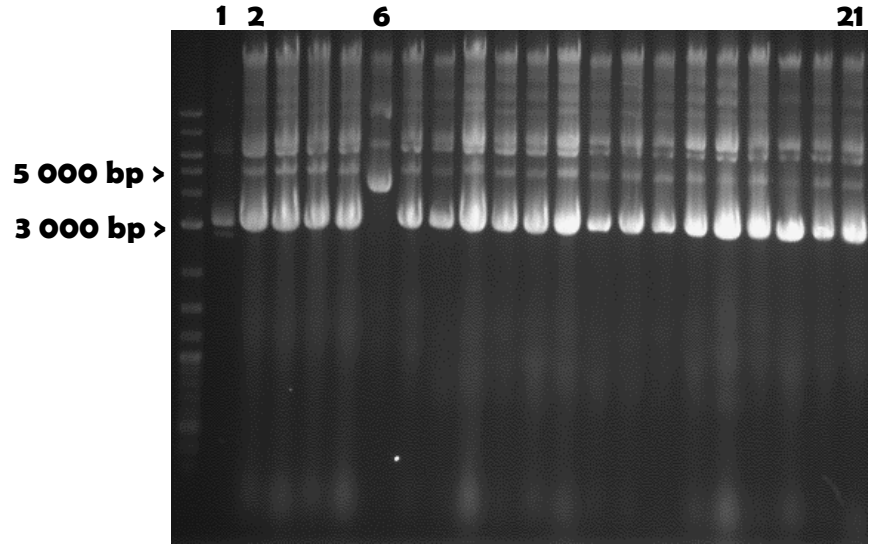

Figure 16. Agarose gel electrophoresis analysis of 20 transformants isolated from the cloning of the *UGT2B7* cDNA into pcDNA3.1(-)-Zeo. Lane 1 is the empty pcDNA3.1/Zeo(-) and lanes 2-21 are transformants.

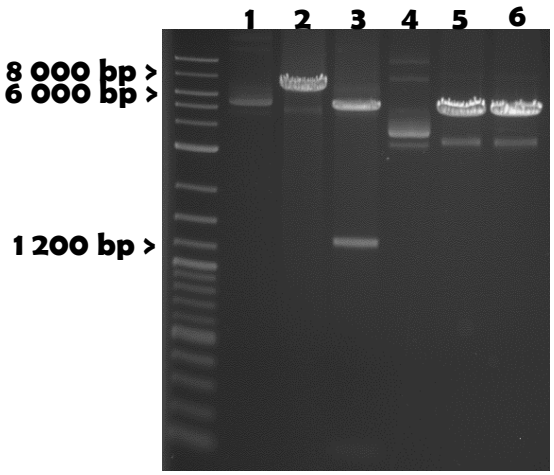

Figure 17. Restriction analysis of transformant 6 (see Figure 16) and the empty pcDNA3.1/Zeo(-)-vector. Lanes 1-3 are unrestricted, *Bam*HI and *Eco*RI restricted transformant 6, respectively. Lanes 4-6 are unrestricted, *Bam*HI and *Eco*RI restricted empty vector pcDNA3.1/Zeo(-), respectively.

*Bam*HI and *Eco*RI restriction analysis of transformant 6 did not correspond to the expected fragments (lanes 2 and 3 in Figure 17). In addition, sequencing of transformant 6 with T7-promoter and BGH-reverse primers resulted in no *UGT2B7* cDNA sequence but a sequence that aligned with genomic *E.coli* DNA (http://blast.ncbi.nlm.nih.gov, results not shown).

4.1.5 Site-directed mutagenesis of the vector pcDNA3.1/Zeo(-)-UGT2B7(1575T)

After unsuccessful amplifications (4.1.1 and 4.1.2) and subclonings (4.1.3 and 4.1.4) of the *UGT2B7* cDNA, the final strategy was to use the in-house available vector pcDNA3.1/Zeo(-)-UGT2B7(1575T). This vector contained a single base pair exchange (A to T) at site 1575 resulting in a premature stop codon of the *UGT2B7* cDNA sequence compared to the reference sequence (Genbank accession NM_001074.2). To achieve the correct sequence, a site-directed mutagenesis reaction was conducted for the vector. For this purpose, two different commercially available mutagenesis kits were used.

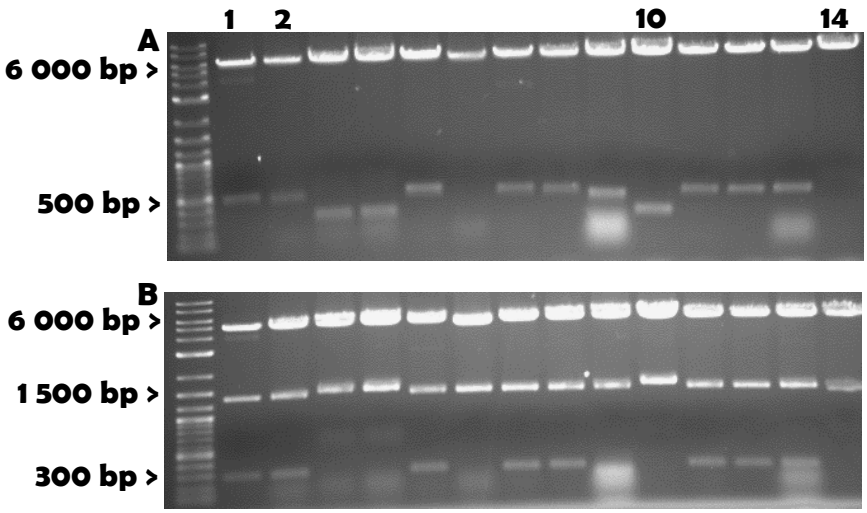

Figure 18. Restriction analysis of selected transformants from the base pair exchange reaction for the pcDNA3.1/Zeo(-)-UGT2B7(1575T). Panel A presents *Bam*HI restrictions and panel B *Eco*RI restrictions. Lane 1 is the template pcDNA3.1/Zeo(-)-UGT2B7(1575T)-vector and lanes 2-14 are transformants from the mutagenesis reaction.

Three reactions were conducted with QuickChange multi-site-directed mutagenesis kit. Reactions with three-step thermocycler protocol and without additional DMSO supplement in the reaction resulted in hundreds of colonies on the plates after the transformation of the mutagenesis reaction. On the other hand, reactions with the two-step thermocycler protocol and 10 % DMSO supplemented reaction, only dozens of colonies were detected after the transformation. Together 22 transformants were sequenced from all reactions with QuickChange multi-site-directed mutagenesis kit and none of them showed the correct T1575A exchange but only the original uncorrect (1575A) sequence.

Another mutagenesis kit, QuickChange II site-directed, was also used from the same manufacturer. Together nine reactions were conducted with this kit. These reactions

resulted in less than 10 colonies on the plates after the transformation. Due to that, subsequent reactions were purified before the transformation and the whole reactions were transformed to achieve higher amount of the colonies. This method resulted in a couple of tens of colonies. However, all sequenced transformants showed no the correct base pair exchange (14 samples) or showed the correct base pair exchange (3 samples) but also a deletion of the coding sequence of the *UGT2B7* cDNA after or before the mutagenesis primer binding sites. In addition, *Eco*RI and *Bam*HI restriction analysis was conducted for 13 transformants from the base pair exchange reactions (Figure 18). Restriction analysis of the pcDNA3.1/Zeo(-)UGT2B7(1575T/A) with *Eco*RI and *Bam*HI should result in fragments of 5010, 1360 and 277 bp, and 6170 and 480 bp, respectively (Appendix 3). However, *Eco*RI restriction analysis resulted in no fragment of 277 bp or a shorter fragment in half of the analysed transformants (lanes 3, 4, 6, 9, 10 and 14 in Figure 18). In addition, *Bam*HI restriction analysis gave similar results; no 480 bp fragment or shorter fragment. These results are in agreement with the sequencing results that showed a deletion of the *UGT2B7* cDNA coding sequence.

4.2 Cloning of the *ABCC3* cDNA encoding the human MRP3

MRP3 is expressed in liver and thus total RNA of this tissue could be used as the source of the *ABCC3* cDNA encoding MRP3 (König et al. 1999a). In addition, later during the study, the pMA-MRP3-plasmid that contains the *ABCC3* cDNA, was available. Amplification of the *ABCC3* cDNA was tried using liver sscDNA or the pMA-MRP3-plasmid as the templates. To coexpress MRP3 with UGT2B7 or UGT1A1 and MRP2, the pcDNA3.1/Hygro(-)-vector was chosen for the expression of the *ABCC3* cDNA. To establish a double- or triple-transfected cell line, all the cDNAs of interest should be cloned in different expression vectors containing different antibiotic resistance genes for the selection of transfected cell lines. The *UGT1A1* cDNA was cloned into pcDNA3.1/Hygro(-)-vector and MRP2 expressing cell line contains G418 resistance.

4.2.1 Cloning of the *ABCC3* cDNA using liver sscDNA as the template

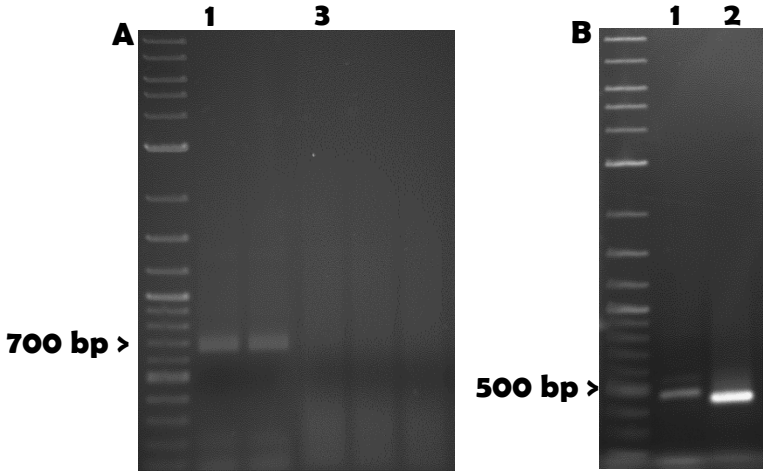

Figure 19. Amplification of the full-length *ABCC3* cDNA (panel A, lanes 3-6) and a β-actin fragment (panel A, lanes 1-2) using liver sscDNA as the template. Amplification the *ABCC3* cDNA control fragment using liver sscDNA (panel B, lane 1) or pCR2.1-TOPO-MRP3-part-plasmid (panel B, lane 2).

Amplification of the full-length *ABCC3* cDNA should result in cDNA fragment of 4620 bp in length. However, several experiments using liver sscDNA resulted in no product (panel A in Figure 19). Amplification of the 661 bp fragment of *β-actin* cDNA was included as a control reaction. In addition, a 450 bp fragment of 3'-end of the *ABCC3* cDNA was also included as a control fragment to the amplification reaction using liver sscDNA and a plasmid that includes this cDNA fragment (panel B in Figure 19). Both control reactions resulted in an amplification product.

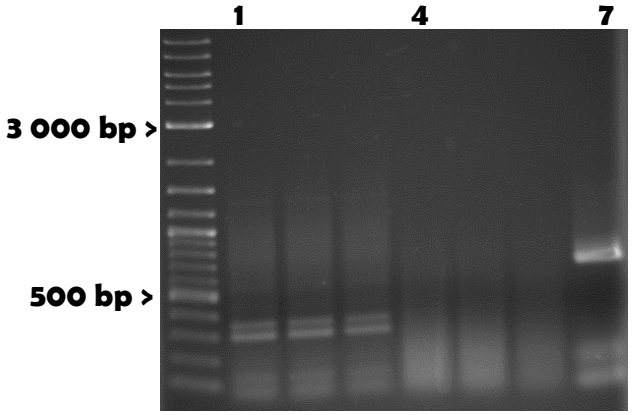

Figure 20. Amplification of 5'-part (lanes 1-3) and 3'-part (lanes 4-6) fragments of the *ABCC3* cDNA using liver sscDNA. Lane 7 represents amplification of the *β-actin* cDNA fragment.

Because the amplification of the full length *ABCC3* cDNA did not result in a correct amplification product, a two fragment amplification strategy was attempted. Primers were designed for amplification of the 5'-part and the 3'-part fragments of the *ABCC3* cDNA corresponding to length of 2470 bp and 2460 bp, respectively. However, the amplification of the both fragments using liver sscDNA resulted in no correct length fragments (Figure 20). The amplification of the control *β-actin* cDNA fragment resulted in the correct

amplification product. In addition to the standard PCR conditions, 3 % DMSO was included into the reaction but it did not have any effect on the amplification (results not shown). Futhermore, amplification of the 3'-part fragment was further tried using two-step PCR conditions and with a liver sscDNA prepared in-house from total RNA isolated from a cryopreserved liver tissue. No amplification was achieved in the presence of 3 % DMSO or without DMSO (results not shown).

4.2.2 Amplification of the *ABCC3* cDNA using pMA-MRP3-plasmid as the template

Because no amplification of the *ABCC3* cDNA was achieved when liver sscDNA was used as the template, another strategy was applied. For this purpose pMA-MRP3-plasmid containing *ABCC3* cDNA was used. However, no amplification of the full-length *ABCC3* cDNA or 5'-part fragment of *ABCC3* cDNA was achieved when pMA-MRP3-plasmid was used as the template (results not shown). However, amplification of the 3'-part fragment was achieved (panel A in Figure 21) and it was successfully cloned into pCR2.1-TOPO, sequenced and a storage culture was prepared (results not shown).

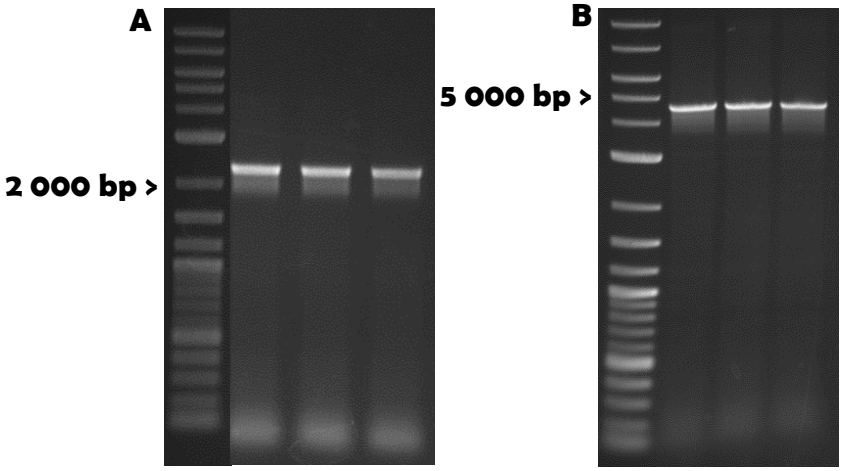

Figure 21. Amplification of the 3'part fragment of the *ABCC3* cDNA (panel A) and the full length *ABCC3* cDNA (panel B) using pMA-MRP3-plasmid or *Not*I-restricted pMA-MRP3-plasmid as the template, respectively.

The pMA-MRP3-plasmid contains a unique *Not*I restriction site right before the start of the *ABCC3* cDNA. Therefore, the plasmid was restricted with *Not*I to simplify the amplification of the full-length *ABCC3* cDNA. Using the *Not*I restricted pMA-MRP3-plasmid as the template, the amplification of the full-length *ABCC3* cDNA was achieved (panel B in Figure 21). The cDNA fragment was cloned into pCR2.1-TOPO-plasmid.

14 transformants from the transformation of cloned *ABCC3* cDNA were analyzed by *Bam*HI restriction analysis. The pCR2.1-TOPO-plasmid contains a unique *Bam*HI restriction site before the cloning site of the plasmid. In addition, the *ABCC3* cDNA contains two internal *Bam*HI restriction sites (Appendix 3). Depending of the orientation of the *ABCC3* cDNA in the pCR2.1-TOPO-plasmid, restriction analysis with *Bam*HI should result in fragments of 294 bp, 2524 bp and 5706 bp (orientation 2) or in fragments of 294 bp, 1855 bp and 6375 bp (orientation 1). Restriction analysis results are shown in Figure 22. All the restrictions resulted in 300 bp and 5700 bp fragments. In addition, restictions resulted in 2500 bp fragments in the case of 10 transformants (lanes 1-10 in Figure 22) and in 1900 bp fragments in the case of 3 transformants (lanes 11-13 in Figure 22). The results are in agreement with expected fragments (see above). Transformant 9 was further sequenced with T7-promoter and M13-reverse primers. The sequencing resulted in the correct sequences of the *ABCC3* cDNA.

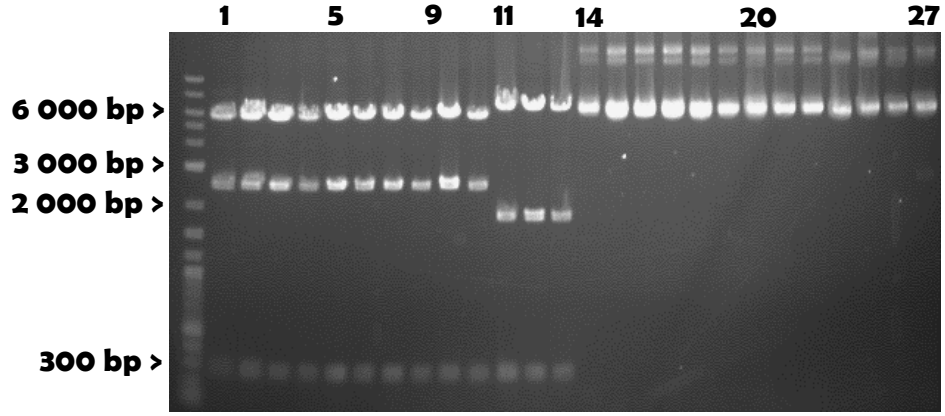

Figure 22. Restriction analysis of the pCR2.1-TOPO-MRP3 transformants Lanes 1-13 are *Bam*HI restricted and lanes 14-27 are respective unrestricted plasmids.

4.2.3 Construction of the pcDNA3.1/Hygro(-)-MRP3

For cloning the *ABCC3* cDNA into the expression vector pcDNA3.1/Hygro(-), the expression vector and the pCR2.1-TOPO-MRP3-vector (orientation 2) were restricted with *Not*I and *Kpn*I. These restriction sites are unique in both vectors and will cut out the *ABCC3* cDNA from the pCR2.1-TOPO-MRP3-plasmid (orientation 2) and allow ligation of the fragment into pcDNA3.1/Hygro(-) (Appendix 3). The restricted fragments were

purified and analyzed by agarose gel electrophoresis before the ligation (panel A in Figure 23). Figure 23 (panel A) presents the restricted vector and the *ABCC3* cDNA. The lengths of the fragments correspond to correct length of the empty vector pcDNA3.1/Hygro(-) (5600 bp) and the *ABCC3* cDNA (4700 bp). The *ABCC3* cDNA fragment was ligated into the pcDNA3.1/Hygro(-)-vector. Almost all analyzed transformants from the ligation reaction showed an insert compared to the empty pcDNA3.1/Hygro(-) (results not shown). Five of transformants were further analyzed by restriction analysis with *Bam*HI (panel B in Figure 23). The *ABCC3* cDNA contains two internal *Bam*HI restriction site and the pcDNA3.1/Hygro(-) contains one (Appendix 3). Restriction analysis should result in the fragments of 7397 bp, 2524 bp and 294 bp in length. Restriction analysis of all five transformant resulted in the correct length fragments (panel B in Figure 23).

The transformant 3 was further sequenced with T7-promoter, oMRP3-Clone-F, oMRP3-seq1, oMRP3-seq2, oMRP3-seq3 and BGH-reverse primers. The sequencing covered the entire MRP3 coding sequence and no base pair exchange was found compared to published reference sequence (Genbank accession NM_003786).

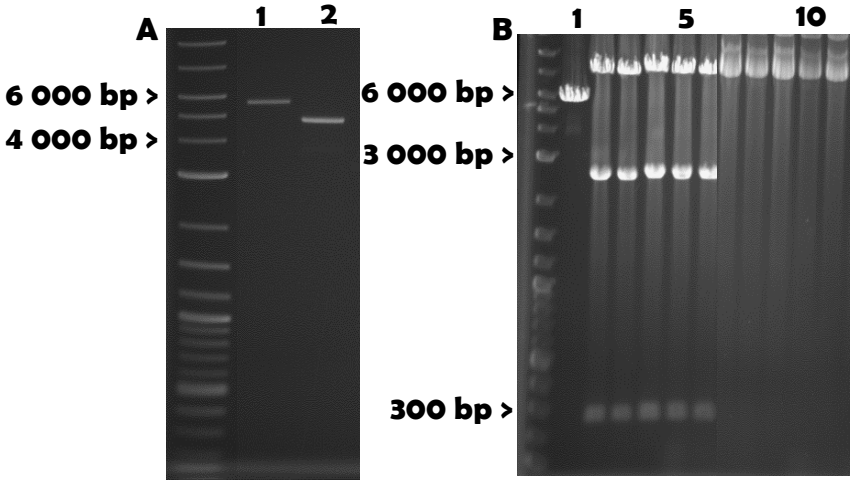

Figure 23. *Not*I and *Kpn*I restricted empty pcDNA3.1/Hygro(-)-vector (panel A, lane 1) and the *ABCC3* cDNA (panel A, lane 2). *Bam*HI restriction analysed empty pcDNA3.1/Hygro(-) (panel B, lane 1), *Bam*HI restriction analysed pcDNA3.1/Hygro(-)-MRP3 transformants (panel B, lanes 2-6) and the respective unrestricted plasmids (panel B, lanes 7-11).

4.3 Establishing MDCK-UGT1A1 and MDCK-UGT1A1-MRP2 cell lines

The *UGT1A1* cDNA was previously cloned into pcDNA3.1/Zeo(-) expression vector in-house and thus there was no need for the cloning of the *UGT1A1* cDNA in this study (Fahrmayr et al. 2012). This vector was used to express UGT1A1 in MDCK and MDCK-MRP2 cells. The newly established MDCK-UGT1A1 and MDCK-UGT1A1-MRP2 could be further used for the transfection of the *ABCC3* cDNA.

4.3.1 Transfection of parental MDCK and MDCK-MRP2 cell with the *UGT1A1* cDNA

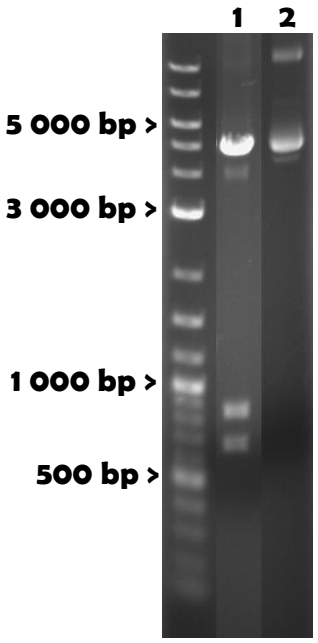

Figure 24. Restriction analysis of pcDNA3.1/Zeo(-)-UGT1A1 with *Eco*RI. Lane 1 is *Eco*RI restricted pcDNA3.1/Zeo(-)-UGT1A1 and lane 2 is unrestricted respective vector.

The pcDNA3.1/Zeo(-)-UGT1A1-vector was isolated from the storage culture and a restriction analysis was carried out. The *UGT1A1* cDNA contains an *Eco*RI restriction site and the pcDNA3.1/Zeo(-)-vector two *Eco*RI restriction sites at both ends of the cloned cDNA fragment (Appendix 3). The restriction analysis should result in fragments of 5100 bp, 920 bp and 730 bp in length. The restriction analysis corresponded to the expected fragments of the pcDNA3.1/Zeo(-)-UGT1A1-vector (Figure 24). The vector was further sequenced with T7-promoter and oUGT1A1-seq1 primers. The sequencing verified the correctness of the entire *UGT1A1* cDNA sequence compared to the reference sequence (GenBank accession NM_000463.2).

The pcDNA3.1/Zeo(-)-vector includes the zeocin resistance gene that allows selection of the stable transfected cells from non-transfected cells using this antibiotic. After the transfection of parental MDCK and MDCK-MRP2 cells with the pcDNA3.1/Zeo(-)-UGT1A1, cells were passaged and cultured in various dilutions in media containing 500 µg/ml of zeocin (Table 23 and 24). This concentration was selected

based on the previously established MDCK-OATP1B1-UGT1A1 cell line transfected with the same vector (Fahrmayr et al. 2012). No cytotoxicity of zeocin to parental MDCK or MDCK-MRP2 cells was determined. No cytotoxicity of the transfection reagent was observed at any stage of the transfection.

Zeocin did not have the desired effect on MDCK-MRP2 cells after the transfection with *UGT1A1* cDNA because all transfection plates of the first passage grew confluent in 6 days. To isolate single colonies of the cells, new passages and very high dilutions were carried out. In addition, zeocin concentration was increased to 1 mg/ml. Number of passages after the transfection and subdilution factors are presented in Table 23. Together 93 colonies were isolated and 20 of them grew enough to produce a clone when MDCK-MRP2 cells were transfected with the *UGT1A1* cDNA.

Table 23. Number of passages and factor of subdilutions for each passage after the transfection of MDCK-MRP2 with the *UGT1A1* cDNA. In addition, number of colonies isolated from transfection plates and number of clones are presented.

Number of the passage (the subdilution plate of the previous passage used for the new passage)	**Factor of the subdilution**	**Colonies isolated**	**Clones**	**Days after the transfection to isolation of colonies**
1 (transfection)	1:5	0	0	-
1 (transfection)	1:10	0	0	-
1 (transfection)	1:20	0	0	-
2 (1:10)	1:1000	12	3	16
2 (1:10)	1:250	0	0	
3 (1:250)	1:100	36	7	26-34
3 (1:250)	1:25			
3 (1:1000)	1:50	0	0	-
4 (1:50)	1:1000	12	1	30
4 (1:50)	1:500			
4 (1:100)	1:1000	33	9	47-58
4 (1:100)	1:250			

Zeocin had stronger effect to MDCK cells transfected with the *UGT1A1* cDNA compared to transfected MDCK-MRP2 cells. The effect was strong enough to allow isolation of single colonies from the highest dilution of the first passage (Table 24). However, subsequent passages were done in higher dilutions to isolate more colonies and have higher probability to have a clone with sufficient expression of *UGT1A1* mRNA.

Together 39 single colonies were isolated and 13 of them grew to produce a clone when parental MDCK cells were transfected with UGT1A1.

Table 24. Number of passages and factor of subdilutions for each passage after the transfection of parental MDCK cells with *UGT1A1* cDNA. In addition, number of colonies isolated and number of clones are presented.

Number of the passage (the subdilution plate of the previous passaged used for the new passage)	**Factor of the subdilution**	**Colonies isolated**	**Clones**	**Days after the transfection to isolation of colonies**
1 (transfection)	1:5	0	0	-
1 (transfection)	1:10	0	0	-
1 (transfection)	1:20	6	4	16
2 (1:10)	1:500	0	0	-
3 (1:500)	1:2000	10	7	30
3 (1:500)	1:4000	14	0	36
4 (1:1000)	1:1000	9	2	42

4.3.2 *UGT1A1* mRNA expression characterization in MDCK-UGT1A1 and MDCK-UGT1A1-MRP2 cell lines

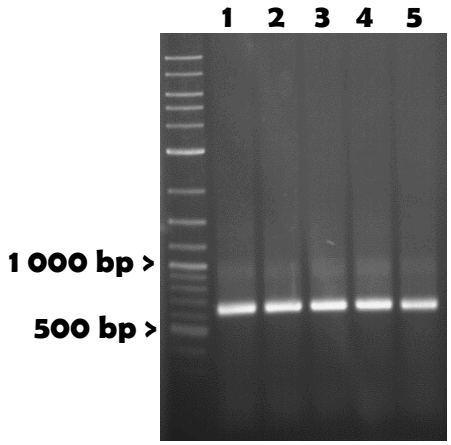

Figure 25. Amplification of the 661 bp fragment of β-actin cDNA from sscDNAs of MDCK-UGT1A1#7 (lane 1), -#11 (lane 2), -#12 (lane 3), MDCK-UGT1A1-MRP2#11 (lane 4) and -#12 (lane 5).

Total RNA of each clone was isolated and reverse transcripted to sscDNA. The cDNA synthesis was evaluated with PCR amplification of the 661 bp fragment of *β-actin* cDNA. Representative amplification of *β-actin* cDNA fragments is presented in Figure 25. Analysis of *UGT1A1* mRNA expression was conducted only if the amplification of the *β-actin* cDNA fragment was successful.

For the analysis of *UGT1A1* mRNA expression, quantitative PCR was used to amplify a 311 bp fragment of the *UGT1A1* cDNA. In addition, the *β-actin* cDNA fragment was amplified in each analysis. Linearity of the analysis was ensured by including four samples of

pcDNA3.1/Zeo(-)-UGT1A1-vector in the range of 1-1000 pg in each run. Correlation coefficient of linearity was 1 in each analysis. In addition, the amount of amplified *β-actin* cDNA fragments and, if expression of *UGT1A1* cDNA was observed, the amount of the *UGT1A1* cDNA fragments was ensured to be in the linear range. Melting curve and agarose gel analysis was also conducted for all amplified *UGT1A1* cDNA fragments. Analysis showed in each case identical melting curve and migration in agarose gel electrophoresis compared to standard samples. Representative agarose gel electrophoresis analysis of qPCR amplified cDNAs is shown in Figure 26.

Together 13 clones of MDCK-UGT1A1 and 20 clones of MDCK-UGT1A1-MRP2 cell lines were analysed with qPCR. Four clones of MDCK-UGT1A1 showed significant expression of *UGT1A1* cDNA (>1%) when normalized to expression of β-actin cDNA. Expression of *UGT1A1* mRNA in these clones is summarized in Table 25. Expression of *UGT1A1* mRNA was observed in none of clones of MDCK-UGT1A1-MRP2, in MDCK-VC (empty vector transfected) or in parental MDCK cells. In addition, a 284 bp fragment of *ABCC2* mRNA was amplified in a couple of analysis of MDCK-UGT1A1-MRP2 cell line clones. Expression of *ABCC2* cDNA in MDCK-MRP2 cells and in four analysed clones of MDCK-UGT1A1-MRP2 were 83 % and 79-89 % of the expression of *β-actin* cDNA, respectively. In addition, no *ABCC2* cDNA expression was observed in MDCK-VC cells.

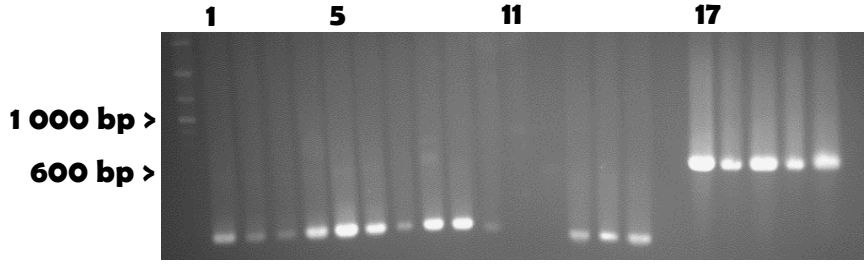

Figure 26. A representative agarose gel analysis of qPCR amplified *UGT1A1*, *ABCC2* and *β-actin* cDNA fragments from sscDNAs of UGT1A1 clones. Lanes 1-4 are 1000-1 pg standards of the vector pcDNA3.1/Zeo(-)-UGT1A1. Lanes 5-10, 11-16 and 17-22 are amplification of fragments of *UGT1A1* (311 bp), *ABCC2* (284 bp) and *β-actin* (661 bp) cDNA from MDCK-UGT1A1#7, -#11, -12#, UGT1A1-MRP2#11, -#12 and control (water) samples, respectively.

Table 25. Expression of *UGT1A1* mRNA in MDCK-UGT1A1 clones 2, 4, 7 and 8. The expression of *UGT1A1* mRNA is normalized to expression of *β-actin* mRNA.

Clone	**mRNA expression of *UGT1A1/β-actin***	**Relative mRNA expression of *UGT1A1***
MDCK-UGT1A1#2	2 %	0.01
MDCK-UGT1A1#4	307 %	2.05
MDCK-UGT1A1#7	150 %	1
MDCK-UGT1A1#8	3 %	0.02

4.3.3 Immunoblot analysis of UGT1A1 protein expression in the MDCK-UGT1A1#4 and MDCK-UGT1A1#7 cell lines

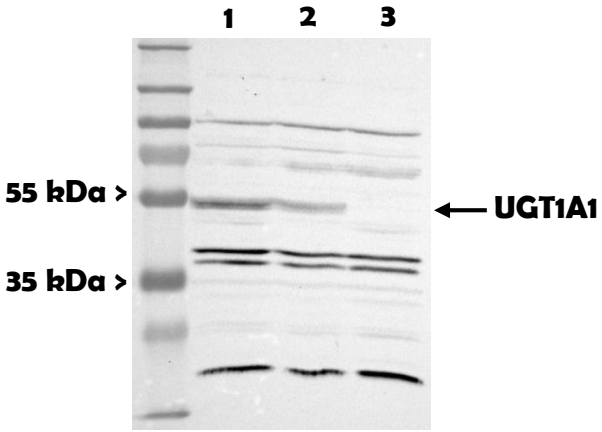

Figure 27. Immunoblot analysis of UGT1A1 in SDS-polyacrylamide gel electrophoresis separated and membrane transferred protein homogenates. Lane 1 is MDCK-UGT1A1#4, lane 2 is MDCK-UGT1A1#7 and lane 3 is MDCK-VC.

Two clones with the highest expression of *UGT1A1* mRNA were further characterized at the protein expression level by immunoblot analysis. UGT1A1 was detected in both analysed clones but not in the control cells (Figure 27). In addition, UGT1A1 showed the correct, approximately 55 kDa molecular weight (Lévesque et al. 2007).

The same membrane was used for the analysis of β-actin expression after stripping off the previous antibodies (Figure 28).

In addition, intensities of UGT1A1 bands and β-actin bands were measured. Relative β-actin expressions were 1.10, 1.00 and 1.13 in MDCK-UGT1A1#4, MDCK-UGT1A1#7 and MDCK-VC cells, respectively. Relative UGT1A1 expressions were 1.89 and 1.00 in MDCK-UGT1A1#4 and MDCK-UGT1A1#7 cells, respectively. There were no significant differences in the β-actin expression levels between three analysed samples. In addition, the expression of UGT1A1 protein was quite comparable to mRNA expression levels of *UGT1A1* in both clones (Table 25).

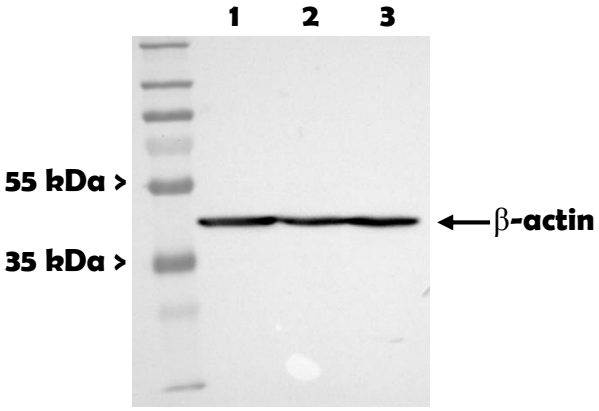

Figure 28. Immunoblot analysis of β-actin in the same membrane as in Figure 27 after stripping of UGT1A1 antibody. Lane 1 is MDCK-UGT1A1#4, lane 2 is MDCK-UGT1A1#7 and lane 3 is MDCK-VC.

5. DISCUSSION

5.1 Cloning of the human *UGT2B7* cDNA

For the establishment of UGT2B7 expressing cell lines, first the *UGT2B7* cDNA has to be cloned. Several methods were tried, but none of the methods were successful and no cloning of this cDNA was achieved. Several research groups have already cloned the human UGT2B7 cDNA earlier, and thus this process should be repeatable with our methods (Ritter et al. 1990; Jin et al. 1993; Coffman et al. 1997; Kurkela et al. 2003). In addition, the *UGT2B7* mRNA is highly and equally expressed in both human kidney and liver (Court et al. 2012). Thus, it was expected that amplification of this cDNA from total kidney sscDNA would result in the correct length amplification (Figure 7). However, it was quite unexpected that several attempts for amplification of this cDNA from total liver sscDNA did not result in any successful amplification. One explanation for unsuccessful amplifications, when using total liver sscDNA as template, could be the quality of the RNA that was used as the template for sscDNA synthesis. In this study, the liver sscDNA was synthesized by using commercially available total liver RNA as the template. However, storage and handling of RNA could have resulted in degradation and loss of

integrity of the RNA and subsequently poor quality of the total liver sscDNA (Holland et al. 2003).

Although, no amplification of the *UGT2B7* cDNA was achieved using liver sscDNA as the template, an amplification product using kidney sscDNA as template was achieved (Figure 7). However, when this cDNA fragment was subcloned and a pair of transformants was sequenced, no *UGT2B7* sequence was found. Instead, a sequence that gave a full correct alignment with a part of the pcDNA3.1-expression vector was found. This strange finding could be a result of contamination of the cloning reactions, or reaction components, with pcDNA3.1-vector. Even if very low DNA amounts, such as ten femtograms are present, plasmid DNA could be transformed into competent cells (Hanahan 1983).

In addition to liver and kidney sscDNA, the *UGT2B7* cDNA was tried to amplified using in-house available pGEM-T-UGT2B7(802C)-vector as the template. This was not used as the first option, because this vector contains a base pair exchange (T802C) in the *UGT2B7* cDNA, which results in an amino acid change compared to the reference sequence. However, despite several attempts, only one successful amplification was achieved although the used template was well defined. Because the template vector for the amplification was circular plasmid DNA, it is possible that this supercoiled conformation of the vector inhibited the amplification reaction and caused unsuccessful amplifications (see also 5.4). Therefore, linearization of the pGEM-T-UGT2B7(802C)-vector with a single cutting enzyme, outside of the *UGT2B7* cDNA, could have aided the amplification. However, despite difficulties in amplification of the *UGT2B7* cDNA using the vector pGEM-T-UGT2B7(802C), a successful amplification was achieved and the cDNA fragment was cloned (Figure 9). Subcloning was followed by a sequencing of a pair of transformants. The results of sequencing corresponded to sequencing results from the cloning reaction of the amplified kidney sscDNA amplified fragment (4.1.1). This suggests that this cloning reaction was also contaminated with pcDNA3.1-expression vector (see above).

5.2 Construction of the expression vector containing the *UGT2B7* cDNA

Because all attempts to amplify *UGT2B7* cDNA were unsuccessful, ligation and restriction based cloning of the *UGT2B7* cDNA fragment was attempted by utilizing the in-house available vector pGEM-T-UGT2B7(802C) and using unique restriction sites in this vector and in the expression vector pcDNA3.1. For the first strategy, pcDNA3.1/Hygro(-) was chosen for the expression of the *UGT2B7* cDNA because this vector contains a different antibiotic selection gene than the expression vector containing the *ABCC2* cDNA encoding MRP2. This strategy would allow construction of MRP2 and UGT2B7 double-transfected cell lines. However, the subcloning was possible only with one pair of single cutting restriction enzymes, *Apa*I and *Bst*XI. Despite several attempts, no correct construct of the expression vector containing the *UGT2B7* cDNA was achieved (4.1.3). A possible explanation for the unsuccessful subclonings could be that *Bst*XI recognizes discontinuous palindromic target sequence (CCANNNNNNTGG, N = A or C). This target sequence is CCAACGCGTTGG in the vector pGEM-T-UGT2B7(802C) and CCACCACACTGG in the vector pcDNA3.1/Hygro(-). This strongly suggests that the restriction did not result in fully compatible sticky ends, which could explain unsuccessful subcloning reactions.

It was also possible to use *Not*I restriction sites for the subcloning of the *UGT2B7* cDNA into pcDNA3.1/Hygro(-). One restriction site is located in the multiple cloning site of the expression vector pcDNA3.1/Hygro(-). However, *Not*I is not a unique restriction site in the vector pGEM-T-UGT2B7(802C) but it is located at both ends of the *UGT2B7* cDNA and restriction with it will release *UGT2B7* cDNA fragment ready for subcloning. Ligation reaction of the above DNA fragment would result in two possibilities of the orientation of the cDNA fragment in the expression vector. In addition, this cloning strategy demands a dephosphorylation reaction for the vector as an additional step before the ligation reaction. Religations of the expression vector would prevent the desired ligation if no dephosphorylation of the free phosphate ends of the restricted expression vector were conducted. However, this did not cause any difficulties because even the amount of potential religations were higher than when using the other cloning strategy, it was not still dominating among analysed transformants (Figure 13). Unfortunately, this cloning strategy did not lead to any correct constructs of pcDNA3.1/Hygro(-)-UGT2B7.

All potential transformants were analysed by restriction analysis and some of them were sequenced, but the outcome was that they did contain neither the expression vector pcDNA3.1/Hygro(-) not the *UGT2B7* cDNA. The identity of these transformants stayed unknown.

The final strategy for subcloning of the *UGT2B7* cDNA was to use the expression vector pcDNA3.1/Zeo(-). This expression vector contains a different antibiotic resistance gene than pcDNA3.1/Hygro(-), but it is also different than in the expression vector containing *ABCC2* cDNA encoding MRP2. This would allow not only the construction of UGT1A1 and MRP2 double-transfected cell lines but also of a triple-transfected cell line with MRP3, if the *ABCC3* cDNA encoding MRP3 is cloned into pcDNA3.1/Hygro(-) expression vector (4.2.3). Nevertheless, subcloning of the *UGT2B7* cDNA into pcDNA3.1/Zeo(-) was attempted with *Apa*I and *Pst*I restrictions of the vectors pGEM-T-UGT2B7(802C) and pcDNA3.1/Zeo(-) and subsequently ligating the restricted DNA fragments. These restriction sites are unique for both vectors and allow subcloning of the *UGT2B7* cDNA in the correct orientation into the expression vector. However, almost all analysed transformants showed the same length as the empty expression vector. This indicates that the expression vector religated with itself and no *UGT2B7* cDNA was ligated into the cloning site. Although two different restriction enzymes were used for the subcloning and no religation should happen. Possibly, one of the restriction enzymes did not work properly and resulted in only single restricted expression vector. This could be caused for example by old stock of the enzyme. A defective enzyme would lead in high amount of religated expression vectors and suppress the desired ligation. However, one transformant showed promising length compared to the empty expression vector, when using this cloning strategy. The sequencing of this transformant resulted only in genomic *E.coli* DNA, which suggests that a recombination event took place in the competent cells, and no correct construct of the *UGT2B7* cDNA in the expression vector was present.

For all above mentioned subcloning strategies, restriction and ligation based cloning methods were used. However, restriction free cloning technique is also available (*e.g.* van den Ent and Löwe 2006 and Unger et al. 2010). Briefly, in this method the cDNA of interest is PCR amplified with specific primers and subsequently ligated into circular vector via a second PCR reaction. Finally, the empty vector is digested and the correct construct is transformed into bacterial cells. This cloning strategy could be used in future

attempts for the construction of the expression vector containing *UGT2B7* cDNA.

5.3 Site-directed mutagenesis of the vector pcDNA3.1/Zeo(-)-UGT2B7(1575T)

UGT2B7 cDNA was already cloned earlier in-house into the expression vector pcDNA3.1/Zeo(-). However, this vector contained a base pair exchange (A1575T) resulting in a premature stop codon compared to the reference sequence of the *UGT2B7* cDNA (Genbank accession NM_001074.2) and thus was not employed as the first option. A site-directed mutagenesis reaction is quite easily conducted with commercially available kits that implement standardized methods (Ling and Robinson 1997). However, despite multiple attempts with two different commercially kits, no correct site-directed mutagenesis of the plasmid was achieved. The main problem with the QuickChange multi-site-directed mutagenesis kit was the high amount of colonies after the transformation of the reaction. This could be a result of unsuccessful restriction of the template vector pcDNA3.1/Zeo(-)-UGT2B7(1575T) after the PCR. This could hindered the detection of the desired transformants, because of high amount of the unrestricted template among all transformants. However, the restriction enzyme was tested in a separate reaction and it worked properly (results not shown). Interestingly, site-directed mutagenesis reactions with the QuickChange II site-directed mutagenesis kit resulted in almost no colonies after the transformation of the reactions. When the reaction conditions were modified, higher amount of colonies were achieved and some of them showed the correct base pair exchange but also major deletions after of before the mutagenesis primer binding sites. This observation strongly suggests that the major problem in the site-directed mutagenesis reactions were strong interactions between the two DNA strands in the vector, which resulted in poor binding of the primers and DNA-polymerase. Poor binding could result in no amplification or partial amplification resulting in deletion of parts of the vector. In addition, we contacted the manufacturer of the mutagenesis kits (Agilent) regarding the difficulties of the site-directed mutagenesis reaction. Their answer was that other customers had also difficulties, when conducting mutagenesis reaction for pcDNA3.1-vectors indicating that the difficulties were caused by strong interactions between DNA strands in the vector. Further optimization of the site-directed mutagenesis

reaction variables such as concentration of DMSO and PCR conditions could possibly result in successful reaction (Ling and Robinson 1997). In addition, several other commercially site-directed mutagenesis kits are available and could be used for the correction of the base pair exchange.

5.4 Cloning of the human *ABCC3* cDNA encoding MRP3

The first step for establishment of MRP3 expressing cell lines is cloning of the *ABCC3* cDNA that encodes MRP3. Earlier several groups have cloned the *ABCC3* cDNA encoding MRP3 using liver sscDNA as the template (Kiuchi et al. 1998; Kool 1999; König et al. 1999a; Paumi et al. 2003). Therefore, the amplification of the full-length *ABCC3* cDNA using liver sscDNA as the template was also attempted in this study. However, no success was achieved despite multiple reactions (Figure 19). As second strategy, *ABCC3* cDNA was attempted to be amplified in two cDNA fragment, which is easier than the amplification of the full length 4600 bp cDNA. No correct amplifications were achieved either with this strategy (Figure 20). As discussed in the case of *UGT2B7* cDNA amplification, the quality of the sscDNA is important for correct amplification of the cDNA of interest. However, in the case of *ABCC3* cDNA, the amount of G and C-bases (GC-content) could also be a significant factor affecting the amplification. The GC-content of the *ABCC3* cDNA is 58 % whereas it is 41 % for the *UGT2B7* cDNA. Average GC-content of the human genome is 41 %, so the *ABCC3* cDNA could be considered as a GC-rich fragment (Lander et al. 2001). PCR amplifications of GC-rich templates could need optimization of PCR conditions, but also additives such as glycerol, DMSO or betaine (Varadaraj and Skinner 1994; Jensen et al. 2010). In this study 3 % DMSO was tried as additive in the amplification reaction without any success. However, even 10-15 % DMSO concentrations were previously used in PCR reactions (Varadaraj and Skinner 1994).

Finally, *ABCC3* cDNA was successfully amplified using a well-defined template, the plasmid pMA-MRP3 (from Dr. Markus Keiser, University of Greifswald, Germany). However, amplification of the full-length cDNA fragment was achieved only when the plasmid was first linearized with a restriction enzyme. When the non-linearized plasmid

was used as template for the amplification, only the 3'-part of the *ABCC3* cDNA was amplified successfully. This supports the idea that GC-richness causes strong interactions between two DNA strands of the *ABCC3* cDNA and the interactions are especially strong at the start of the cDNA. For example, if the first 40 base pairs starting from the first base of the oMRP3-F binding site are analysed, the GC-content is as high as 75 %.

The amplification of the *ABCC3* cDNA was finally achieved and it was successfully cloned into the expression vector pcDNA3.1/Hygro(-) and the correctness of the sequence was verified by sequencing and it corresponded to the reference sequence (Genbank accession NM_003786). This successful cloning strongly suggests that materials and methods used for all cloning reactions during this study in principle were proper and worked well. This also indicated that the difficulties with sscDNA clonings of *UGT2B7* and *ABCC3* cDNAs were associated more with the template and/or with the sequence itself. In addition, subcloning issues of the *UGT2B7* cDNA could be associated mainly with the cDNA itself, because the *ABCC3* cDNA was cloned in the same expression vector as the *UGT2B7* cDNA was attempted to be cloned and also the same DNA ligation and purification methods were used. However, in the case of *UGT2B7* cDNA, restriction reactions and enzymes might also have been the cause for difficulties (see 5.2).

5.5 Establishing MDCK-UGT1A1 and MDCK-UGT1A1-MRP2 cell lines

For the establishment of single- and double-transfected UGT1A1 cell lines, the already established expression vector containing the *UGT1A1* cDNA was used (Fahmayr et al. 2012). In this study, the same expression vector and methods were used to establish MDCK-UGT1A1 and MDCK-UGT1A1-MRP2 cell lines as in the previous study for MDCK-OATP1B1-UGT1A1-MRP2 cell line. However, unexpected difficulties were faced with double-transfected cells, because the selection antibiotic zeocin did not properly inhibit the growth of the transfected cells when MRP2 was present, even if the concentration of zeocin was the same as in the previous study (Fahrmayr et al. 2012). Subsequently, the concentration of zeocin was increased from 0.5 mg/ml to 1 mg/ml for MDCK-UGT1A1-MRP2 transfected cells, which resulted in better selection of single colonies. Despite concentration increment, no cell clones expressing *UGT1A1* mRNA

were achieved for double-transfected cells. Proper expression of UGT1A1 was achieved for two clones of single transfected cells.

An explanation for this unsuccessful transfection of MDCK-MRP2 cells with the *UGT1A1* cDNA could be the expression of efflux transporter MRP2. It could be that MRP2 transports zeocin out of the cells and thus it decreases antibiotic effect. This should be investigated with further studies by determinating the concentration dependent cytotoxicity of zeocin to parental and MRP2 transfected MDCK cells. However, this does not explain why Fahrmayr and coworkers (2012) were able to establish MDCK-OATP1B1-UGT1A1-MRP2 cell line. On the other hand, they were not able to establish MDCK-OATP1B3-UGT1A1-MRP2 cell line because exactly the same difficulties with zeocin as in this study (unpublished observation by Christina Fahrmayr 2012). It could be speculated that OATP1B1 contributes to transport of zeocin and concentrates it into cells even if MRP2 transports it out of cells. However, this has to be clarified. In the future, the MDCK-UGT1A1-MRP2 cell line could be attempted to establish by transfection of MDCK-UGT1A1 cell line, which was established in this study, with the expression vector containing *ABCC2* cDNA encoding MRP2 and G418 resistance gene. On the other hand, establishment of MDCK-UGT1A1-MRP2 cell line was recently published using hygromycin as the selection antibiotic in the expression vector containing the *UGT1A1* cDNA (Ge et al. 2015). However, characterization of this cell line was not published in the study and no further conclusions of the expression of UGT1A1 in it could be drawn.

Establishment of MDCK-UGT1A1 cell line in this study was successful and protein and mRNA expression level of *UGT1A1* were characterized. In the studies of Fahrmayr and co-workers (2012 and 2013), mRNA expression level of *UGT1A1* was reported to be approximately 50 %, 250 % and 180 % of *β-actin* mRNA expression level in MDCK-OATP1B1-UGT1A1, MDCK-OATP1B1-UGT1A1-MRP2 and MDCK-OATP1B1-CYP3A4-UGT1A1-MRP2 cell lines, respectively. The expression levels of *UGT1A1* mRNA found in this study, 150 % and 300 % of *β-actin* mRNA expressions, are in the same range as in the previous study. However, none of the MDCK-UGT1A1-MRP2 clones and most of the MDCK-UGT1A1 clones did not express sufficient amounts of *UGT1A1* mRNA although they were resistant to zeocin. In addition to the possible contribution of MRP2 to zeocin resistance (see above), integration of the transfected

cDNA into the genome of cells plays a role key for obtaining sufficient expression of the cDNA of interest after the transfection (Büssow et al. 2015). Because the integration is unpredictable and could be of low frequency, it might be one of the reasons for insufficient expression of *UGT1A1* mRNA in most of the clones analysed in this study.

5.6 Future prospects

Multi-transfected cell lines expressing drug transporters and metabolizing enzymes are recognized as valuable tools for *in vitro* evaluation of drug transport and metabolism (Brouwer et al. 2013; Zamek-Gliszczynski et al. 2014). The most advanced models available at the moment are double-transfected cell lines MDCK-OATP1B1/3-MRP2, triple-transfected cell lines MDCK-OATP1B1-MRP2-MRP3, MDCK-OATP1B1-MRP2-MRP4 and MDCK-OATP1B1-UGT1A1-MRP2, and quadruble-transfected cell lines MDCK-OATP1B1-CYP3A4-UGT1A1-MRP2 and MDCK-OATP1B1-OATP1B3-OATP2B1-MRP2 (Cui et al. 2001; Fehrenbach et al. 2003; Kopplow et al. 2005; Hirouchi et al. 2009; Fahrmayr et al. 2012 and Fahrmayr et al. 2013). However, there are no reports of cell lines expressing both basolaterally localized MRP3 and any UGT or any cell lines co-expressing UGT2B7 with a transporter. The expression vector containing *ABCC3* cDNA encoding MRP3 was established in this study. In addition, MDCK-UGT1A1 cell line was established. Both of these could be used in the future for the establishment of a MDCK-UGT1A1-MRP3 cell line and further for the establishment of a MDCK-UGT1A1-MRP2-MRP3 cell line. This cell line could be a valuable tool for understanding the interplay between glucuronidation and basolateral efflux transport and to identify substrates and inhibitors for both efflux transporters MRP2 and MRP3 and for the drug metabolizing enzyme UGT1A1. Although, no expression vector containing *UGT2B7* cDNA could be established in this study, despite several different strategies and attempts, there are still several methods available for the construction of the expression vector and subsequent expression of UGT2B7 in MDCK cells.

6. CONCLUSIONS

Cloning of the *UGT2B7* cDNA and construction a mammalian expression vector containing this cDNA for the subsequent expression of UGT2B7 in MDCK cells for drug metabolism studies were attempt in this study without success. *ABCC3* cDNA encoding the efflux transporter MRP3 was successfully cloned into mammalian expression vector that could be used in future experiments for the expression of MRP3 in MDCK cells or other mammalian cells for drug metabolism studies. In addition, a novel cell line MDCK-UGT1A1 was established and it could be used for drug metabolism studies and more importantly, for the coexpression of drug efflux transporters such as MRP3 and MRP2. These cell lines could be used for studying the interplay between glucuronidation and efflux transport of drug molecules and drug candidates.

REFERENCES

Achour B, Russell MR, Barber J, Rostami-Hodjegan A: Simultaneous quantification of the abundance of several cytochrome P450 and uridine 5'-diphospho-glucuronosyltransferase enzymes in human liver microsomes using multiplexed targeted proteomics. Drug Metab Dispos 42: 500-510, 2014

Aithal GP, Ramsay L, Daly AK et al.: Hepatic Adducts, Circulating Antibodies, and Cytokine Polymorphisms in Patients with Diclofenac Hepatotoxicity. Hepatology 39: 1430-1440, 2004

Akita H, Suzuki H, Hirohashi T, Takikawa H, Sugiyama Y: Transport activity of human MRP3 expressed in Sf9 cells: Comparative studies with rat MRP3. Pharm Res 19: 34-41, 2002

Ambudkar SV, Dey S, Hrycyna CA, Ramachandra M, Pastan I, Gottesman MM: Biochemical, cellular, and pharmacological aspects of the multidrug transporter. Annu Rev Pharmacol Toxicol 39: 361-398, 1999

Ambudkar SV, Kimchi-Sarfaty C, Sauna ZE, Gottesman MM: P-glycoprotein: From genomics to mechanism. Oncogene 22: 7468-7485, 2003

Amidon GL, Lennernas H, Shah VP, Crison JR: A theoretical basis for a biopharmaceutic drug classification: The correlation of in vitro drug product dissolution and in vivo bioavailability. Pharm Res 12: 413-420, 1995

Anderson S, Luffer-Atlas D, Knadler MP: Predicting circulating human metabolites: How good are we? Chem Res Toxicol 22: 243-256, 2009

Baer BR, DeLisle RK, Allen A: Benzylic oxidation of gemfibrozil-1-O-ß-glucuronide by P450 2C8 leads to heme alkylation and irreversible inhibition. Chem Res Toxicol 22: 1298-1309, 2009

Bakos E, Evers R, Sinkó E, Váradi A, Borst P, Sarkadi B: Interactions of the human multidrug resistance proteins MRP1 and MRP2 with organic anions. Mol Pharmacol 57: 760-768, 2000

Baltes S, Fedrowitz M, Tortós CL, Potschka H, Löscher W: Valproic acid is not a substrate for P-glycoprotein or multidrug resistance proteins 1 and 2 in a number of in vitro and in vivo transport assays. J Pharmacol Exp Ther 320: 331-343, 2007

Bélanger A, Pelletier G, Labrie F, Barbier O, Chouinard S: Inactivation of androgens by UDP-glucuronosyltransferase enzymes in humans. Trends Endocrinol Metab 14: 473-479, 2003

Belinsky MG, Dawson PA, Shchaveleva I et al.: Analysis of the in vivo functions of Mrp3. Mol Pharmacol 68: 160-168, 2005

Benet LZ, Broccatelli F, Oprea TI: BDDCS applied to over 900 drugs. AAPS J 13: 519-547, 2011

Borst P, Oude Elferink R: Mammalian ABC transporters in health and disease. Annu Rev Biochem 71: 537-592, 2002

Borst P, De Wolf C, Van De Wetering K: Multidrug resistance-associated proteins 3, 4, and 5. Pflug Arch Eur J Physiol 453: 661-673, 2007

Bosma PJ, Seppen J, Goldhoorn B et al.: Bilirubin UDP-glucuronosyltransferase 1 is the only relevant bilirubin glucuronidating isoform in man. J Biol Chem 269: 17960-17964, 1994

Brouwer KLR, Keppler D, Hoffmaster KA et al.: In vitro methods to support transporter evaluation in drug discovery and development. Clin Pharmacol Ther 94: 95-112, 2013

Büssow K: Stable mammalian producer cell lines for structural biology. Curr Opin Struct Biol 32: 81-90, 2015

Caldwell J, Gardner I, Swales N: An introduction to drug disposition: The basic principles of absorption, distribution, metabolism, and excretion. Toxicol Pathol 23: 102-114, 1995

Chen C-, Chin JE, Ueda K et al.: Internal duplication and homology with bacterial transport proteins in the mdr1 (P-glycoprotein) gene from multidrug-resistant human cells. Cell 47: 381-389, 1986

Chen G, Giambrone NE, Lazarus P: Glucuronidation of trans-3'-hydroxycotinine by UGT2B17 and UGT2B10. Pharmacogenet Genomics 2012

Chu X-, Huskey S-W, Braun MP, Sarkadi B, Evans DC, Evers R: Transport of Ethinylestradiol Glucuronide and Ethinylestradiol Sulfate by the Multidrug Resistance Proteins MRP1, MRP2, and MRP3. J Pharmacol Exp Ther 309: 156-164, 2004

Chu X-, Strauss JR, Mariano MA et al.: Characterization of mice lacking the multidrug resistance protein Mrp2 (Abcc2). J Pharmacol Exp Ther 317: 579-589, 2006

Chu X-, Bleasby K, Yabut J et al.: Transport of the dipeptidyl peptidase-4 inhibitor sitagliptin by human organic anion transporter 3, organic anion transporting polypeptide 4C1, and multidrug resistance P-glycoprotein. J Pharmacol Exp Ther 321: 673-683, 2007

Chu X-, Liang Y, Cai X et al.: Metabolism and renal elimination of gaboxadol in humans: Role of UDP-glucuronosyltransferases and transporters. Pharm Res 26: 459-468, 2009

Coffman BL, Rios GR, King CD, Tephly TR: Human UGT2B7 catalyzes morphine glucuronidation. Drug Metab Dispos 25: 1-4, 1997

Court MH, Duan SX, Von Moltke LL et al.: Interindividual variability in acetaminophen glucuronidation by human liver microsomes: Identification of relevant acetaminophen UDP-glucuronosyltransferase isoforms. J Pharmacol Exp Ther 299: 998-1006, 2001

Court MH, Krishnaswamy S, Hao Q et al.: Evaluation of 3'-azido-3'-deoxythymidine, morphine, and codeine as probe substrates for udp-glucuronosyltransferase 2B7 (UGT2B7) in human liver microsomes: Specificity and influence of the UGT2B7*2 polymorphism. Drug Metab Dispos 31: 1125-1133, 2003

Court MH, Zhang X, Ding X, Yee KK, Hesse LM, Finel M: Quantitative distribution of mRNAs encoding the 19 human UDP-glucuronosyltransferase enzymes in 26 adult and 3 fetal tissues. Xenobiotica 42: 266-277, 2012

Cui Y, König J, Buchholz U, Spring H, Leier I, Keppler D: Drug resistance and ATP-dependent conjugate transport mediated by the apical multidrug resistance protein, MRP2, permanently expressed in human and canine cells. Mol Pharmacol 55: 929-937, 1999

Cui Y, König J, Keppler D: Vectorial transport by double-transfected cells expressing the human uptake transporter SLC21A8 and the apical export pump ABCC2. Mol Pharmacol 60: 934-943, 2001

Cvetkovic M, Leake B, Fromm MF, Wilkinson GR, Kim RB: OATP and P-glycoprotein transporters mediate the cellular uptake and excretion of fexofenadine. Drug Metab Dispos 27: 866-871, 1999

Dalvie D, Scott Obach R, Kang P et al.: Assessment of three human in vitro systems in the generation of major human excretory and circulating metabolites. Chem Res Toxicol 22: 357-368, 2009

Damme K, Nies AT, Schaeffeler E, Schwab M: Mammalian MATE (SLC47A) transport proteins: Impact on efflux of endogenous substrates and xenobiotics. Drug Metab Rev 43: 499-523, 2011

de Waart DR, Paulusma CC, Kunne C, Oude Elferink RPJ: Multidrug resistance associated protein 2 mediates transport of prostaglandin E2. Liver Int 26: 362-368, 2006

de Waart DR, Van De Wetering K, Kunne C, Duijst S, Paulusma CC, Oude Elferink RPJ: Oral availability of cefadroxil depends on ABCC3 and ABCC4. Drug Metab Dispos 40: 515-521, 2012

Deeley RG, Westlake C, Cole SPC: Transmembrane transport of endo- and xenobiotics by mammalian ATP-binding cassette multidrug resistance proteins. Physiol Rev 86: 849-899, 2006

Delaforge M, Pruvost A, Perrin L, André F: Cytochrome P450-mediated oxidation of

glucuronide derivatives: Example of estradiol-17ß-glucuronide oxidation to 2-hydroxy-estradiol-17ß- glucuronide by CYP 2C8. Drug Metab Dispos 33: 466-473, 2005

Di L: The role of drug metabolizing enzymes in clearance. Expert Opin Drug Metab Toxicol 10: 379-393, 2014

D'Incalci M, Rossi C, Zucchetti M et al.: Pharmacokinetics of etoposide in patients with abnormal renal and hepatic function. Cancer Res 46: 2566-2571, 1986

Dong D, Ako R, Hu M, Wu B: Understanding substrate selectivity of human UDP-glucuronosyltransferases through QSAR modeling and analysis of homologous enzymes. Xenobiotica 42: 808-820, 2012

Doyle AL, Yang W, Abruzzo LV et al.: A multidrug resistance transporter from human MCF-7 breast cancer cells. Proc Natl Acad Sci U S A 95: 15665-15670, 1998

Drozdzik M, Gröer C, Penski J et al.: Protein abundance of clinically relevant multidrug transporters along the entire length of the human intestine. Mol Pharm 11: 3547-3555, 2014

EMA (European Medicines Agency): ICH guideline M3(R2) on non-clinical safety studies for the conduct of human clinical trials and marketing authorisation for pharmaceuticals, 2009. Available online: www.ema.europa.eu/docs/en_GB/document_library/Scientific_guideline/2009/09/WC500002720.pdf (accessed 22.11.2015).

EMA (European Medicines Agency), Committee for Human Medicinal Products (CHMP): Guideline on the investigation of drug interactions, 2012. Available online: www.ema.europa.eu/ema/pages/includes/document/open_document.jsp?webContentId=WC500129606 (accessed 22.11.2015).

Ethell BT, Ekins S, Wang J, Burchell B: Quantitative structure activity relationships for the glucuronidation of simple phenols by expressed human UGT1A6 and UGT1A9. Drug Metab Dispos 30: 734-738, 2002

Evers R, Kool M, van Deemter L et al.: Drug export activity of the human canalicular multispecific organic anion transporter in polarized kidney MDCK cells expressing cMOAT (MRP2) cDNA. J Clin Invest 101: 1310-1319, 1998

Evers R, De Haas M, Sparidans R et al.: Vinblastine and sulfinpyrazone export by the multidrug resistance protein MRP2 is associated with glutathione export. Br J Cancer 83: 375-383, 2000

Fagerholm U: Prediction of human pharmacokinetics - Renal metabolic and excretion clearance. J Pharm Pharmacol 59: 1463-1471, 2007

Fagerholm U: Prediction of human pharmacokinetics - Biliary and intestinal clearance and enterohepatic circulation. J Pharm Pharmacol 60: 535-542, 2008

Fahrmayr C, König J, Auge D, Mieth M, Fromm MF: Identification of drugs and drug metabolites as substrates of multidrug resistance protein 2 (MRP2) using triple-transfected MDCK-OATP1B1-UGT1A1-MRP2 cells. Br J Pharmacol 165: 1836-1847, 2012

Fahrmayr C, König J, Auge D et al.: Phase i and II metabolism and MRP2-mediated export of bosentan in a MDCKII-OATP1B1-CYP3A4-UGT1A1-MRP2 quadruple-transfected cell line. Br J Pharmacol 169: 21-33, 2013

Fallon JK, Neubert H, Hyland R, Goosen TC, Smith PC: Targeted quantitative proteomics for the analysis of 14 UGT1As and -2Bs in human liver using NanoUPLC-MS/MS with selected reaction monitoring. J Proteome Res 12: 4402-4413, 2013

FDA (U.S. Department of Health and Human Services, Food and Drug Administration, Center for Drug Evaluation and Research (CDER)): Safety Testing of Drug Metabolites, 2008. Available online: www.fda.gov/Drugs/GuidanceComplianceRegulatoryInformation/Guidances/UCM079266 (accessed 22.11.2015).

FDA (U.S. Department of Health and Human Services, Food and Drug Administration, Center for Drug Evaluation and Research (CDER): Drug Interaction Studies - Study Design, Data Analysis, Implications for Dosing, and Labeling Recommendations, 2012. Available online: www.fda.gov/downloads/Drugs/GuidanceComplianceRegulatoryInformation/Guidances/UCM292362.pdf (accessed 22.11.2015)

Fehrenbach T, Cui Y, Faulstich H, Keppler D: Characterization of the transport of the bicyclic peptide phalloidin by human hepatic transport proteins. Naunyn-Schmiedeberg's Arch Pharmacol 368: 415-420, 2003

Ferslew BC, Köck K, Bridges AS, Brouwer KLR: Role of multidrug resistance-associated protein 4 in the basolateral efflux of hepatically derived enalaprilat. Drug Metab Dispos 42: 1567-1574, 2014

Fromm MF, Kauffmann H-, Fritz P et al.: The effect of rifampin treatment on intestinal expression of human MRP transporters. Am J Pathol 157: 1575-1580, 2000

Fromm MF: Importance of P-glycoprotein at blood-tissue barriers. Trends Pharmacol Sci 25: 423-429, 2004

Gallagher CJ, Kadlubar FF, Muscat JE, Ambrosone CB, Lang NP, Lazarus P: The UGT2B17 gene deletion polymorphism and risk of prostate cancer. A case-control study in Caucasians. Cancer Detect Prev 31: 310-315, 2007

Gauthier-Landry L, Bélanger A, Barbier O: Multiple roles for udp-glucuronosyltransferase (UGT)2B15 and UGT2B17 enzymes in androgen metabolism and prostate cancer evolution. J Steroid Biochem Mol Biol 145: 187-192, 2015

Ge S, Yin T, Xu B, Gao S, Hu M: Curcumin Affects Phase II Disposition of Resveratrol Through Inhibiting Efflux Transporters MRP2 and BCRP. Pharm Res 2015

Gerk PM, Li W, Megaraj V, Vore M: Human multidrug resistance protein 2 transports the therapeutic bile salt tauroursodeoxycholate. J Pharmacol Exp Ther 320: 893-899, 2007

Ghibellini G, Leslie EM, Brouwer KLR: Methods to evaluate biliary excretion of drugs in humans: An updated review. Mol Pharm 3: 198-211, 2006

Ghosal A, Hapangama N, Yuan Y et al.: Identification of human UDP-glucuronosyltransferase enzyme(s) responsible for the glucuronidation of ezetimibe (ZETIA). Drug Metab Dispos 32: 314-320, 2004

Giacomini KM, Huang S-, Tweedie DJ et al.: Membrane transporters in drug development. Nat Rev Drug Discov 9: 215-236, 2010

Glavinas H, Méhn D, Jani M, Oosterhuis B, Herédi-Szabó K, Krajcsi P: Utilization of membrane vesicle preparations to study drug-ABC transporter interactions. Expert Opin Drug Metab Toxicol 4: 721-732, 2008

Gottesman MM, Fojo T, Bates SE: Multidrug resistance in cancer: Role of ATP-dependent transporters. Nat Rev Cancer 2: 48-58, 2002

Gramec Skledar D, Troberg J, Lavdas J, Mašic LP, Finel M: Differences in the glucuronidation of bisphenols F and S between two homologous human UGT enzymes, 1A9 and 1A10. Xenobiotica 45: 511-519, 2015

Grant CE, Valdimarsson G, Hipfner DR, Almquist KC, Cole SPC, Deeley RG: Overexpression of multidrug resistance-associated protein (MRP) increases resistance to natural product drugs. Cancer Res 54: 357-361, 1994

Gregus Z, Klaassen CD: Biliary excretion. J Clin Pharmacol 27: 537-541, 1987

Guillemette C, Lévesque É, Rouleau M: Pharmacogenomics of human uridine diphospho-glucuronosyltransferases and clinical implications. Clin Pharmacol Ther 96: 324-339, 2014

Han Y-, Busler D, Hong Y, Tian Y, Chen C, Rodrigues AD: Transporter studies with the 3-O-sulfate conjugate of 17a- ethinylestradiol: Assessment of human liver drug transporters. Drug Metab Dispos 38: 1072-1082, 2010

Hanahan D: Studies on transformation of Escherichia coli with plasmids. J Mol Biol 166: 557-580, 1983

Hanioka N, Ozawa S, Jinno H, Ando M, Saito Y, Sawada J: Human liver UDP-glucuronosyltransferase isoforms involved in the glucuronidation of 7-ethyl-10-hydroxycamptothecin. Xenobiotica 31: 687-699, 2001

Hao X-, Widersten M, Ridderstrom M, Hellman U, Mannervik B: Co-variation of glutathione transferase expression and cytostatic drug resistance in HeLa cells: Establishment of class Mu glutathione transferase M3-3 as the dominating isoenzyme. Biochem J 297: 59-67, 1994

Harbourt DE, Fallon JK, Ito S et al.: Quantification of human uridine-diphosphate glucuronosyl transferase 1A isoforms in liver, intestine, and kidney using nanobore liquid chromatography-tandem mass spectrometry. Anal Chem 84: 98-105, 2012

Hediger MA, Clémençon B, Burrier RE, Bruford EA: The ABCs of membrane transporters in health and disease (SLC series): Introduction. Mol Asp Med 34: 95-107, 2013

Herédi-Szabó K, Glavinas H, Kis E et al.: Multidrug resistance protein 2-mediated estradiol-17ßcuronide transport potentiation: In vitro-in vivo correlation and species specificity. Drug Metab Dispos 37: 794-801, 2009

Hilgendorf C, Ahlin G, Seithel A, Artursson P, Ungell A-, Karlsson J: Expression of thirty-six drug transporter genes in human intestine, liver, kidney, and organotypic cell lines. Drug Metab Dispos 35: 1333-1340, 2007

Hillgren KM, Keppler D, Zur AA et al.: Emerging transporters of clinical importance: An update from the international transporter consortium. Clin Pharmacol Ther 94: 52-63, 2013

Hirouchi M, Kusuhara H, Onuki R, Ogilvie BW, Parkinson A, Sugiyama Y: Construction of triple-transfected cells [organic anion-transporting polypeptide (OATP) 1B1/multidrug resistance-associated protein (MRP) 2/MRP3 and OATP1B1/MRP2/MRP4] for analysis of the sinusoidal function of MRP3 and MRP4. Drug Metab Dispos 37: 2103-2111, 2009

Hoffmann U, Kroemer HK: The ABC transporters MDR1 and MRP2: Multiple functions in disposition of xenobiotics and drug resistance. Drug Metab Rev 36: 669-701, 2004

Holland NT, Smith MT, Eskenazi B, Bastaki M: Biological sample collection and processing for molecular epidemiological studies. Mutat Res Rev Mutat Res 543: 217-234, 2003

Holmes DS, Quigley M: A rapid boiling method for the preparation of bacterial plasmids. Anal Biochem 114: 193-197, 1981

Hoskin PJ, Hanks GW: Morphine: Pharmacokinetics and clinical practice. Br J Cancer 62: 705-707, 1990

Huang L, Hoffman T, Vore M: Adenosine triphosphate-dependent transport of estradiol-17ß (ß-D- glucuronide) in membrane vesicles by MDR1 expressed in insect

cells. Hepatology 28: 1371-1377, 1998

Huisman MT, Smit JW, Crommentuyn KML et al.: Multidrug resistance protein 2 (MRP2) transports HIV protease inhibitors, and transport can be enhanced by other drugs. AIDS 16: 2295-2301, 2002

Huls M, Brown CDA, Windass AS et al.: The breast cancer resistance protein transporter ABCG2 is expressed in the human kidney proximal tubule apical membrane. Kidney Int 73: 220-225, 2008

Imai Y, Asada S, Tsukahara S, Ishikawa E, Tsuruo T, Sugimoto Y: Breast cancer resistance protein exports sulfated estrogens but not free estrogens. Mol Pharmacol 64: 610-618, 2003

Imaoka T, Kusuhara H, Adachi M, Schuetz JD, Takeuchi K, Sugiyama Y: Functional involvement of multidrug resistance-associated protein 4 (MRP4/ABCC4) in the renal elimination of the antiviral drugs adefovir and tenofovir. Mol Pharmacol 71: 619-627, 2007

Ishiguro N, Maeda K, Saito A et al.: Establishment of a set of double transfectants coexpressing organic anion transporting polypeptide 1B3 and hepatic efflux transporters for the characterization of the hepatobiliary transport of telmisartan acylglucuronide. Drug Metab Dispos 36: 796-805, 2008

Ishizuka H, Konno K, Shiina T et al.: Species differences in the transport activity for organic anions across the bile canalicular membrane. J Pharmacol Exp Ther 290: 1324-1330, 1999

Jedlitschky G, Leier I, Buchholz U, Barnouin K, Kurz G, Keppler D: Transport of glutathione, glucuronate, and sulfate conjugates by the MRP gene-encoded conjugate export pump. Cancer Res 56: 988-994, 1996

Jedlitschky G, Tirschmann K, Lubenow LE et al.: The nucleotide transporter MRP4 (ABCC4) is highly expressed in human platelets and present in dense granules, indicating a role in mediator storage. Blood 104: 3603-3610, 2004

Jensen MA, Fukushima M, Davis RW: DMSO and betaine greatly improve amplification of GC-rich constructs in de novo synthesis. PLoS ONE 5: 2010

Jeong EJ, Lin H, Hu M: Disposition mechanisms of raloxifene in the human intestinal Caco-2 model. J Pharmacol Exp Ther 310: 376-385, 2004

Jeong EJ, Liu X, Jia X, Chen J, Hu M: Coupling of conjugating enzymes and efflux transporters: Impact on bioavailability and drug interactions. Curr Drug Metab 6: 455-468, 2005

Ji B, Ito K, Suzuki H, Sugiyama Y, Horie T: Multidrug resistance-associated protein2 (MRP2) plays an important role in the biliary excretion of glutathione conjugates of 4-

hydroxynonenal. Free Radic Biol Med 33: 370-378, 2002

Jin C, Miners JO, Lillywhite KJ, Mackenzie PI: Complementary deoxyribonucleic acid cloning and expression of a human liver uridine diphosphate-glucuronosyltransferase glucuronidating carboxylic acid-containing drugs. J Pharmacol Exp Ther 264: 475-479, 1993

Kaivosaari S, Finel M, Koskinen M: N-glucuronidation of drugs and other xenobiotics by human and animal UDP-glucuronosyltransferases. Xenobiotica 41: 652-669, 2011

Kamdem LK, Liu Y, Stearns V et al.: In vitro and in vivo oxidative metabolism and glucuronidation of anastrozole. Br J Clin Pharmacol 70: 854-869, 2010

Kamiie J, Ohtsuki S, Iwase R et al.: Quantitative atlas of membrane transporter proteins: Development and application of a highly sensitive simultaneous LC/MS/MS method combined with novel in-silico peptide selection criteria. Pharm Res 25: 1469-1483, 2008

Kamisako T, Leier I, Gui Y et al.: Transport of monoglucuronosyl and bisglucuronosyl bilirubin by recombinant human and rat multidrug resistance protein 2. Hepatology 30: 485-490, 1999

Kartenbeck J, Leuschner U, Mayer R, Keppler D: Absence of the canalicular isoform of the MRP gene - encoded conjugate export pump from the hepatocytes in Dubin-Johnson syndrome. Hepatology 23: 1061-1066, 1996

Keppler D: The roles of MRP2, MRP3, OATP1B1, and OATP1B3 in conjugated hyperbilirubinemia. Drug Metab Dispos 42: 561-565, 2014

King CD, Rios GR, Green MD, Tephly TR: UDP-Glucuronosyltransferases. Curr Drug Metab 1: 143-161, 2000

Kitamura Y, Kusuhara H, Sugiyama Y: Functional characterization of multidrug resistance-associated protein 3 (Mrp3/Abcc3) in the basolateral efflux of glucuronide conjugates in the mouse small intestine. J Pharmacol Exp Ther 332: 659-666, 2010

Kiuchi Y, Suzuki H, Hirohashi T, Tyson CA, Sugiyama Y: cDNA cloning and inducible expression of human multidrug resistance associated protein 3 (MRP3). FEBS Lett 433: 149-152, 1998

Komura H, Iwaki M: In vitro and in vivo small intestinal metabolism of CYP3A and UGT substrates in preclinical animals species and humans: Species differences. Drug Metab Rev 43: 476-498, 2011

König J, Rost D, Cui Y, Keppler D: Characterization of the human multidrug resistance protein isoform MRP3 localized to the basolateral hepatocyte membrane. Hepatology 29: 1156-1163, 1999a

König J, Nies AT, Cui Y, Leier I, Keppler D: Conjugate export pumps of the multidrug resistance protein (MRP) family: Localization, substrate specificity, and MRP2-mediated drug resistance. Biochim Biophys Acta Biomembr 1461: 377-394, 1999b

König J, Müller F, Fromm MF: Transporters and drug-drug interactions: Important determinants of drug disposition and effects. Pharmacol Rev 65: 944-966, 2013

Kool M, De Haas M, Scheffer GL et al.: Analysis of expression of cMOAT (MRP2), MRP3, MRP4, and MRP5, homologues of the multidrug resistance-associated protein gene (MRP1), in human cancer cell lines. Cancer Res 57: 3537-3547, 1997

Kool M, Van Der Linden M, De Haas M et al.: MRP3, an organic anion transporter able to transport anti-cancer drugs. Proc Natl Acad Sci U S A 96: 6914-6919, 1999

Kopplow K, Letschert K, König J, Walter B, Keppler D: Human hepatobiliary transport of organic anions analyzed by quadruple-transfected cells. Mol Pharmacol 68: 1031-1038, 2005

Kosoglou T, Statkevich P, Johnson-Levonas AO, Paolini JF, Bergman AJ, Alton KB: Ezetimibe: A review of its metabolism, pharmacokinetics and drug interactions. Clin Pharmacokinet 44: 467-494, 2005

Krumpochova P, Sapthu S, Brouwers JF et al.: Transportomics: Screening for substrates of ABC transporters in body fluids using vesicular transport assays. FASEB J 26: 738-747, 2012

Kurkela M, Garcia-Horsmant JA, Luukkanen L et al.: Expression and characterization of recombinant human UDP-glucuronosyltransferases (UGTs): UGT1A9 is more resistant to detergent inhibition than the other UGTs and was purified as an active dimeric enzyme. J Biol Chem 278: 3536-3544, 2003

Kwatra D, Budda B, Vadlapudi AD, Vadlapatla RK, Pal D, Mitra AK: Transfected MDCK cell line with enhanced expression of CYP3A4 and P-glycoprotein as a model to study their role in drug transport and metabolism. Mol Pharm 9: 1877-1886, 2012

Laakkonen L, Finel M: A molecular model of the human UDP-glucuronosyltransferase 1A1, its membrane orientation, and the interactions between different parts of the enzyme. Mol Pharmacol 77: 931-939, 2010

Lagas JS, Fan L, Wagenaar E et al.: P-glycoprotein (P-gp/Abcb1), Abcc2, and Abcc3 determine the pharmacokinetics of etoposide. Clin Cancer Res 16: 130-140, 2010a

Lagas JS, Sparidans RW, Wagenaar E, Beijnen JH, Schinkel AH: Hepatic clearance of reactive glucuronide metabolites of diclofenac in the mouse is dependent on multiple ATP-binding cassette efflux transporters. Mol Pharmacol 77: 687-694, 2010b

Lander ES, Linton LM, Birren B et al.: Initial sequencing and analysis of the human genome. Nature 409: 860-921, 2001

Lautala P, Ethell BT, Taskinen J, Burchell B: The specificity of glucuronidation of entacapone and tolcapone by recombinant human UDP-glucuronosyltransferases. Drug Metab Dispos 28: 1385-1389, 2000

Lavé T, Chapman K, Goldsmith P, Rowland M: Human clearance prediction: Shifting the paradigm. Expert Opin Drug Metab Toxicol 5: 1039-1048, 2009

Lee K, Belinsky MG, Bell DW, Testa JR, Kruh GD: Isolation of MOAT-B, a widely expressed multidrug resistance-associated protein/canalicular multispecific organic anion transporter-related transporter. Cancer Res 58: 2741-2747, 1998

Lee Y-A, Cui Y, König J et al.: Identification and functional characterization of the natural variant MRP3-Arg1297His of human multidrug resistance protein 3 (MRP3/ABCC3). Pharmacogenetics 14: 213-223, 2004

Leggas M, Adachi M, Scheffer GL et al.: Mrp4 confers resistance to topotecan and protects the brain from chemotherapy. Mol Cell Biol 24: 7612-7621, 2004

Leier I, Hummel-Eisenbeiss J, Cui Y, Keppler D: ATP-dependent para-aminohippurate transport by apical multidrug resistance protein MRP2. Kidney Int 57: 1636-1642, 2000

Leslie EM, Ito K-, Upadhyaya P, Hecht SS, Deeley RG, Cole SPC: Transport of the ß-O-glucuronide conjugate of the tobacco-specific carcinogen 4-(methylnitrosamino)-1-(3-pyridyl)-1-butanol (NNAL) by the multidrug resistance protein 1 (MRP1): Requirement for glutathione or a non-sulfur-containing analog. J Biol Chem 276: 27846-27854, 2001

Letschert K, Komatsu M, Hummel-Eisenbeiss J, Keppler D: Vectorial transport of the peptide CCK-8 by double-transfected MDCKII cells stably expressing the organic anion transporter OATP1B3 (OATP8) and the export pump ABCC2. J Pharmacol Exp Ther 313: 549-556, 2005

Lévesque E, Girard H, Journault K, Lépine J, Guillemette C: Regulation of the UGT1A1 bilirubin-conjugating pathway: Role of a new splicing event at the UGT1A locus. Hepatology 45: 128-138, 2007

Li H, Jin H-, Kim W et al.: Involvement of P-glycoprotein, multidrug resistance protein 2 and breast cancer resistance protein in the transport of belotecan and topotecan in Caco-2 and MDCKII cells. Pharm Res 25: 2601-2612, 2008a

Li M, Yuan H, Li N et al.: Identification of interspecies difference in efflux transporters of hepatocytes from dog, rat, monkey and human. Eur J Pharm Sci 35: 114-126, 2008b

Li N, Zhang Y, Hua F, Lai Y: Absolute difference of hepatobiliary transporter multidrug resistance-associated protein (MRP2/Mrp2) in liver tissues and isolated hepatocytes from rat, dog, monkey, and human. Drug Metab Dispos 37: 66-73, 2009

Lin JH, Wong BK: Complexities of glucuronidation affecting in vitro-in vivo

extrapolation. Curr Drug Metab 3: 623-646, 2002

Ling MM, Robinson BH: Approaches to DNA mutagenesis: An overview. Anal Biochem 254: 157-178, 1997

Lo W-, Chiou Y-, Hsu Y- et al.: Enzymatic and nonenzymatic synthesis of glutathione conjugates: Application to the understanding of a parasite's defense system and alternative to the discovery of potent glutathione S-transferase inhibitors. Bioconjugate Chem 18: 109-120, 2007

Loe DW, Almquist KC, Deeley RG, Cole SPC: Multidrug resistance protein (MRP)-mediated transport of leukotriene C4 and chemotherapeutic agents in membrane vesicles: Demonstration of glutathione-dependent vincristine transport. J Biol Chem 271: 9675-9682, 1996

Loi C-, Smith DA, Dalvie D: Which metabolites circulate? Drug Metab Dispos 41: 933-951, 2013

Mahmood I: Interspecies scaling of biliary excreted drugs: A comparison of several methods. J Pharm Sci 94: 883-892, 2005

Maliepaard M, Scheffer GL, Faneyte IF et al.: Subcellular localization and distribution of the Breast Resistance Protein Transporter in normal human tissues. Cancer Res 61: 3458-3464, 2001

Manautou JE, De Waart DR, Kunne C et al.: Altered disposition of acetaminophen in mice with a disruption of the Mrp3 gene. Hepatology 42: 1091-1098, 2005

Mao Q, Unadkat JD: Role of the Breast Cancer Resistance Protein (BCRP/ABCG2) in Drug Transport—an Update. AAPS J 17: 65-82, 2015

Marchetti S, De Vries NA, Buckle T et al.: Effect of the ATP-binding cassette drug transporters ABCB1, ABCG2, and ABCC2 on erlotinib hydrochloride (Tarceva) disposition in in vitro and in vivo pharmacokinetic studies employing Bcrp1-/-/Mdr1a/1b-/- (triple-knockout) and wild-type mice. Mol Cancer Ther 7: 2280-2287, 2008

Matsunaga N, Wada S, Nakanishi T, Ikenaga M, Ogawa M, Tamai I: Mathematical modeling of the in vitro hepatic disposition of mycophenolic acid and its glucuronide in sandwich-cultured human hepatocytes. Mol Pharm 11: 568-579, 2014

Matsushima S, Maeda K, Ishiguro N, Igarashi T, Sugiyama Y: Investigation of the inhibitory effects of various drugs on the hepatic uptake of fexofenadine in humans. Drug Metab Dispos 36: 663-669, 2008

Mayer R, Kartenbeck J, Büchler M, Jedlitschky G, Leier I, Keppler D: Expression of the MRP gene-encoded conjugate export pump in liver and its selective absence from the canalicular membrane in transport-deficient mutant hepatocytes. J Cell Biol 131:

137-150, 1995

McGill MR, Jaeschke H: Metabolism and disposition of acetaminophen: Recent advances in relation to hepatotoxicity and diagnosis. Pharm Res 30: 2174-2187, 2013

Minematsu T, Hashimoto T, Usui T, Kamimura H: Characterization of renal tubular apical efflux of zonampanel, an a-amino-3-hydroxy-5- methylisoxazole-4-propionate receptor antagonist, in humans. Xenobiotica 38: 1191-1202, 2008

Miners JO, Smith PA, Sorich MJ, McKinnon RA, Mackenzie PI: Predicting Human Drug Glucuronidation Parameters: Application of In Vitro and In Silico Modeling Approaches. Annu Rev Pharmacol Toxicol 44: 1-25, 2004

Miners JO, Bowalgaha K, Elliot DJ, Baranczewski P, Knights KM: Characterization of niflumic acid as a selective inhibitor of human liver microsomal UDP-glucuronosyltransferase 1A9: Application to the reaction phenotyping of acetaminophen glucuronidation. Drug Metab Dispos 39: 644-652, 2011

Ming X, Thakker DR: Role of basolateral efflux transporter MRP4 in the intestinal absorption of the antiviral drug adefovir dipivoxil. Biochem Pharmacol 79: 455-462, 2010

Mizuno N, Takahashi T, Kusuhara H, Schuetz JD, Niwa T, Sugiyama Y: Evaluation of the role of Breast Cancer Resistance Protein (BCRP/ABCG2) and Multidrug Resistance-Associated Protein 4 (MRP4/ABCC4) in the urinary excretion of sulfate and glucuronide metabolites of edaravone (MCI-186; 3-methyl-1-phenyl-2-pyrazolin-5-one). Drug Metab Dispos 35: 2045-2052, 2007

Morello KC, Wurz GT, DeGregorio MW: Pharmacokinetics of selective estrogen receptor modulators. Clin Pharmacokinet 42: 361-372, 2003

Mutsaers HAM, Caetano-Pinto P, Seegers AEM et al.: Proximal tubular efflux transporters involved in renal excretion of p-cresyl sulfate and p-cresyl glucuronide: Implications for chronic kidney disease pathophysiology. Toxicol Vitro 29: 1868-1877, 2015

Nagy N, Kuipers HF, Frymoyer AR et al.: 4-Methylumbelliferone treatment and hyaluronan inhibition as a therapeutic strategy in inflammation, autoimmunity, and cancer. Front Immunol 6: 2015

Neve EPA, Artursson P, Ingelman-Sundberg M, Karlgren M: An integrated in vitro model for simultaneous assessment of drug uptake, metabolism, and efflux. Mol Pharm 10: 3152-3163, 2013

Nezasa K-, Tian X, Zamek-Gliszczynski MJ, Patel NJ, Raub TJ, Brouwer KLR: Altered hepatobiliary disposition of 5 (and 6)-carboxy-2',7'- dichlorofluorescein in Abcg2 (Bcrp1) and Abcc2 (Mrp2) knockout mice. Drug Metab Dispos 34: 718-723, 2006

Ng KH, Lim BG, Wong KP: Sulfate conjugating and transport functions of MDCK distal tubular cells. Kidney Int 63: 976-986, 2003

Ni Z, Bikadi Z, Rosenberg MF, Mao Q: Structure and function of the human breast cancer resistance protein (BCRP/ABCG2). Curr Drug Metab 11: 603-617, 2010

Ninomiya M, Ito K, Horie T: Functional analysis of dog multidrug resistance-associated protein 2 (Mrp2) in comparison with rat Mrp2. Drug Metab Dispos 33: 225-232, 2005

Nishimura M, Naito S: Tissue-specific mRNA expression profiles of human ATP-binding cassette and solute carrier transporter superfamilies. Drug Metab Pharmacokinet 20: 452-477, 2005

Nowell SA, Massengill JS, Williams S et al.: Glucuronidation of 2-hydroxyamino-1-methyl-6-phenylimidazo[4,5-b]pyridine by human microsomal UDP-glucuronosyltransferases: Identification of specific UGT1A family isoforms involved. Carcinogenesis 20: 1107-1114, 1999

Obach SR: Pharmacologically active drug metabolites: Impact on drug discovery and pharmacotherapy. Pharmacol Rev 65: 578-640, 2013

Obach RS, Lombardo F, Waters NJ: Trend analysis of a database of intravenous pharmacokinetic parameters in humans for 670 drug compounds. Drug Metab Dispos 36: 1385-1405, 2008

Oda S, Fukami T, Yokoi T, Nakajima M: A comprehensive review of UDP-glucuronosyltransferase and esterases for drug development. Drug Metab Pharmacokinet 30: 30-51, 2015

Ohno S, Nakajin S: Determination of mRNA expression of human UDP-glucuronosyltransferases and application for localization in various human tissues by real-time reverse transcriptase-polymerase chain reaction. Drug Metab Dispos 37: 32-40, 2009

Ohtsuki S, Schaefer O, Kawakami H et al.: Simultaneous absolute protein quantification of transporters, cytochromes P450, and UDP-glucuronosyltransferases as a novel approach for the characterization of individual human liver: Comparison with mRNA levels and activities. Drug Metab Dispos 40: 83-92, 2012

Oleschuk CJ, Deeley RG, Cole SPC: Substitution of Trp1242 of TM17 alters substrate specificity of human multidrug resistance protein 3. Am J Physiol Gastrointest Liver Physiol 284: G280-G289, 2003

Oude Elferink RPJ, Meijer DKF, Kuipers F, Jansen PLM, Groen AK, Groothuis GMM: Hepatobiliary secretion of organic compounds; molecular mechanisms of membrane transport. Biochim Biophys Acta Rev Biomembr 1241: 215-268, 1995

Patel CG, Ogasawara K, Akhlaghi F: Mycophenolic acid glucuronide is transported by

multidrug resistance-associated protein 2 and this transport is not inhibited by cyclosporine, tacrolimus or sirolimus. Xenobiotica 43: 229-235, 2013

Paul D, Standifer KM, Inturrisi CE, Pasternak GW: Pharmacological characterization of morphine-6ß-glucuronide, a very potent morphine metabolite. J Pharmacol Exp Ther 251: 477-483, 1989

Paulusma CC, Bosma PJ, Zaman GJR et al.: Congenital jaundice in rats with a mutation in a multidrug resistance-associated protein gene. Science 271: 1126-1128, 1996

Paulusma CC, Van Geer MA, Evers R et al.: Canalicular multispecific organic anion transporter/multidrug resistance protein 2 mediates low-affinity transport of reduced glutathione. Biochem J 338: 393-401, 1999

Paumi CM, Wright M, Townsend AJ, Morrow CS: Multidrug resistance protein (MRP) 1 and MRP3 attenuate cytotoxic and transactivating effects of the cyclopentenone prostaglandin, 15-deoxy-d 12,14prostaglandin J2 in MCF7 breast cancer cells. Biochemistry 42: 5429-5437, 2003

Pellegatti M: Preclinical in vivo ADME studies in drug development: A critical review. Expert Opin Drug Metab Toxicol 8: 161-172, 2012

Pratt S, Chen V, Perry III WI, Starling JJ, Dantzig AH: Kinetic validation of the use of carboxydichlorofluorescein as a drug surrogate for MRP5-mediated transport. Eur J Pharm Sci 27: 524-532, 2006

Priebe W, Krawczyk M, Kuo MT, Yamane Y, Savaraj N, Ishikawa T: Doxorubicin- and daunorubicin-glutathione conjugates, but not unconjugated drugs, competitively inhibit leukotriene C4 transport mediated by MRP/GS-X pump. Biochem Biophys Res Commun 247: 859-863, 1998

Quan E, Wang H, Dong D, Zhang X, Wu B: Characterization of chrysin glucuronidation in UGT1A1-overexpressing HeLa cells: Elucidating the transporters responsible for efflux of glucuronide. Drug Metab Dispos 43: 433-443, 2015

Raftogianis R, Creveling C, Weinshilboum R, Weisz J: Estrogen metabolism by conjugation. J Natl Cancer Inst Monographs 113-124, 2000

Ray AS, Cihlar T, Robinson KL et al.: Mechanism of active renal tubular efflux of tenofovir. Antimicrob Agents Chemother 50: 3297-3304, 2006

Rees DC, Johnson E, Lewinson O: ABC transporters: The power to change. Nat Rev Mol Cell Biol 10: 218-227, 2009

Ritter JK, Sheen YY, Owens IS: Cloning and expression of human liver UDP-glucuronosyltransferase in COS-1 cells: 3,4-catechol estrogens and estriol as primary substrates. J Biol Chem 265: 7900-7906, 1990

Rius M, Nies AT, Hummel-Eisenbeiss J, Jedlitschky G, Keppler D: Cotransport of reduced glutathione with bile salts by MRP4 (ABCC4) localized to the basolateral hepatocyte membrane. Hepatology 38: 374-384, 2003

Rius M, Thon WF, Keppler D, Nies AT: Prostanoid transport by multidrug resistance protein 4 (MRP4/ABCC4) localized in tissues of the human urogenital tract. J Urol 174: 2409-2414, 2005

Rost D, Mahner S, Sugiyama Y, Stremmel W: Expression and localization of the multidrug resistance-associated protein 3 in rat small and large intestine. Am J Physiol Gastrointest Liver Physiol 282: G720-G726, 2002

Roth M, Obaidat A, Hagenbuch B: OATPs, OATs and OCTs: The organic anion and cation transporters of the SLCO and SLC22A gene superfamilies. Br J Pharmacol 165: 1260-1287, 2012

Rowland A, Miners JO, Mackenzie PI: The UDP-glucuronosyltransferases: Their role in drug metabolism and detoxification. Int J Biochem Cell Biol 45: 1121-1132, 2013

Ruiz-Garcia A, Bermejo M, Moss A, Casabo VG: Pharmacokinetics in drug discovery. J Pharm Sci 97: 654-690, 2008

Ryu S, Kawabe T, Nada S, Yamaguchi A: Identification of basic residues involved in drug export function of human multidrug resistance-associated protein 2. J Biol Chem 275: 39617-39624, 2000

Sallustio BC, Sabordo L, Evans AM, Nation RL: Hepatic Disposition of Electrophilic Acyl Glucuronide Conjugates. Curr Drug Metab 1: 163-180, 2000

Sato Y, Nagata M, Tetsuka K et al.: Optimized methods for targeted peptide-based quantification of human uridine 59-diphosphate-glucuronosyltransferases in biological specimens using liquid chromatography-tandem mass spectrometry. Drug Metab Dispos 42: 885-889, 2014

Scheffer GL, Kool M, De Haas M et al.: Tissue distribution and induction of human multidrug resistant protein 3. Lab Invest 82: 193-201, 2002

Schinkel AH, Jonker JW: Mammalian drug efflux transporters of the ATP binding cassette (ABC) family: An overview. Adv Drug Deliv Rev 55: 3-29, 2003

Schwab N, Skopp G: Identification and preliminary characterization of UDP-glucuronosyltransferases catalyzing formation of ethyl glucuronide. Anal Bioanal Chem 406: 2325-2332, 2014

Scialis RJ, Csanaky IL, Goedken MJ, Manautou JE: Multidrug resistance-associated protein 3 plays an important role in protection against acute toxicity of diclofenac. Drug Metab Dispos 43: 944-950, 2015

Seelheim P, Wüllner A, Galla H-: Substrate translocation and stimulated ATP hydrolysis of human ABC transporter MRP3 show positive cooperativity and are half-coupled. Biophys Chem 171: 31-37, 2013

Seelig A: A general pattern for substrate recognition by P-glycoprotein. Eur J Biochem 251: 252-261, 1998

Sharom FJ: ABC multidrug transporters: Structure, function and role in chemoresistance. Pharmacogenomics 9: 105-127, 2008

Shawahna R, Uchida Y, Declèves X et al.: Transcriptomic and quantitative proteomic analysis of transporters and drug metabolizing enzymes in freshly isolated human brain microvessels. Mol Pharm 8: 1332-1341, 2011

Shi S, Li Y: Interplay of drug-metabolizing enzymes and transporters in drug absorption and disposition. Curr Drug Metab 15: 915-941, 2014

Shitara Y, Hirano M, Sato H, Sugiyama Y: Gemfibrozil and its glucoronide inhibit the organic anion transporting polypeptide 2 (OATP2/OATP1B1:SLC21A6)-mediated hepatic uptake and CYP2C8-mediated metabolism of cerivastatin: Analysis of the mechanism of the clinically relevant drug-drug interaction between cerivastatin and gemfibrozil. J Pharmacol Exp Ther 311: 228-236, 2004

Smith PA, Soric MJ, McKinnon RA, Miners JO: In silico insights: Chemical and structural characteristics associated with uridine diphosphate-glucuronosyltransferase substrate selectivity. Clin Exp Pharmacol Physiol 30: 836-840, 2003

Smith DA, Dalvie D: Why do metabolites circulate? Xenobiotica 42: 107-126, 2012

Smitherman PK, Townsend AJ, Kute TE, Morrow CS: Role of Multidrug Resistance Protein 2 (MRP2, ABCC2) in Alkylating Agent Detoxification: MRP2 Potentiates Glutathione S-Transferase A1-1-Mediated Resistance to Chlorambucil Cytotoxicity. J Pharmacol Exp Ther 308: 260-267, 2004

Stingl JC, Bartels H, Viviani R, Lehmann ML, Brockmöller J: Relevance of UDP-glucuronosyltransferase polymorphisms for drug dosing: A quantitative systematic review. Pharmacol Ther 141: 92-116, 2014

Stouch TR, Gudmundsson O: Progress in understanding the structure-activity relationships of P-glycoprotein. Adv Drug Deliv Rev 54: 315-328, 2002

Sugawara I, Akiyama S, Scheper RJ, Itoyama S: Lung resistance protein (LRP) expression in human normal tissues in comparison with that of MDR1 and MRP. Cancer Lett 112: 23-31, 1997

Sun D, Jones NR, Manni A, Lazarus P: Characterization of raloxifene glucuronidation: Potential role of UGT1A8 genotype on raloxifene metabolism in vivo. Cancer Prev Res 6: 719-730, 2013

Suzuki H, Sugiyama Y: Role of metabolic enzymes and efflux transporters in the absorption of drugs from the small intestine. Eur J Pharm Sci 12: 3-12, 2000

Suzuki M, Suzuki H, Sugimoto Y, Sugiyama Y: ABCG2 transports sulfated conjugates of steroids and xenobiotics. J Biol Chem 278: 22644-22649, 2003

Szafraniec MJ, Szczygiel M, Urbanska K, Fiedor L: Determinants of the activity and substrate recognition of breast cancer resistance protein (ABCG2). Drug Metab Rev 46: 459-474, 2014

Takusagawa S, Ushigome F, Nemoto H et al.: Intestinal absorption mechanism of mirabegron, a potent and selective ß3-adrenoceptor agonist: Involvement of human efflux and/or influx transport systems. Mol Pharm 10: 1783-1794, 2013

Taniguchi K, Wada M, Kohno K et al.: A human canalicular multispecific organic anion transporter (cMOAT) gene is overexpressed in cisplatin-resistant human cancer cell lines with decreased drug accumulation. Cancer Res 56: 4124-4129, 1996

Thiebaut F, Tsuruo T, Hamada H, Gottesman MM, Pastan I, Willingham MC: Cellular localization of the multidrug-resistance gene product P-glycoprotein in normal human tissues. Proc Natl Acad Sci U S A 84: 7735-7738, 1987

Tong Z, Yerramilli U, Surapaneni S, Kumar G: The interactions of lenalidomide with human uptake and efflux transporters and UDP-glucuronosyltransferase 1A1: Lack of potential for drug-drug interactions. Cancer Chemother Pharmacol 73: 869-874, 2014

Uchida Y, Ohtsuki S, Katsukura Y et al.: Quantitative targeted absolute proteomics of human blood-brain barrier transporters and receptors. J Neurochem 117: 333-345, 2011

Unger T, Jacobovitch Y, Dantes A, Bernheim R, Peleg Y: Applications of the Restriction Free (RF) cloning procedure for molecular manipulations and protein expression. J Struct Biol 172: 34-44, 2010

Van Aubel RAMH, Smeets PHE, Peters JGP, Bindels RJM, Russel FGM: The MRP4/ABCC4 gene encodes a novel apical organic anion transporter in human kidney proximal tubules: Putative efflux pump for urinary cAMP and cGMP. J Am Soc Nephrol 13: 595-603, 2002

Van Aubel RAMH, Smeets PHE, Van Den Heuvel JJMW, Russel FGM: Human organic anion transporter MRP4 (ABCC4) is an efflux pump for the purine end metabolite urate with multiple allosteric substrate binding sites. Am J Physiol Renal Physiol 288: F327-F333, 2005

van de Wetering K, Zelcer N, Kuil A et al.: Multidrug resistance proteins 2 and 3 provide alternative routes for hepatic excretion of morphine-glucuronides. Mol Pharmacol 72: 387-394, 2007

van de Wetering K, Burkon A, Feddema W et al.: Intestinal breast cancer resistance

protein (BCRP)/Bcrp1 and multidrug resistance protein 3 (MRP3)/Mrp3 are involved in the pharmacokinetics of resveratrol. Mol Pharmacol 75: 876-885, 2009a

van de Wetering K, Feddema W, Helms JB, Brouwers JF, Borst P: Targeted Metabolomics Identifies Glucuronides of Dietary Phytoestrogens as a Major Class of MRP3 Substrates In Vivo. Gastroenterology 137: 1725-1735, 2009b

van den Ent F, Löwe J: RF cloning: A restriction-free method for inserting target genes into plasmids. J Biochem Biophys Methods 67: 67-74, 2006

van der Schoor LWE, Verkade HJ, Kuipers F, Jonker JW: New insights in the biology of ABC transporters ABCC2 and ABCC3: Impact on drug disposition. Expert Opin Drug Metab Toxicol 11: 273-293, 2015

Varadaraj K, Skinner DM: Denaturants or cosolvents improve the specificity of PCR amplification of a G + C-rich DNA using genetically engineered DNA polymerases. Gene 140: 1-5, 1994

Varma MVS, Feng B, Obach RS et al.: Physicochemical determinants of human renal clearance. J Med Chem 52: 4844-4852, 2009

Varma MVS, Chang G, Lai Y et al.: Physicochemical property space of hepatobiliary transport and computational models for predicting rat biliary excretion. Drug Metab Dispos 40: 1527-1537, 2012

Vasiliou V, Vasiliou K, Nebert DW: Human ATP-binding cassette (ABC) transporter family. Hum Genomics 3: 281-290, 2009

Vasilyeva A, Durmus S, Li L et al.: Hepatocellular shuttling and recirculation of sorafenib-glucuronide is dependent on Abcc2, Abcc3, and Oatp1a/1b. Cancer Res 75: 2729-2736, 2015

Veal GJ, Back DJ: Metabolism of zidovudine. Gen Pharmacol Vasc Syst 26: 1469-1475, 1995

Vermeir M, Annaert P, Mamidi RNVS, Roymans D, Meuldermans W, Mannens G: Cell-based models to study hepatic drug metabolism and enzyme induction in humans. Expert Opin Drug Metab Toxicol 1: 75-90, 2005

Vree TB, Verwey-Van Wissen CPWGM: Pharmacokinetics and metabolism of codeine in humans. Biopharm Drug Dispos 13: 445-460, 1992

Wakabayashi Y, Maruyama S, Hachimura K, Ohwada T: Activated charcoal interrupts enteroenteric circulation of phenobarbital. Clin Toxicol 32: 419-424, 1994

Walle T, Hsieh F, DeLegge MH, Oatis Jr. JE, Walle UK: High absorption but very low bioavailability of oral resveratrol in humans. Drug Metab Dispos 32: 1377-1382, 2004

Wang L, Prasad B, Salphati L et al.: Interspecies variability in expression of

hepatobiliary transporters across human, dog, monkey, and rat as determined by quantitative proteomics. Drug Metab Dispos 43: 367-374, 2015

Wikberg T, Vuorela A, Ottoila P, Taskinen J: Identification of major metabolites of the catechol-O-methyltransferase inhibitor entacapone in rats and humans. Drug Metab Dispos 21: 81-92, 1993

Williams JA, Hyland R, Jones BC et al.: Drug-drug interactions for UDP-glucuronosyltransferase substrates: A pharmacokinetic explanation for typically observed low exposure (AUC 1/AUC) ratios. Drug Metab Dispos 32: 1201-1208, 2004

Wittgen HGM, Van Den Heuvel JJMW, Van Den Broek PHH et al.: Transport of the coumarin metabolite 7-hydroxycoumarin glucuronide is mediated via multidrug resistance-associated proteins 3 and 4. Drug Metab Dispos 40: 1076-1079, 2012

Wortelboer HM, Usta M, Van Der Velde AE et al.: Interplay between MRP Inhibition and Metabolism of MRP Inhibitors: The Case of Curcumin. Chem Res Toxicol 16: 1642-1651, 2003

Wu C-, Benet LZ: Predicting drug disposition via application of BCS: Transport/absorption/ elimination interplay and development of a biopharmaceutics drug disposition classification system. Pharm Res 22: 11-23, 2005

Wu B, Basu S, Meng S, Wang X, Hu M: Regioselective sulfation and glucuronidation of phenolics: Insights into the structural basis. Curr Drug Metab 12: 900-916, 2011

Xia CQ, Milton MN, Gan L-: Evaluation of drug-transporter interactions using in vitro and in vivo models. Curr Drug Metab 8: 341-363, 2007

Yamada A, Maeda K, Kamiyama E et al.: Multiple human isoforms of drug transporters contribute to the hepatic and renal transport of olmesartan, a selective antagonist of the angiotensin II AT1-receptor. Drug Metab Dispos 35: 2166-2176, 2007

Yang X, Gandhi YA, Duignan DB, Morris ME: Prediction of biliary excretion in rats and humans using molecular weight and quantitative structure-pharmacokinetic relationships. AAPS Journal 11: 511-525, 2009

Yang X, Gandhi YA, Morris ME: Biliary excretion in dogs: Evidence for a molecular weight threshold. Eur J Pharm Sci 40: 33-37, 2010

Yasunaga M, Takemura M, Fujita K, Yabuuchi H, Wada M: Molecular cloning and functional characterization of cynomolgus monkey multidrug resistance-associated protein 2 (MRP2). Eur J Pharm Sci 35: 326-334, 2008

Yu L, Shen Q, Zhou Q et al.: In vitro characterization of ABC transporters involved in the absorption and distribution of liensinine and its analogs. J Ethnopharmacol 150: 485-491, 2013

Zamek-Gliszczynski MJ, Hoffmaster KA, Nezasa K-, Tallman MN, Brouwer KLR: Integration of hepatic drug transporters and phase II metabolizing enzymes: Mechanisms of hepatic excretion of sulfate, glucuronide, and glutathione metabolites. Eur J Pharm Sci 27: 447-486, 2006a

Zamek-Gliszczynski MJ, Hoffmaster KA, Humphreys JE, Tian X, Nezasa K-, Brouwer KLR: Differential involvement of Mrp2 (Abcc2) and Bcrp (Abcg2) in biliary excretion of 4-methylumbelliferyl glucuronide and sulfate in the rat. J Pharmacol Exp Ther 319: 459-467, 2006b

Zamek-Gliszczynski MJ, Nezasa K-, Tian X et al.: Evaluation of the role of multidrug resistance-associated protein (Mrp) 3 and Mrp4 in hepatic basolateral excretion of sulfate and glucuronide metabolites of acetaminophen, 4-methylumbelliferone, and harmol in Abcc3-/- and Abcc4-/- mice. J Pharmacol Exp Ther 319: 1485-1491, 2006c

Zamek-Gliszczynski MJ, Day JS, Hillgren KM, Phillips DL: Efflux transport is an important determinant of ethinylestradiol glucuronide and ethinylestradiol sulfate pharmacokinetics. Drug Metab Dispos 39: 1794-1800, 2011

Zamek-Gliszczynski MJ, Lee CA, Poirier A et al.: ITC recommendations for transporter kinetic parameter estimation and translational modeling of transport-mediated PK and DDIs in humans. Clin Pharmacol Ther 94: 64-79, 2013

Zamek-Gliszczynski MJ, Chu X, Polli JW, Paine MF, Galetin A: Understanding the transport properties of metabolites: Case studies and considerations for drug development. Drug Metab Dispos 42: 650-664, 2014

Zelcer N, Saeki T, Reid G, Beijnen JH, Borst P: Characterization of Drug Transport by the Human Multidrug Resistance Protein 3 (ABCC3). J Biol Chem 276: 46400-46407, 2001

Zelcer N, Reid G, Wielinga P et al.: Steroid and bile acid conjugates are substrates of human multidrug-resistance protein (MRP) 4 (ATP-binding cassette C4). Biochem J 371: 361-367, 2003

Zelcer N, Van De Wetering K, Hillebrand M et al.: Mice lacking multidrug resistance protein 3 show altered morphine pharmacokinetics and morphine-6-glucuronide antinociception. Proc Natl Acad Sci U S A 102: 7274-7279, 2005

Zelcer N, Wetering KVD, Waart RD et al.: Mice lacking Mrp3 (Abcc3) have normal bile salt transport, but altered hepatic transport of endogenous glucuronides. J Hepatol 44: 768-775, 2006

Zeng H, Liu G, Rea PA, Kruh GD: Transport of amphipathic anions by human multidrug resistance protein 3. Cancer Res 60: 4779-4784, 2000

Zeng H, Chen Z-, Belinsky MG, Rea PA, Kruh GD: Transport of methotrexate (MTX)

and folates by multidrug resistance protein (MRP) 3 and MRP1: Effect of polyglutamylation on MTX transport. Cancer Res 61: 7225-7232, 2001

Zenser TV, Lakshmi VM, Davis BB: N-glucuronidation of benzidine and its metabolites: Role in bladder cancer. Drug Metab Dispos 26: 856-859, 1998

Zhang D, Frost CE, He K et al.: Investigating the enteroenteric recirculation of apixaban, a factor Xa inhibitor: Administration of activated charcoal to bile duct-cannulated rats and dogs receiving an intravenous dose and use of drug transporter knockout rats. Drug Metab Dispos 41: 906-915, 2013

Zimmerman EI, Roberts JL, Li L et al.: Ontogeny and sorafenib metabolism. Clin Cancer Res 18: 5788-5795, 2012

APPENDIX 1

Recipes and concentrations of the reagent solutions.

Final concentration of the reagents are presented in the parenthesis. All the reagents and materials used here are presented in *MATERIALS AND METHODS*.

Agarose gel 0.8 %

1.6 g	Agarose	(0.8 %)
Ad. 200 ml	1X TAE-buffer	

Boil the agarose solution in the microwave oven, cool it down to approximately 50 °C and cast the gel.

Agarose gel 1.5 %

3 g	Agarose	(1.5 %)
Ad. 200 ml	1X TAE-buffer	

Boil the agarose solution in the microwave oven, cool it down to approximately 40 °C and cast the gel.

1X TAE-buffer

242 g	TRIS-Base	(40 mM)
57.1 g	Acetic Acid	(19 mM)
18.61 g	EDTA disodium salt dehydrate	(1 mM)
Ad. 1 l	Water	

Adjust pH to 8 with 32 % hydrochloric acid.

Dilute in the multiple of 50 with water before use to give 1X TAE.

STET

8 g	Saccharose	(8 %)
5 g	Triton X 100	(5 %)
5 ml	500 mM TRIS-HCl water solution pH 8.0	(25 mM)
5 ml	500 mM EDTA water solution pH 8.0	(25 mM)
Ad. 100 ml	Water	

STETL

5 ml	STET solution	
50 µl	50 mg/ml (1 000 000 U/ml) lysozyme water solution	(10 000 U/ml)

10 % Running gel

50 µl	10 % SDS water solution	(0.1 %)
25 µl	10 % APS water solution	(0.05 %)
2.5 µl	TEMED	(0.05 %)
1.25 ml	1.5 M TRIS-HCl water solution pH 8.8	(370 mM)
1.65 ml	30 % Acrylamide/Bis-acrylamide solution	(10 %)
2.05 ml	Water	

4 % Stacking gel

25 µl	10 % SDS water solution	(0.1 %)
25 µl	10 % APS water solution	(0.1 %)
2.5 µl	TEMED	(0.1 %)
0.625 ml	500 mM TRIS-HCl water solution pH 6.8	(125 µM)
0.325 ml	30 % Acrylamide/Bis-acrylamide solution	(4 %)
1.525 ml	Water	

Transfer buffer

3.034 g	TRIS-Base	(25 mM)
14.42 g	Glycin	(190 mM)
200 ml	Methanol	(20 %)
Ad. 1000 ml	Water	

1X Running buffer

30.25 g	TRIS-Base	(25 mM)
144 g	Glycin	(190 mM)
10 g	SDS	(0.1 %)
Ad. 1000 ml	Water	

Dilute 10 times with water before use.

6X Lämmli buffer

3.0 g	SDS	(12 %)
15 g	Glycerol	(60 %)
3.0 ml	500 mM TRIS-HCl water solution pH 6.8	(60 mM)
100 mg	Bromophenol blue	(0.4 %)
Ad. 25 ml	Water	

4X Loading buffer

80 µl	5 X Lämmli buffer	(4X)
20 µl	2 M DTT water solution	(400 mM)

PBST

100 ml	10X PBS water solution prepared using commercial PBS powder	(1X)
1 ml	Tween 20	(0.1 %)
Ad. 1000 ml	Water	

5 % Milk

5 g	Milk powder	(5 %)
Ad. 100 ml	PBST	

Protein staining solution

0.2 g	Ponceau S	(0.2 %)
3 g	Trichloroacetic acid	(3 %)
Ad. 100 ml	Water	

APPENDIX 2

Recipes and concentrations of the cell and bacterial media and related solutions.

Final concentration of the reagents are presented in the parenthesis. All the reagents and materials used here are presented in *MATERIALS AND METHODS*.

Agar Plates with 100 µg/ml ampicillin

40 g	LB-Agar	(4 %)
Ad. 1 l	Water	

Autoclave and add 2 ml of 50 mg/ml ampicillin water solution when agar solution is cooled down to approximately 40 °C and pour to petri plates immediately.

LB-media with 50 µg/ml ampicillin

25 g	LB-medium	(2.5 %)
Ad. 1 l	Water	

Autoclave and add 1 ml of 50 mg/ml ampicillin water solution just before use.

500 mM sodium butyrate solution

2.75 g	Sodium butyrate	(500 mM)
Ad. 50 ml	DPBS	

Sterile filter with 0.2 µm syringe filter.

G418 solution

5 g	G418	(0.1 g/ml)
Ad. 50 ml	DPBS	

Sterile filter with 0.2 µm syringe filter.

FBS

500 ml of FBS is thawed in room temperature, heat inactivated for 30 minutes at 56˚C water bath and divided in aliquots which are stored at -20 °C.

Cell culture media for parental MDCK cells (MEM-PS)

500 ml	MEM	
55 ml	FBS	(10 %)
5.7 ml	Penicillin (10 000 U/ml) and Streptomycin (10 mg/ml) solution in PBS	(1 %)

Cell culture media for MDCK-MRP2 and MDCK-VC cells (MEM-PS-G418)

500 ml	MEM	
55 ml	FBS	(10 %)
5.7 ml	Penicillin (10 000 U/ml) and Streptomycin (10 mg/ml) solution in PBS	(1 %)
4.6 ml	G418 0.1 g/ml	(0.8 mg/ml)

Cell culture media for MDCK UGT1A1 cells (MEM-PS-Zeocin)

500 ml	MEM	
55 ml	FBS	(10 %)
5.7 ml	Penicillin (10 000 U/ml) and Streptomycin (10 mg/ml) solution in PBS	(1 %)
2.85 ml	Zeocin 100 mg/ml in water	(0.5 mg/ml)

Cell culture media for MDCK-MRP2-UGT1A1 cells (MEM-PS-G418-Zeocin)

500 ml	MEM	
55 ml	FBS	(10 %)
5.7 ml	Penicillin (10 000 U/ml) and Streptomycin (10 mg/ml) solution in PBS	(1 %)
4.6 ml	G418 0.1 g/ml	(0.8 mg/ml)
5.7 ml	Zeocin 100 mg/ml in water	(1 mg/ml)

APPENDIX 3

Charts of the plasmids used in the study including selected restriction enzymes, primer binding sites and sizes of the plasmids

Charts of the plasmids pCR2.1-TOPO-UGT2B7, pGEM-T-UGT2B7, pcDNA3.1/Hygro(-), pcDNA3.1/Hygro(-)-UGT2B7 (correct orientation), pcDNA3.1/Hygro(-)-UGT2B7 (wrong orientation), pcDNA3.1/Zeo(-), pcDNA3.1/Zeo(-)-UGT2B7, pCR2.1-TOPO-MRP3 (orientation 1), pCR2.1-TOPO-MRP3 (orientation 2), pcDNA3.1/Hygro(-)-MRP3 and pcDNA3.1/Zeo(-)-UGT1A1 are presented in Figures 1-11, respectively. Table 1-11 present location of the restriction sites and binding sites of the primers in the respective plasmids.

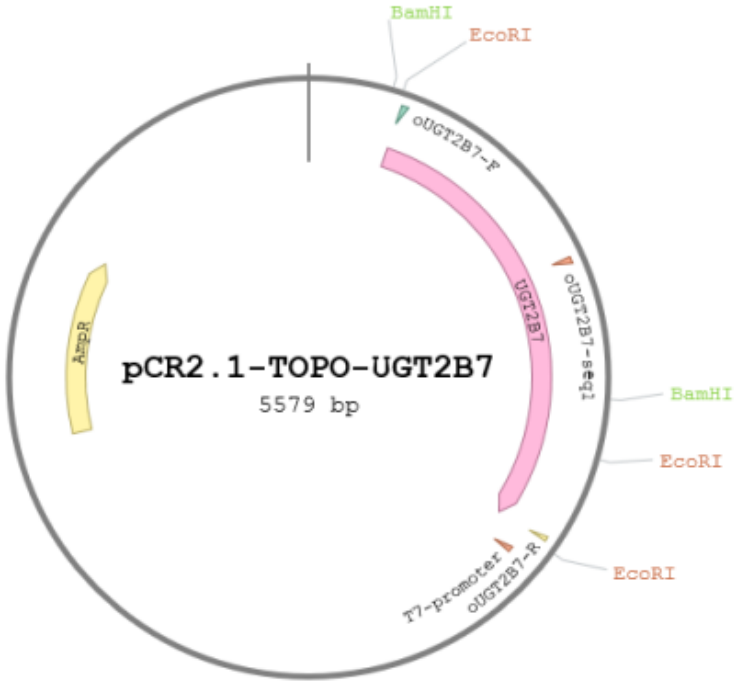

Figure 1. Chart of the plasmid pCR2.1-TOPO-UGT2B7. Restriction sites used in this study are indicated. In addition, position of the *UGT2B7* cDNA, ampicillin resistance gene (AmpR) and primer binding sites are indicated (created in www.benchling.com).

Table 1. Selected restriction sites and primer binding sites in the plasmid pCR2.1-TOPO-UGT2B7.

Restriction site	**Start site**	**Primer**	**Start site**
*Bam*HI	253	oUGT2B7-F	315
*Bam*HI	1461	oUGT2B7-seq1	1032
*Eco*RI	284	oUGT2B7-R	1919
*Eco*RI	1641	T7-promoter	2012
*Eco*RI	1950		

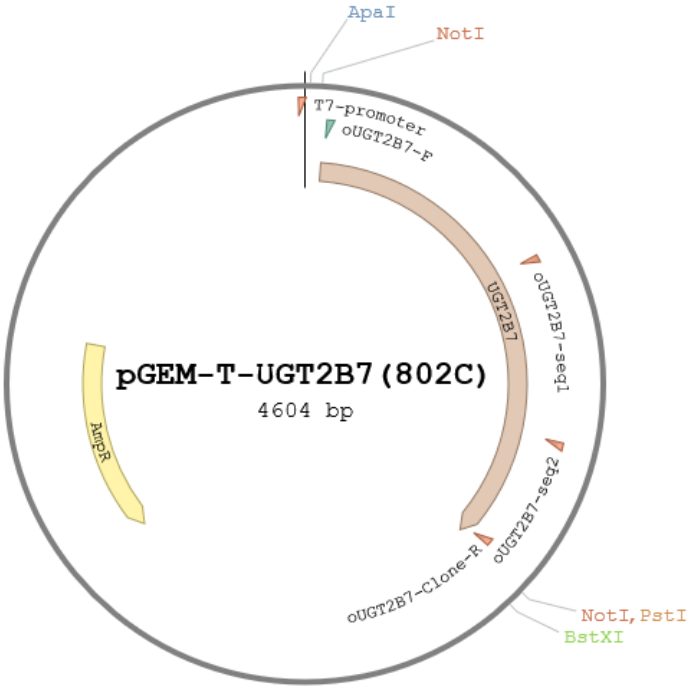

Figure 2. Chart of the plasmid pGEM-T-UGT2B7(802C). Restriction sites used in this study are indicated. In addition, position of the *UGT2B7* cDNA, ampicillin resistance gene (AmpR) and primer binding sites are indicated (created in www.benchling.com).

Table 2. Selected restriction sites and primer binding sites in the plasmid pGEM-T-UGT2B7(802C).

Restriction site	Start site	Primer	Start site
*Apa*I	15	T7-promoter	3
*Bst*XI	1754	oUGT2B7-F	83
*Not*I	44	oUGT2B7-seq1	800
*Not*I	1713	oUGT2B7-seq2	1339
*Pst*I	1724	oUGT2B7-Clone-R	1658

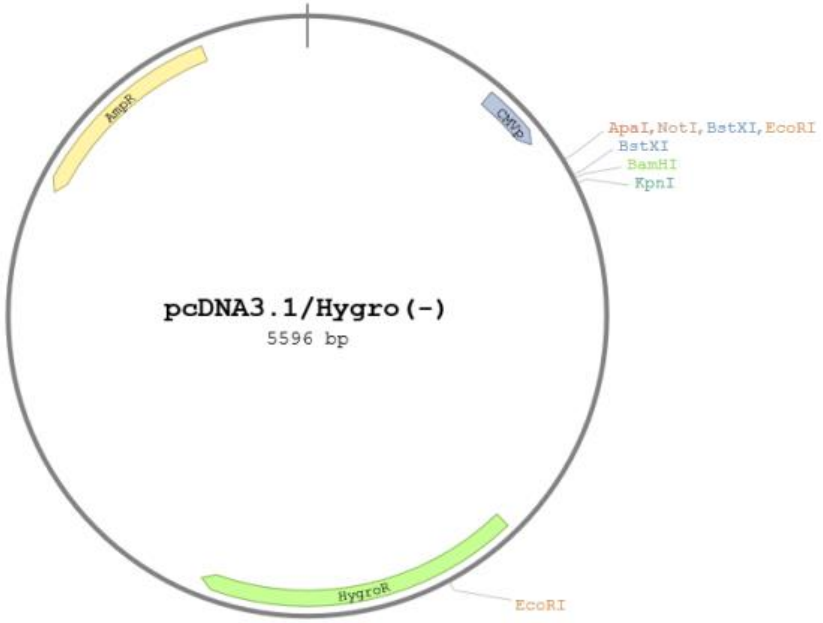

Figure 3. Chart of the vector pcDNA3.1/Hygro(-). Restriction sites used in this study are indicated. In addition, positions of ampicillin resistance gene (AmpR), hygromycin resistance gene (HygroR) and cytomegalovirus promoter (CMVp) are indicated (created in www.benchling.com).

Table 3. Selected restriction sites sites in the vector pcDNA3.1/Hygro(-).

Restriction site	Start site	Restriction site	Start site
*Apa*I	914	*Eco*RI	955
*Bam*HI	978	*Eco*RI	2361
*Bst*XI	941	*Kpn*I	994
*Bst*XI	967	*Not*I	928

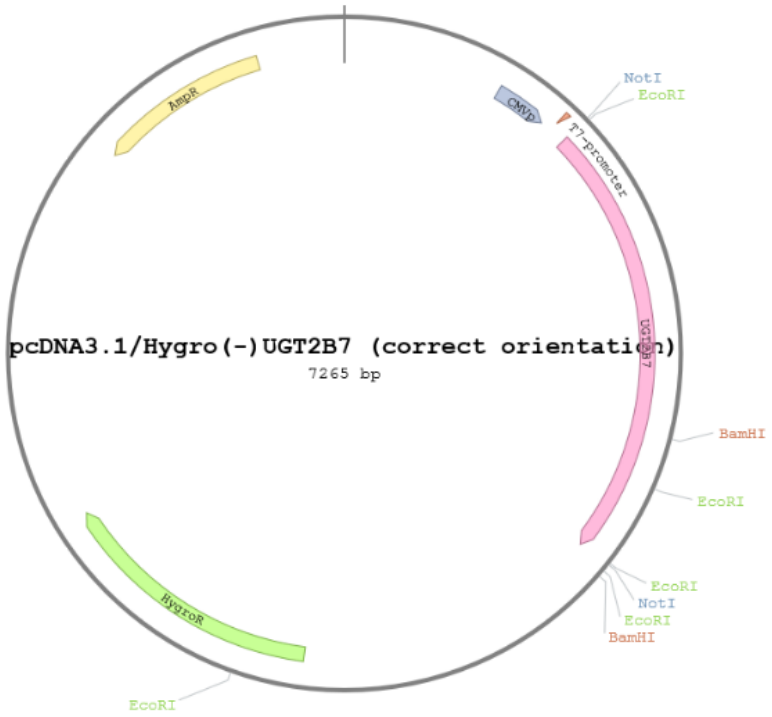

Figure 4. Chart of the vector pcDNA3.1/Hygro(-)-UGT2B7 (correct orientation). Restriction sites used in this study are indicated. In addition, positions of ampicillin resistance gene (AmpR), hygromycin resistance gene (HygroR), cytomegalovirus promoter (CMVp) and T7-promoter primer are indicated (created in www.benchling.com).

Table 4. Selected restriction sites and primer binding sites in the vector pcDNA3.1/Hygro(-)-UGT2B7 (correct orientation).

Restriction site	Start site	Restriction site/Primer	Start site
*Bam*HI	2113	*Eco*RI	2624
*Bam*HI	2647	*Eco*RI	4030
*Eco*RI	937	*Not*I	928
*Eco*RI	2293	*Not*I	2597
*Eco*RI	2590	T7-promoter	882

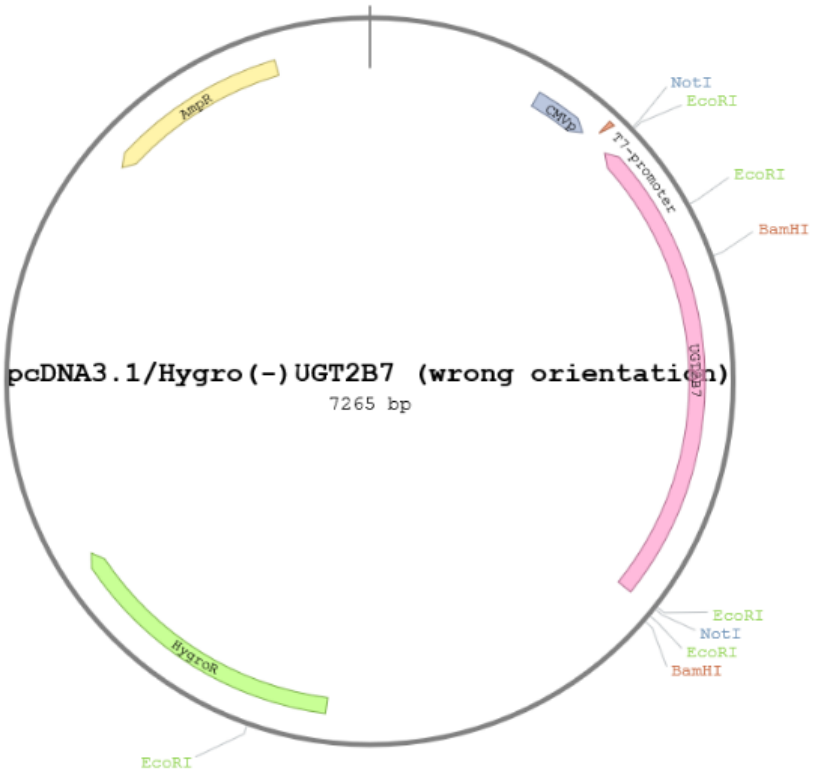

Figure 5. Chart of the vector pcDNA3.1/Hygro(-)-UGT2B7 (wrong orientation). Restriction sites used in this study are indicated. In addition, positions of ampicillin resistance gene (AmpR), hygromycin resistance gene (HygroR), cytomegalovirus promoter (CMVp) and T7-promoter primer are indicated (created in www.benchling.com).

Table 5. Selected restriction sites and primer binding sites in the vector pcDNA3.1/Hygro(-)-UGT2B7 (wrong orientation).

Restriction site	**Start site**	**Restriction site/Primer**	**Start site**
*Bam*HI	1412	*Eco*RI	2624
*Bam*HI	2647	*Eco*RI	4030
*Eco*RI	937	*Not*I	928
*Eco*RI	1232	*Not*I	2597
*Eco*RI	2590	T7-promoter	882

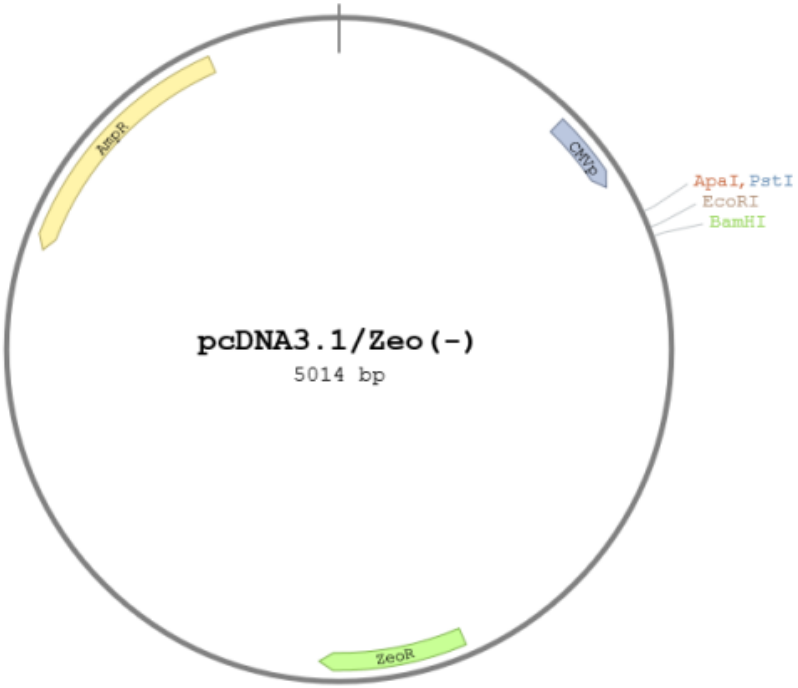

Figure 6. Chart of the vector pcDNA3.1/Zeo(-). Restriction sites used in this study are indicated. In addition, positions of ampicillin resistance gene (AmpR), zeocin resistance gene (ZeoR) and cytomegalovirus promoter (CMVp) are indicated (created in www.benchling.com).

Table 6. Selected restriction site sites in pcDNA3.1/Zeo(-).

Restriction site	Start site
*Apa*I	914
*Bam*HI	978
*Eco*RI	955
*Pst*I	954

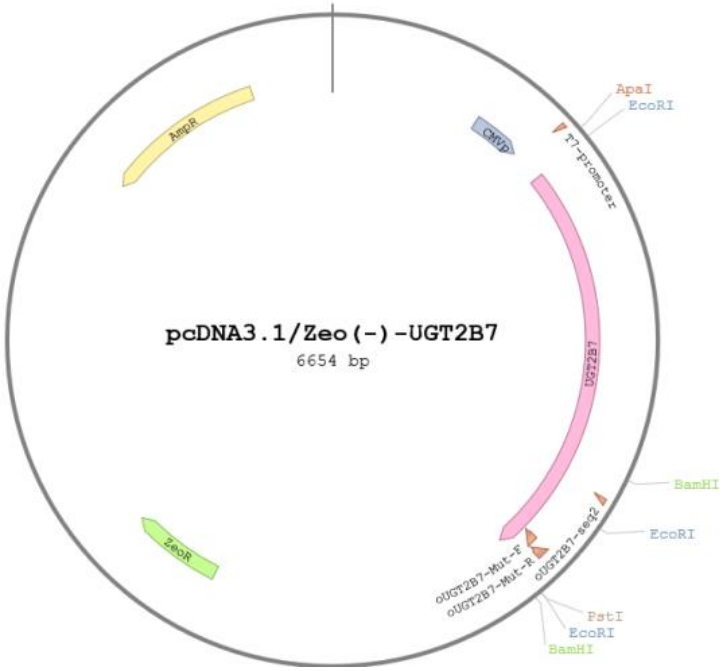

Figure 7. Chart of the vector pcDNA3.1/Zeo(-)-UGT2B7. Restriction sites used in this study are indicated. In addition, positions of ampicillin resistance gene (AmpR), zeocin resistance gene (ZeoR), cytomegalovirus promoter (CMVp) and primers are indicated (created in www.benchling.com).

Table 7. Selected restriction sites and primer binding sites in pcDNA3.1/Zeo(-)-UGT2B7.

Restriction site	Start site	Restriction site/Primer	Start site
*Apa*I	914	*Eco*RI	2595
*Bam*HI	2133	*Pst*I	2594
*Bam*HI	2618	T7-promoter	882
*Eco*RI	950	oUGT2B7-seq2	2243
*Eco*RI	2313	oUGT2B7-Mut-F	2477
		oUGT2B7-Mut-R	2523

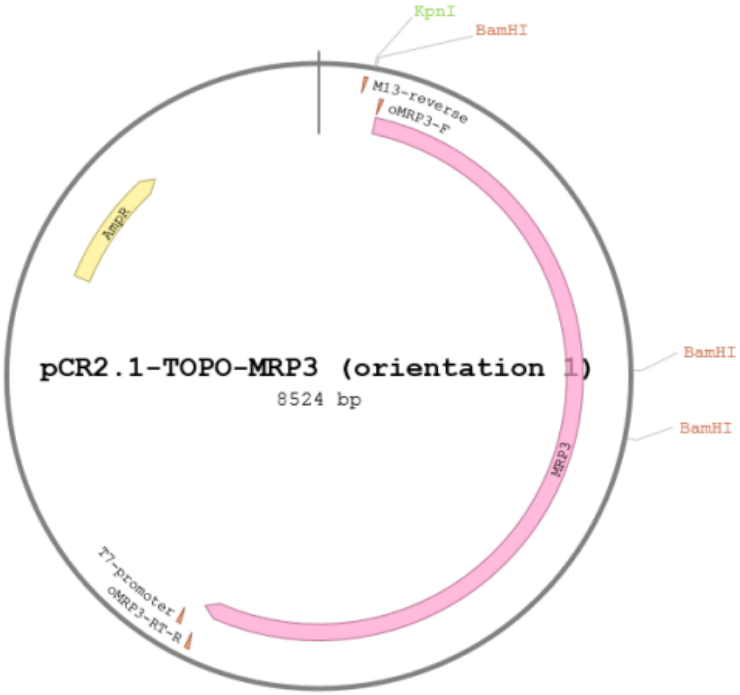

Figure 8. Chart of the plasmid pCR2.1-TOPO-MRP3 (orientation 1). Restriction sites used in this study are indicated. In addition, positions of ampicillin resistance gene (AmpR) and primers are indicated (created in www.benchling.com).

Table 8 Selected restriction sites and primer binding sites in the plasmid pCR2.1-TOPO-MRP3 (orientation 1).

Restriction site	Start site	Restriction site/Primer	Start site
*Bam*HI	253	*Not*I	4922
*Bam*HI	2108	M13-reverse	221
*Bam*HI	2402	oMRP3-F	312
*Kpn*I	245	oMRP3-RT-R	4867
		T7-promoter	4957

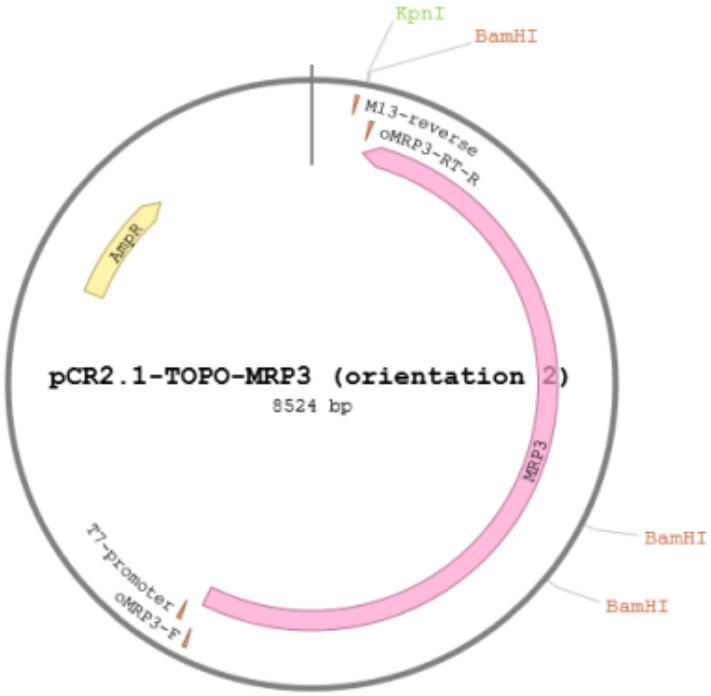

Figure 9. Chart of the plasmid pCR2.1-TOPO-MRP3 (orientation 2). Restriction sites used in this study are indicated. In addition, positions of ampicillin resistance gene (AmpR) and primers are indicated (created in www.benchling.com).

Table 9. Selected restriction sites and primer binding sites in the plasmid pCR2.1-TOPO-MRP3 (orientation 1).

Restriction site	Start site	Restriction site/Primer	Start site
*Bam*HI	253	*Not*I	4922
*Bam*HI	2777	M13-reverse	221
*Bam*HI	3071	oMRP3-F	4870
*Kpn*I	245	oMRP3-RT-R	315
		T7-promoter	4957

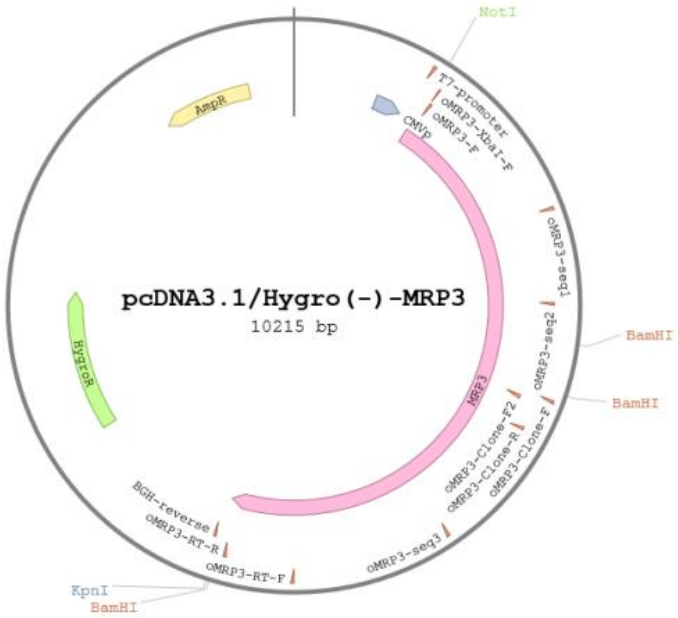

Figure 10. Chart of the vector pcDNA3.1/Hygro(-)-MRP3. Restriction sites used in this study are indicated. In addition, positions of ampicillin resistance gene (AmpR), hygromycin resistance gene (HygroR), cytomegalovirus promoter (CMVp) and primers are indicated (created in www.benchling.com).

Table 10. Restriction site and primer binding sites in the vector pcDNA3.1/Hygro (-)-MRP3.

Restriction site/Primer	Start site	Primer	Start site
*BamH*I	2779	oMRP3-seq2	2552
*BamH*I	3073	oMRP3-Clone-F	3145
*BamH*I	5597	oMRP3-Clone-F2	3188
*Kpn*I	5613	oMRP3-Clone-R	3344
*Not*I	928	oMRP3-seq3	4155
T7-promoter	882	oMRP3-RT-F	5128
oMRP3-*Xba*I-F	975	oMRP3-RT-R	5538
oMRP3-F	983	BGH-reverse	5640
oMRP3-seq1	1980		

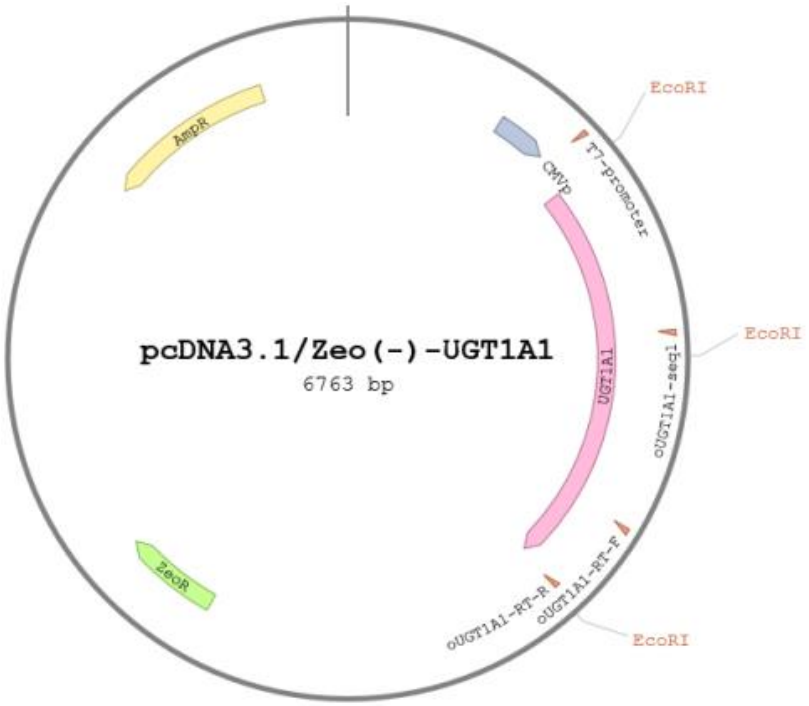

Figure 11. Chart of the vector pcDNA3.1/Zeo(-)-UGT1A1. Restriction sites used in this study are indicated. In addition, positions of ampicillin resistance gene (AmpR), zeocin resistance gene (ZeoR), cytomegalovirus promoter (CMVp) and primers are indicated (created in www.benchling.com).

Table 11. Restriction site and primer binding sites in pcDNA3.1/Zeo(-)-UGT1A1.

Restriction site	Start site	Primer	Start site
*Eco*RI	955	T7-promoter	882
*Eco*RI	1681	oUGT1A1-seq1	1614
*Eco*RI	2596	oUGT1A1-RT-F	2299
		oUGT1A1-RT-R	2569